

INFORMATION TO USERS

This was produced from a copy of a document sent to us for microfilming. While the most advanced technological means to photograph and reproduce this document have been used, the quality is heavily dependent upon the quality of the material submitted.

The following explanation of techniques is provided to help you understand markings or notations which may appear on this reproduction.

1. The sign or "target" for pages apparently lacking from the document photographed is "Missing Page(s)". If it was possible to obtain the missing page(s) or section, they are spliced into the film along with adjacent pages. This may have necessitated cutting through an image and duplicating adjacent pages to assure you of complete continuity.
2. When an image on the film is obliterated with a round black mark it is an indication that the film inspector noticed either blurred copy because of movement during exposure, or duplicate copy. Unless we meant to delete copyrighted materials that should not have been filmed, you will find a good image of the page in the adjacent frame.
3. When a map, drawing or chart, etc., is part of the material being photographed the photographer has followed a definite method in "sectioning" the material. It is customary to begin filming at the upper left hand corner of a large sheet and to continue from left to right in equal sections with small overlaps. If necessary, sectioning is continued again--beginning below the first row and continuing on until complete.
4. For any illustrations that cannot be reproduced satisfactorily by xerography, photographic prints can be purchased at additional cost and tipped into your xerographic copy. Requests can be made to our Dissertations Customer Services Department.
5. Some pages in any document may have indistinct print. In all cases we have filmed the best available copy.

University
Microfilms
International

300 N. ZEEB ROAD, ANN ARBOR, MI 48106
18 BEDFORD ROW, LONDON WC1R 4EJ, ENGLAND

7916203

LOWN, JEAN A.

THE ANODIC AMPEROMETRIC DETERMINATION OF
ARSENIC AT A PLATINUM FLOW-THROUGH DETECTOR.

IOWA STATE UNIVERSITY, PH.D., 1979

University
Microfilms
International

300 N. ZEEB ROAD, ANN ARBOR, MI 48106

The anodic amperometric determination of arsenic
at a platinum flow-through detector

by

Jean A. Lown

A Dissertation Submitted to the
Graduate Faculty in Partial Fulfillment of
The Requirements for the Degree of
DOCTOR OF PHILOSOPHY

Department: Chemistry
Major: Analytical Chemistry

Approved:

Signature was redacted for privacy.

In Charge of ~~Major~~ Work

Signature was redacted for privacy.

For the ~~Major~~ Department

Signature was redacted for privacy.

For the ~~Graduate~~ College

Iowa State University
Ames, Iowa

1979

TABLE OF CONTENTS

| | Page |
|--|------|
| I. INTRODUCTION | 1 |
| II. LITERATURE SURVEY | 6 |
| A. Sample Pretreatment and Dissolution | 6 |
| 1. Wet ashing | 6 |
| 2. Dry ashing | 7 |
| 3. Oxygen combustion | 8 |
| 4. Fusion | 8 |
| B. Preconcentration and Isolation of Arsenic Species | 8 |
| 1. Coprecipitation | 9 |
| 2. Liquid-liquid extraction | 9 |
| 3. Volatilization | 10 |
| 4. Ion-exchange | 11 |
| C. Methods Used for Arsenic Determination | 11 |
| 1. Non-electroanalytical techniques | 12 |
| a. Titrations with visual end-points | 12 |
| b. Molecular absorption spectroscopy | 12 |
| c. Atomic spectroscopy | 13 |
| d. Neutron activation analysis | 14 |
| e. X-ray fluorescence | 15 |
| f. Gas chromatography | 15 |
| 2. Electroanalytical techniques | 16 |
| a. Potentiometric titrations | 16 |
| b. Amperometric titrations | 16 |
| c. Coulometric titrations | 17 |
| d. Polarography | 17 |
| e. Anodic stripping voltammetry | 19 |
| III. CHOICE OF ELECTRODE MATERIAL FOR THE DETERMINATION OF ARSENIC | 20 |
| A. Introduction | 20 |
| B. Experimental | 21 |

| | Page |
|---|------|
| 1. Instrumentation and apparatus | 21 |
| 2. Reagents | 22 |
| 3. Procedure | 23 |
| C. Cyclic Voltammetry of Arsenic at a Gold Disk | 23 |
| D. Cyclic Voltammetry of Arsenic at a Platinum Disk | 38 |
| E. Conclusions | 66 |
| IV. EVALUATION OF THE Pt FLOW-THROUGH DETECTOR | 67 |
| A. Introduction | 67 |
| B. Experimental | 68 |
| 1. Description of the flow system | 68 |
| 2. Detector and instrumentation | 71 |
| C. Detector Response | 74 |
| 1. Current as a function of time for As(III) | 74 |
| 2. Relationship between oxide growth on Pt electrode and current decay for oxidation of As(III) | 82 |
| 3. Pseudo I-E curve for As(III) in 0.5 <u>M</u> HClO ₄ | 91 |
| 4. Dependence of current on flow rate | 94 |
| 5. Calibration curve for As(III) in 0.1 <u>M</u> HClO ₄ | 99 |
| D. Conclusion | 103 |
| V. CHOICE OF REDUCING AGENT FOR As(V) | 110 |
| A. Introduction | 110 |
| B. Experimental | 110 |
| 1. Procedure | 110 |
| 2. Standardization of As(V) | 111 |
| C. Results and Discussion | 112 |
| 1. Reducing columns | 112 |

| | Page |
|--|------|
| a. Metals | 112 |
| b. Redox resins | 113 |
| 2. Iodide | 114 |
| 3. Stannous | 118 |
| 4. Copper(I) | 120 |
| 5. Titanium(III) | 120 |
| 6. Sulfur(IV) | 120 |
| 7. Hydrazine | 121 |
| D. Conclusions | 122 |
| VI. INTERFERENCES | 124 |
| A. Introduction | 124 |
| B. Experimental | 124 |
| 1. Reagents | 124 |
| 2. Procedure | 125 |
| C. Results and Discussion | 125 |
| D. Conclusion | 128 |
| VII. DETERMINATION OF ARSENIC IN ORCHARD LEAVES | 129 |
| A. Introduction | 129 |
| B. Experimental | 129 |
| C. Results and Discussion | 129 |
| 1. Choice of eluent | 129 |
| 2. Dissolution of orchard leaves and reduction of As(V) | 130 |
| D. Conclusion | 140 |
| VIII. SUGGESTIONS FOR FUTURE RESEARCH | 145 |
| IX. BIBLIOGRAPHY | 146 |
| X. ACKNOWLEDGEMENTS | 158 |

LIST OF TABLES

| | Page |
|---|------|
| Table I-1. Concentration of arsenic found in nature | 4 |
| Table III-1. Limiting current produced at Au disk for various concentrations of As(III) in 1.0 M HClO ₄ | 31 |
| Table III-2. Dependence of limiting current on rotation speed of Au disk for As(III) in 1.0 M HClO ₄ | 32 |
| Table III-3. Limiting current produced at Pt disk for various concentrations of As(III) in 0.5 M HClO ₄ | 52 |
| Table III-4. Dependence of limiting current on rotation speed of Pt disk for As(III) in 0.5 M HClO ₄ | 60 |
| Table IV-1. Current as a function of time for As(III) in 0.5 M HClO ₄ passing through Pt flow-through electrochemical detector | 79 |
| Table IV-2. Current at 1.0 V <u>vs.</u> SCE on negative potential sweep <u>vs.</u> time potential of Pt disk held at 1.35 V <u>vs.</u> SCE for As(III) in 0.5 M HClO ₄ | 83 |
| Table IV-3. Current <u>vs.</u> time for As(III) in 0.5 M HClO ₄ flowing through Pt wire electrochemical detector held at 1.0 V <u>vs.</u> SCE for 7 hours | 88 |
| Table IV-4. Pseudo current-voltage curve for As(III) in 0.5 M HClO ₄ through Pt wire flow-through detector | 91 |

| | Page |
|---|------|
| Table IV-5. Dependence of current on flow rate of As(III) in 0.5 <u>M</u> HClO ₄ through Pt wire detector | 98 |
| Table IV-6. Dependence of current on flow rate for Br ⁻ in 0.5 <u>M</u> HClO ₄ through Pt wire detector | 102 |
| Table IV-7. Calibration curve for As(III) in 0.1 <u>M</u> HClO ₄ at Pt wire detector | 104 |
| Table VI-1. Interference study | 126 |
| Table VII-1. Constituents present in NBS SRM 1571 (orchard leaves) | 139 |

LIST OF FIGURES

| | Page |
|---|------|
| Figure III-1. Cyclic voltammograms of As(III) in 1.0 <u>M</u> HClO ₄ at a Au disk | 25 |
| Figure III-2. Limiting current produced at Au disk during positive potential scan for various concentrations of As(III) in 1.0 <u>M</u> HClO ₄ | 30 |
| Figure III-3. Dependence of limiting current on rotation speed of Au disk during positive potential scan for As(III) in 1.0 <u>M</u> HClO ₄ | 34 |
| Figure III-4. Effect of Cl ⁻ on the cyclic voltammetry of As(III) in 1.0 <u>M</u> HClO ₄ at a Au disk | 37 |
| Figure III-5. Cyclic voltammograms of As(III) in 0.5 <u>M</u> HClO ₄ at a Pt disk | 40 |
| Figure III-6. Variation of potential limit applied to Pt disk during negative scan for As(III) in 0.5 <u>M</u> HClO ₄ | 44 |
| Figure III-7. Variation of potential limit applied to Pt disk during positive scan for As(III) in 0.5 <u>M</u> HClO ₄ | 46 |
| Figure III-8. Variation of rotation speed of Pt disk for As(III) in 0.5 <u>M</u> HClO ₄ | 49 |
| Figure III-9. Variation of potential scan rate of Pt disk for As(III) in 0.5 <u>M</u> HClO ₄ | 50 |
| Figure III-10. Limiting current produced at Pt disk for various concentrations of As(III) in 0.5 <u>M</u> HClO ₄ | 54 |

| | Page |
|--|------|
| Figure III-11. Change in onset of formation of Pt oxide in the presence of As(III) | 56 |
| Figure III-12. Dependence of limiting current on rotation speed of Pt disk for As(III) in 0.5 <u>M</u> HClO ₄ | 59 |
| Figure III-13. Effect of Cl ⁻ on the cyclic voltammetry at a Pt disk for As(III) in 0.5 <u>M</u> HClO ₄ | 62 |
| Figure III-14. Cyclic voltammetry of As(V) in 0.5 <u>M</u> HClO ₄ at Pt disk | 65 |
| Figure IV-1. Schematic diagram of flow-through system used for determination of As(III) | 70 |
| Figure IV-2. Pt wire flow-through electrochemical detector | 73 |
| Figure IV-3. Current as a function of time for As(III) in 0.5 <u>M</u> HClO ₄ passing through Pt flow-through electrochemical detector held at various potentials | 77 |
| Figure IV-4. Cyclic voltammograms of As(III) in 0.5 <u>M</u> HClO ₄ at Pt disk as varied time potential held at 1.35 V <u>vs.</u> SCE | 85 |
| Figure IV-5. Current at 1.0 V <u>vs.</u> SCE during negative potential scan <u>vs.</u> time potential of Pt disk held at 1.35 V <u>vs.</u> SCE for As(III) in 0.5 <u>M</u> HClO ₄ | 87 |

| | Page |
|--|------|
| Figure IV-6. Current <u>vs.</u> time for As(III) in 0.5 <u>M</u> HClO ₄ flowing through Pt wire electrochemical detector held at 1.0 V <u>vs.</u> SCE for 7 hours | 90 |
| Figure IV-7. Pseudo current-voltage curve for As(III) in 0.5 <u>M</u> HClO ₄ through Pt wire flow-through detector | 93 |
| Figure IV-8. Dependence of current on flow rate of As(III) in 0.5 <u>M</u> HClO ₄ through Pt wire detector | 97 |
| Figure IV-9. Dependence of current on flow rate for Br ⁻ in 0.5 <u>M</u> HClO ₄ through Pt wire detector | 101 |
| Figure IV-10. Calibration curve for As(III) in 0.1 <u>M</u> HClO ₄ at Pt wire flow-through detector | 106 |
| Figure IV-11. Typical signal peak for As(III) in 0.1 <u>M</u> HClO ₄ at Pt flow-through detector | 108 |
| Figure V-1. Effect of I ⁻ on cyclic voltammetry of As(III) in 0.5 <u>M</u> HClO ₄ at Pt disk | 117 |
| Figure VII-1. Effect of hydrazine sulfate on signal peaks for As(III) in samples with high acid concentrations | 132 |
| Figure VII-2. Reduction of As(III) with N ₂ H ₄ ·H ₂ SO ₄ in presence of HClO ₄ and H ₂ SO ₄ | 135 |
| Figure VII-3. Reduction of As(III) with N ₂ H ₄ ·H ₂ SO ₄ in presence of H ₂ SO ₄ | 138 |

| | Page |
|---|------|
| Figure VII-4. Signal peaks used to construct calibration curve and signal peak due to As(III) in NBS orchard leaves | 142 |
| Figure VII-5. Calibration curve for NBS orchard leaves sample | 144 |

I. INTRODUCTION

Throughout history, the word arsenic has become synonymous with the word poison. For thousands of years arsenic has been used as an effective solution to many awkward situations that develop in human affairs. In fact, during the nineteenth century arsenic was the most popular poison utilized by homicidal practitioners (1). This popularity is portrayed in Kessling's play "Arsenic and Old Lace." It is interesting to note that a larger amount of arsenic is needed to cause death than the amount of beryllium, cadmium, cobalt, copper, indium, mercury, selenium, silver, tantalum, tellurium, thallium or vanadium (2). However, the names of these elements do not connote the concept of toxicity to the general public as strongly as does arsenic.

The toxicity of an arsenic compound is dependent upon the valence state in which the arsenic is found. The most toxic form of arsenic is arsine (AsH_3). The next most toxic form is As(III). The least toxic form is As(V). Generally, the organic arsenic compounds are less toxic than the inorganic arsenic compounds (3). The fatal dosage of arsenic is between 120 and 180 mg, depending on the chemical form of the arsenic species (4). The relative toxicity of the various forms of arsenic can be explained, in part, by examining the rate by which the body adsorbs

and excretes the arsenic species. The more toxic trivalent arsenic compounds are retained in the tissues in greater amounts and are excreted more slowly than the less toxic pentavalent arsenic compounds (5).

The mode of action within the human body is different for the various arsenic species. Arsine is primarily a hemolytic agent. Inhalation of arsine leads to rapid hemolysis of red blood cells, resulting in anemia, and to the presence of hemoglobin in the urine, resulting in renal damage. Arsine is fatal and there is no known antidote. Trivalent arsenic has a high affinity for sulfhydryl groups. As a result, sulfhydryl enzyme systems essential to cellular metabolism are inhibited. Fat and carbohydrate metabolism as well as cellular respiration are blocked (6). 2,3-Dimercaptopropanol has been used successfully as an antidote for victims of As(III) poisoning (7). Pentavalent arsenic inhibits ATP synthesis by replacing stable phosphoryl groups (8). The symptoms of arsenic poisoning include stomach pains, profuse diarrhea, skin ulcerations, muscular cramps, sighing respiration, frontal headaches and depression (2).

The possible carcinogenic nature of arsenic has been studied for over a century without a clear decision. There appears to be a strong correlation between the amount of arsenic exposure and the incidence of both skin and

respiratory cancer in humans (9, 10). Yet, all attempts to produce tumors in experimental animals by exposure to arsenic compounds have failed (11-13).

Arsenic has some remarkable attributes that have failed to receive notice because of its poor public image. The medicinal virtues of arsenic have been acclaimed for 2,500 years. Arsenic sulfide reportedly was used by Hippocrates to cure "ulcers" and similar disorders (7). Potassium arsenite, prepared as a 1% solution in ethanol, was known as "Fowler's solution" and was used at one time in the treatment of psoriasis (5). In 1919, Paul Ehrlich introduced the arsenical Salvarsan for the clinical treatment of syphilis (14). Although most of the arsenic compounds used for medical purposes have been replaced by more effective agents, arsonic acids are still widely used as growth stimulants for swine and poultry. The arsonic acids alter the bacterial metabolism in the intestinal tract resulting in improved nutrition (15, 16).

Additionally, there are quite a few commercial uses for arsenic compounds. There are a number of very important applications in agriculture. Compounds of arsenic have been used both as insecticides and herbicides. Arsenic compounds have been utilized as defoliants in cotton fields. Without defoliants, mechanical cotton pickers could not be

used. Arsenic compounds are used as wood preservatives. Small quantities of arsenic trioxide are used in glass making to remove the greenish color imparted to the glass by the metal contaminants in the raw materials. The makers of semiconductors have found a number of applications for compounds of arsenic as dopants. These are just a few of the varied uses for arsenic. There is no satisfactory substitute for arsenic in many of these applications (17, 18).

Surprisingly enough, arsenic is an ubiquitous element (6). Therefore, the finding of arsenic in a given sample is not significant unless the concentration is compared to the values normally found for that sample. Table I-1

Table I-1. Concentration of arsenic found in nature

| Substance | Concentration (ppm) |
|-----------------|---------------------|
| Water | 0.01 - 1.0 |
| Soil | 1.0 - 500 |
| Grass | 0.1 - 1.6 |
| Vegetables | 0.0 - 2.9 |
| Grains | 0.11 - 0.16 |
| Meat | 0.06 - 1.07 |
| Milk | 0.01 - 0.05 |
| Fish | 2.0 - 9.0 |
| Shrimp, lobster | 1.5 - 100 |

illustrates the levels commonly found in many environmental food samples (2, 19, 20). Schroeder and Balassa estimated that a typical adult in the United States consumes between 0.4 and 1.0 mg of arsenic every day (19). Of course, diets unusually rich in seafoods would supply much more arsenic.

The U.S. Public Health Service has set the maximum allowable level of arsenic in drinking water at 0.05 ppm (21).

More research is needed to investigate the effects of arsenic consumption on health. More definitive research is needed to establish the relationship between the amount of exposure to arsenic and the incidence of cancer. In order to perform this research, satisfactorily sensitive analytical methods are mandatory. If the analysis is to be performed routinely, the method must be fairly simple and inexpensive. With these goals in mind, an effort was made to develop an electroanalytical method for the determination of arsenic. This thesis describes the development of an anodic amperometric method for the determination of arsenic in a Pt flow-through detector. Using the method developed, arsenic can be determined routinely at the nanogram level with only a minimum number of interferences.

II. LITERATURE SURVEY

An attempt will not be made here to review exhaustively the vast volume of literature pertaining to arsenic determinations. The literature has been reviewed recently in several publications (22, 23). The intention of this chapter is to summarize the accepted analytical procedures. The following topics will be discussed: sample pretreatment and dissolution, isolation of the arsenic species and methods available for the determination of arsenic.

A. Sample Pretreatment and Dissolution

With most samples it is necessary to go through a dissolution step and convert the arsenic present to an inorganic form. There are four ways of accomplishing dissolution: wet ashing, dry ashing, oxygen combustion and fusion. Each of these approaches will be briefly described.

1. Wet ashing

When working with biological materials, great care must be exercised to prevent sample loss by volatilization while the organic matter is being destroyed. This is particularly true if halides are present because the halide complexes of As(III) are quite volatile. Consequently, a reflux condenser is generally used during the digestion step (24). Nitric acid should be the only acid present

during the early stages of the ashing procedure if the sample contains a high concentration of halide ions (25). This suggestion stems from the fact that reduction processes must be prevented in the digestion flask. If sulfuric acid is added initially, charring can occur as the nitric acid disappears. Charring results in the production of carbon and the subsequent creation of a reducing environment within the reaction flask. In a reducing environment, As(III) can be produced and the volatile halide complexes of As(III) can escape from the sample (26). Nitric acid digestion has been used for vegetation, animal tissues, and sewage. The nitric acid can be removed by adding 1:1 H_2SO_4 and evaporating the sample until fumes of sulfur trioxide appear (27). For samples requiring more vigorous digestion, combinations of nitric, sulfuric and perchloric acid are used (28, 29, 30). The perchloric acid is generally not added until the oxidation process is nearly completed.

Steel and iron ore samples are dissolved with a mixture of nitric and sulfuric acids (31, 32, 33) or with a mixture of nitric and hydrochloric acid (34, 35).

2. Dry ashing

The most widely used dry ashing procedure involves the use of magnesium oxide and magnesium nitrate. The dry ashing method has been widely investigated by the Association

of Official Analytical Chemists (A.O.A.C.) (36-39). The accepted procedure requires the formation of a slurry containing the sample, magnesium oxide, cellulose powder and water. The slurry is pre-charred until the evolution of smoke ceases. After cooling, magnesium nitrate is added. The sample is placed in a muffle furnace and ashed for two hours at 550°C. Coal samples, mixed with MgO, are directly ignited at 650°C. Satisfactory recoveries have been reported (22).

3. Oxygen combustion

Biological materials can be digested by igniting them with a spark in an oxygen atmosphere (40). A Schoniger flask is typically used (41). Both dilute NaOH (42) and HCl have been used as the absorption solution for the combustion products (43).

4. Fusion

Fusions are routinely used for the dissolution of silicate and carbonate sediments (44). NaOH fusion has been used to leach arsenic from minerals placed in a silver or nickel crucible (45). Arsenic losses are reported to be no greater than 0.5% even when a residue remains.

B. Preconcentration and Isolation of Arsenic Species

There are four principal methods for preconcentrating the arsenic present in a sample and separating the arsenic

from the other species which would interfere with the analysis. These four methods are coprecipitation, liquid-liquid extraction, volatilization and ion-exchange. Each of these methods will be described.

1. Coprecipitation

Several transition metal hydroxides can serve as efficient collectors for As(V). Coprecipitation with $\text{Fe}(\text{OH})_3$ at pH 7 has been implemented to collect As(V) with a recovery of 99% (22, 46, 47, 24). Pentavalent arsenic can also be carried down by the hydroxides of Ce, Zr, In, Ti and Al (48). At pH 9 to 10, $\text{La}(\text{OH})_3$ can likewise be used to coprecipitate As(V). Hydrated MnO_2 has also been utilized (50). For As(III), efficient collection has been obtained only with the hydroxides of Zn and In at pH 8.5 (49).

Thionalide is the most commonly used organic reagent for arsenic cocrystallization. The reagent is selective for As(III). Consequently, a prior reduction step to convert As(V) to As(III) is mandatory (22, 24). Recovery of the arsenic present is about 95%.

2. Liquid-liquid extraction

Most of the liquid-liquid extractions implemented for the isolation of arsenic are specific for As(III). This is a particularly advantageous fact when attempting to remove

interfering elements. Many interferences can be eliminated by performing a preliminary extraction while the arsenic is in the pentavalent form. Arsenic can be reduced to the trivalent state and, subsequently, be extracted after all the other interferences have been removed. The most common method for extracting arsenic involves forming AsCl_3 and extracting the AsCl_3 into chloroform or carbon tetrachloride. The AsCl_3 is then back-extracted into an aqueous solution (31, 34, 51, 52). If the pH of the sample is between 2 and 5, various dithiocarbamates can extract As(III) from an aqueous solution. Two examples are diethylammonium dithiocarbamate in chloroform (54) and ammonium dithiocarbamate in methyl isobutyl ketone (55). Di-2-ethylhexyldithiophosphoric acid in decane and diethyldithiophosphoric acid can also be used to extract trivalent arsenic (53).

3. Volatilization

The forms of arsenic that are volatile are the trihalides and the arsines. Arsenic trichloride is often distilled from hot solutions containing a high concentration of hydrochloric acid (29, 32, 56-58). Trivalent antimony will also distill under these conditions. During recent years, there has been a rapid increase in the use of arsine generation as a means of separating arsenic from

its original matrix. The arsenic is reduced to the trivalent state with SnCl_2 , KI or TiCl_3 (59, 60). The arsine is generated by passing the acidified As(III) sample through a column of zinc (61) or magnesium (60). Alternately, NaBH_4 can be used to generate arsine directly from As(V) (62).

4. Ion-exchange

Ion-exchange resins can serve as a tool for separating arsenic from either cationic or anionic species. In an acidic environment, both trivalent and pentavalent arsenic are neutral species. Consequently, arsenic will not be retained on a cation-exchange resin when the pH of the solution is low. Complete separation of arsenic from the ions of Al, Fe, Co, Ni, Cu, Mg, Pb, Cd, Au, Sr, Cr, Zn, Ca, Mn and Bi is possible in acidic solutions. Distribution coefficients have been calculated in acids more concentrated than 0.1 M (63-68). Anion-exchange resins have been used to separate As(III), Bi(III) and Sb(III) in HCl (69, 70). When an anion-exchange resin is converted to the acetate form and acetic acid is used as an eluent, As(III) can be separated from the halides (71, 72).

C. Methods Used for Arsenic Determination

A great deal of effort has been expended searching for practical methods for the determination of arsenic. The

analyst can choose from a broad spectrum of techniques. The techniques available include titrations, molecular absorption spectroscopy, atomic spectroscopy, neutron activation analysis, X-ray fluorescence and gas chromatography as well as many electroanalytical techniques. The principal methods used will be presented.

1. Non-electroanalytical techniques

a. Titrations with visual end-points An iodimetric titration can be used to determine the amount of arsenic in both organic and inorganic compounds. Excess KI is added to an acidic sample. The liberated iodine is titrated with thiosulfate using starch as the indicator (73-76, 66). Titrations based upon the oxidation of As(III) to As(V) are also used. One such titrant is ceric sulfate. Osmium tetroxide catalyzes the reaction between the As(III) and the ceric ions while ferrous phenanthroline serves as the indicator (77).

b. Molecular absorption spectroscopy The most widely used technique for the determination of arsenic is molecular absorption spectroscopy. The two reagents most commonly used with the spectroscopic measurements are silver diethyldithiocarbamate (Ag-DDC) and ammonium molybdate. When using the Ag-DDC reagent, arsine must be generated initially. The arsine is then swept into a 0.5%

solution of Ag-DDC in pyridine. A red chromophore is formed and the color intensity is measured at 533 nm. The method is sensitive to 0.05 ppm (26, 36-39, 78, 79). When ammonium molybdate is used as the color forming reagent, the arsenic must be initially present in the pentavalent form. The reaction between As(V) and acidified molybdate forms an arsenomolybdate which, when reduced, forms a blue complex. The color intensity is monitored at 866 nm (24, 34, 44, 58, 80-85). The molybdenum blue method is suitable for samples from 0.2 to 2 ppm arsenic (86).

c. Atomic spectroscopy There are two problems encountered in the determination of arsenic by atomic absorption spectroscopy. The first problem concerns the poor stability of the hollow cathode lamp. The second problem is created by the fact that the most sensitive resonance lines of arsenic exist in the vacuum ultraviolet region of the electromagnetic spectrum. Unfortunately, the common air-acetylene flame absorbs strongly in the vacuum ultraviolet region as well. With a hollow cathode lamp and an air-acetylene flame, a commonly attained detection limit is 1 ppm (87). An extensive list of interferences has been reported including Mg(II), Al(III), Ca(II), Fe(III), Co(II) and Ni(II). The use of a nitrogen shielded nitrous oxide-acetylene flame eliminates these interferences (88, 89). The use of an electrodeless discharge

tube has been recommended in place of the hollow cathode lamp (87, 90). Nonflame atomic absorption techniques are also available. Detection limits of 0.01 ppm have been reported using a carbon rod atomizer (22). When a graphite furnace is used as an atomizer, 0.5 ppb arsenic can be detected (28, 91).

Emission spectroscopic methods have also been applied. Flame emission techniques are generally not sensitive enough because of the inadequate excitation energies produced by the flame. However, plasma discharge sources have proven to be very efficient excitation sources for observing arsenic emissions. Detection limits as low as 0.1 ppb have been obtained using RF plasma sources while monitoring the 228.8 nm arsenic line (92, 93). By interfacing an arsine generator to a helium dc discharge, arsenic content down to 0.01 ppb can be determined (61).

d. Neutron activation analysis With the advent of high resolution solid state detectors, neutron activation analysis has become a more attractive technique for arsenic determinations. In most environmental samples, however, the detection limit is only a few ppm because of the high activity of the ^{24}Na present. Since the gamma activity in these samples has to decay for several days before measurement, the sensitivity to arsenic is greatly reduced. In samples where the gamma activity of ^{24}Na is

not a problem, the induced gamma activity of ^{76}As is measured by monitoring the photopeak at 559 KeV. This peak generally appears as the middle peak in a triplet composed of ^{82}Br ($t_{1/2} = 35.3$ hours), ^{76}As ($t_{1/2} = 26.5$ hours) and ^{122}Sb ($t_{1/2} = 67.2$ hours). The counting must be done as soon as possible after irradiation because ^{76}As has the shortest half-life in the triplet. Using a neutron flux of 10^{-12} neutrons $\text{cm}^{-2} \text{sec}^{-1}$, sub-ppm arsenic levels can be measured. Elemental separations are generally needed prior to analysis (94-97).

e. X-ray fluorescence Arsenic has been determined in complex matrices such as rocks, soils, river and sea sediments, air filters and water samples by X-ray fluorescence (98-100). Detection down to 50 ppb is possible for water samples (23).

f. Gas chromatography If arsenic compounds are transformed to volatile derivatives, detection by gas chromatography is possible. Total arsenic content can be determined by the separation of arsenic trichloride (101, 102), arsenic trifluoride (103) or the trimethylsilyl derivatives (104). Arsenic can also be determined by gas chromatography following conversion of the arsenic species to triphenyl arsine (105, 106). Speciation of organo-arsenic compounds is possible after formation of the corresponding arsines (107, 108, 109). Flame ionization

detectors, microwave emission detectors, mass spectrometers and nitrous oxide-acetylene flame spectrometric detectors have been used (22). The microwave emission detector has a detection limit of approximately 30 pg (110).

2. Electroanalytical techniques

a. Potentiometric titrations Accurate potentiometric titrations can be performed using ceric sulfate as the titrant. The titration is normally carried out in 0.1 M H_2SO_4 or 0.2 M HCl using KIO_3 and KI as catalysts (111). Indirect methods using ion-selective electrodes are also available. One such method involves the addition of an excess amount of AgNO_3 . If the solution is neutral, silver arsenate precipitates quantitatively. A silver ion-selective electrode is utilized to determine the amount of unreacted silver ions (112). The detection limit is reported to be 7 ppm. Another indirect method involves the precipitation of As(V) with lanthanum nitrate at pH of 8.65. The excess lanthanum is titrated with a standard solution of fluoride using a fluoride ion-selective electrode to locate the end-point. Concentrations down to 0.75 ppm have been measured (113).

b. Amperometric titrations Various amperometric titrations have been developed to determine arsenic. The following titrants have been used for the oxidation of

As(III) to As(V): BrO_3^- (114-116), Ce(IV) (117), MnO_4^- (118), I_2 (119, 120), Br_2 (121) and $\text{Cr}_2\text{O}_7^{=}$ (122). Generally, a Pt microelectrode serves as the indicator electrode and a saturated calomel electrode serves as the reference electrode. Biamperometric detection is possible also using two Pt electrodes (121, 123) or a Pt electrode in combination with a graphite electrode (124). A detection range of 0.02 to 100 mg is typical (23). The technique is not useful for trace levels of arsenic.

c. Coulometric titrations Coulometric titrations can be conducted with a high degree of precision. One of the most popular methods for determining arsenic is the coulometric generation of iodine on Pt electrodes with the subsequent titration of As(III). A neutral or slightly basic medium is required. Both visual and amperometric end-point detection have been implemented (125, 126). Nonaqueous solvents such as methanol, ethanol, acetonitrile and isopropanol have been used to determine trivalent arsenic in the presence of Sn(II) and Sb(III) (123, 127, 128). Electrogenerated bromine at Pt (119, 121) or vitreous carbon (129) has also been used to coulometrically titrate the As(III).

d. Polarography A vast amount of literature has been written about the dc polarographic determination of arsenic at the dropping mercury electrode. Excellent

reviews are available (130, 131). The pentavalent arsenic compounds do not exhibit polarographic behavior in alkaline, neutral or moderately acidic media. A distinctive wave corresponding to the reduction of As(V) to As(III) is observed in 11.5 M HCl, however. The reduction wave disappears entirely if the concentration of the HCl is less than 9 M (132). Pentavalent arsenic also shows polarographic activity if it is allowed to complex with pyrogallol in 1.0 to 3.0 M HClO₄ (133). A reduction wave for As(III) is observed in acidic, neutral and basic media. In alkaline solutions, the pH should be less than 13 in order to reduce As(III) (134-136). Reduction of As(III) to arsenic metal in an acidic environment is a complicated phenomenon. The size and shape of the various reduction waves obtained are functions of the acid concentration (130). Maxima suppressors such as gelatin (137) or methylene blue (56, 138) must be added to the sample to obtain any useful analytical data. Detection of less than 1×10^{-4} M arsenic is difficult (139, 140). Better results are often obtained using an organic acid as the supporting electrolyte. Lactic acid (141), citric acid (142-144), ascorbic acid (145, 31), oxalic acid (146) and acetic acid (147) are examples of supporting electrolytes that have been used. A detection limit of 0.1 ppm is not unusual when an organic acid is the supporting electrolyte.

In an alkaline medium, As(III) can be oxidized to As(V) by dc polarography. The detection limit is about 1×10^{-4} M arsenic (148, 149).

In addition to the determination of arsenic by dc polarography, differential pulse polarography (150-152, 37) and normal pulse polarography have been applied (32, 153, 153). The detection limits are 0.01 ppm for differential pulse (152) and 0.03 ppm for normal pulse (154).

e. Anodic stripping voltammetry Applying the technique of anodic stripping voltammetry, trace levels of arsenic can be determined. Gold (30, 155, 156), platinum (157, 158), mercury (159-161) and graphite (162, 163) electrode surfaces have been utilized as working electrodes. The As(III) in the sample is first deposited as arsenic metal onto the electrode surface. After a sufficiently large quantity of arsenic metal has accumulated, the potential applied to the electrode is scanned in a positive direction. When the potential becomes large enough to oxidize the deposited arsenic metal to As(V), a stripping peak results. The size of the stripping peak is proportional to the concentration of arsenic in the sample. Under optimum conditions, the detection limit is 0.3 ppb (30). However, inter-metallic compounds often form between arsenic and other metal species present in the sample. These inter-metallic compounds interfere with the anodic stripping process.

III. CHOICE OF ELECTRODE MATERIAL FOR THE DETERMINATION OF ARSENIC

A. Introduction

When an electroanalytical method is being developed, the first decision to be made regards the material used to fabricate the working electrode. Various electrode materials are available to the researcher including platinum, gold, mercury and glassy carbon. In order to evaluate which electrode material would be the best for the electroanalytical determination of arsenic, cyclic voltammetry was used. Cyclic voltammetry is a technique commonly used to study electrochemical processes.

The working electrode used to obtain a cyclic voltammogram can take on a variety of shapes. But, because the hydrodynamic theory has been worked out most successfully for a disk shaped electrode, the disk electrode is very commonly utilized. The disk is attached to the end of a stainless steel or brass shaft. An inert shroud of Teflon covers the shaft and the sides of the disk. Consequently, only the end surface of the disk is exposed. The shaft is connected to a motor and is rotated about an axis perpendicular to the disk. The disk is placed in the test solution. As the disk rotates in the solution, the potential applied to the disk is varied in a cyclic manner.

By varying the rotation speed, the potential scan rate and the potential limits, a great deal of mechanistic information about the electrochemical reaction can be obtained. This chapter describes the cyclic voltammetry of arsenic at both platinum and gold surfaces. Experimental data illustrate why platinum is the preferred electrode material for the electroanalytical determination of As(III).

B. Experimental

1. Instrumentation and apparatus

The three electrode potentiostat used is described in reference 164. The radius of the platinum disk was 3.77 mm while the radius of the gold disk was 3.72 mm. The disk electrodes and the rotator were obtained from the Pine Instrument Co. in Grove City, PA. The cyclic voltammograms was recorded with a Plotamatic Model 815 X-Y recorder from Bolt, Beranek and Newman, Inc., of Santa Anna, CA. The electrode potential was measured with a Model 345 digital voltmeter from Data Technology Corp. of Santa Anna, CA.

The electrolysis cell was constructed from pyrex with a capacity of approximately 500 ml. The chamber containing the Pt counter electrode was separated from the test solution by a fritted glass disk. The counter electrode chamber was filled with the supporting electrolyte. The reference electrode, a commercial SCE filled with saturated

NaCl in place of saturated KCl, was placed in a chamber connected to the test solution through a Luggin capillary. The capillary and the reference electrode chamber were filled with the supporting electrolyte. The Luggin capillary tip was placed as close as possible to the surface of the working electrode.

The electrode surfaces were polished according to standard metallographic procedures. The final polishing step was accomplished using 0.3 μm alumina on a Buehler Microcloth with water as the lubricant.

2. Reagents

All the chemicals used to conduct the experiments were Analytical Reagent Grade. The supporting electrolytes, 0.5 M HClO_4 and 1.0 M HClO_4 , were prepared from reagent grade perchloric acid obtained from the G. Frederick Smith Chemical Co. of Columbus, OH. All the water was triply distilled. Demineralization occurred after the first distillation. The second distillation was from an alkaline permanganate solution.

The stock solutions of As(III) and As(V) were prepared in volumetric flasks by dissolving the corresponding arsenic oxides in a minimum amount of 5 M NaOH. Triply distilled water was used as the diluent. The solutions were prepared fresh weekly.

3. Procedure

The electrode was pretreated prior to each experiment by polishing with 0.3 μm alumina. The electrode was then thoroughly rinsed with water. The test solutions were deaerated with prepurified N_2 . The potential applied to the disk was scanned between the prescribed limits until reproducible current-potential curves were procured.

C. Cyclic Voltammetry of Arsenic at a Gold Disk

Figure III-1 portrays the cyclic voltammograms obtained using a gold disk in the 1.0 M HClO_4 supporting electrolyte alone, and after aliquots of As(III) were added to the supporting electrolyte. The current-potential (I-E) curve for the supporting electrolyte will be explained first followed by the explanation of the I-E curve obtained with the As(III) present in the solution.

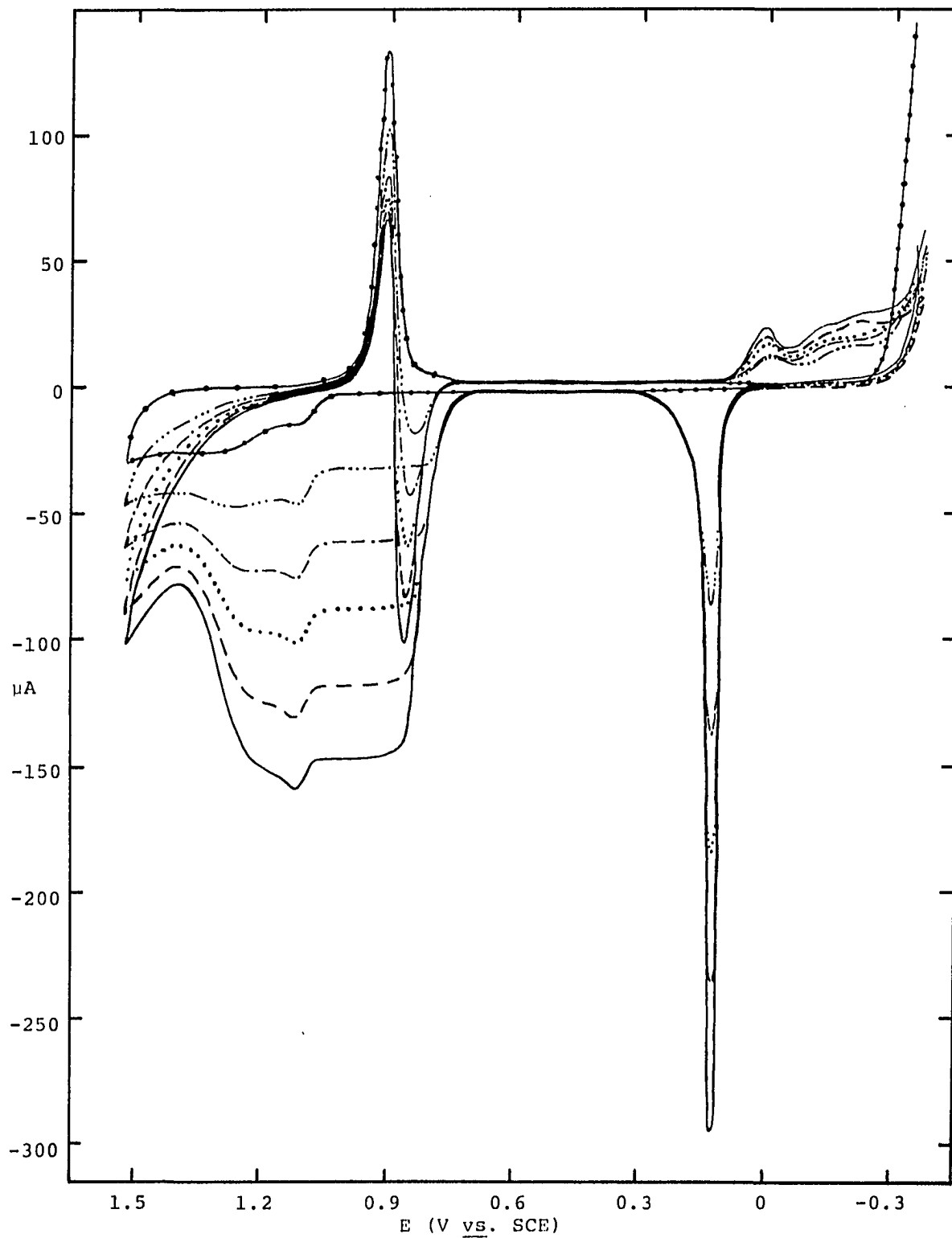
When the cyclic voltammetry for the HClO_4 is recorded starting at 0.0 V vs. SCE and the potential is scanned in a positive direction, virtually no current flows until the potential reaches about 1.1 V vs. SCE. Beyond 1.1 V vs. SCE, the gold metal surface becomes oxidized. The surface is oxidized with the concomitant flow of anodic current. The gold oxide continues to form as the potential is increased. At 1.5 V vs. SCE, the potential applied to the electrode is high enough to cause the oxidation of the

Figure III-1. Cyclic voltammograms of As(III) in 1.0 M
HClO₄ at a Au disk

Rotation speed - 3600 rev min⁻¹

Potential scan rate - 1 V min⁻¹

—•—•— 1.0 M HClO₄
—••• 1.44 x 10⁻⁵ M As₂O₃
1.0 M HClO₄
- - • 2.88 x 10⁻⁵ M As₂O₃
1.0 M HClO₄
••••• 4.32 x 10⁻⁵ M As₂O₃
1.0 M HClO₄
- - - 5.76 x 10⁻⁵ M As₂O₃
1.0 M HClO₄
———— 7.20 x 10⁻⁵ M As₂O₃
1.0 M HClO₄



water present in the test solution to oxygen gas. The current would go completely off-scale if the potential was increased further. Instead, the direction of the potential scan is reversed. The current rapidly drops to zero and stays at zero because, as the applied potential decreases, the driving force necessary for continued formation of gold oxide no longer exists. At 0.9 V vs. SCE, the potential is no longer positive enough to sustain an oxide film on the gold surface. The peak at 0.9 V vs. SCE corresponds to the reduction of the gold oxide to gold metal. Once the oxide has been removed, no current flows until the potential is approximately -0.2 V vs. SCE. Below -0.2 V vs. SCE, the water in the test solution undergoes reduction to hydrogen gas. Again, rather than allowing the current to shoot off-scale, the direction of the potential scan is reversed (165, 166).

The cyclic voltammogram obtained after As(III) is added to the solution exhibits an oxidation plateau beginning at 0.8 V vs. SCE. This plateau corresponds to the oxidation of As(III) to As(V). As the potential is scanned in the positive direction, the region where gold oxide formation occurs is reached. The current due to the gold oxide formation initially adds to the current plateau resulting from the oxidation of As(III) to As(V). But, as the gold oxide continues to form, the oxidation

process for As(III) is inhibited. Consequently, the current decreases as the potential increases. At 1.5 V vs. SCE, some of the water in the sample is oxidized to oxygen gas. When the direction of the potential scan is reversed, the current decays to zero because the presence of a heavy gold oxide film on the electrode surface prevents the further oxidation of As(III). At 0.9 V vs. SCE, the gold oxide is reduced to gold metal. Once the gold oxide has been removed from the electrode surface, the oxidation process for As(III) is resumed. An anodic peak results from this oxidation process until the potential of the disk becomes too low to perpetuate the reaction. No more current flows until the potential drops to 0.1 V vs. SCE. Below 0.1 V vs. SCE, arsenic metal plates out on the gold electrode. If the potential becomes negative enough, As(III) can be reduced to arsine. When the direction of the potential scan is reversed, a stripping peak due to the oxidation of the deposited arsenic metal to As(III) is produced (30, 155, 156).

The limiting current for the oxidation process of As(III) to As(V) at a rotating disk electrode is given by Equation III-1 (167).

$$I_{\ell} = \frac{-nFAD_{\text{red}}C_{\text{red}}^b}{1.61 D_{\text{red}}^{1/3} \nu^{1/6} \omega^{-1/2} + \frac{D_{\text{red}}}{k}} \quad (\text{III-1})$$

In Equation III-1:

I_l = limiting current (mA);

n = number of electrons involved in the oxidation process (equivalents mole⁻¹);

F = Faraday's constant (coulombs/equivalent);

A = electrode surface area (cm²);

D_{red} = diffusion coefficient of electroactive species (cm² s⁻¹);

C_{red}^b = concentration of the reduced species in the solution (moles l⁻¹);

ω = rotation speed of electrode (radians s⁻¹);

k = heterogeneous rate constant (cm s⁻¹);

ν = kinematic viscosity of the solution to the electrode (cm² s⁻¹).

According to Equation III-1, a plot of the limiting current vs. the concentration of As(III) in the solution should be linear. Experimentally, this is the case as illustrated by Figure III-2 and Table III-1. The data were obtained from Figure III-1. The data were corrected for the residual current because Equation III-1 applies only to faradaic processes. For the case at hand, Equation III-1 describes only the current produced from the oxidation of As(III) to As(V). Before a large amount of gold oxide forms, the heterogeneous rate constant is fairly large and the second term in the denominator of Equation III-1 is negligible

Figure III-2. Limiting current produced at Au disk during positive potential scan for various concentrations of As(III) in 1.0 M HClO₄

Rotation speed - 3600 rev min⁻¹

Potential scan rate - 1 V min⁻¹

■ 0.90 V vs. SCE

● 1.20 V vs. SCE

○ 1.30 V vs. SCE

□ 1.50 V vs. SCE

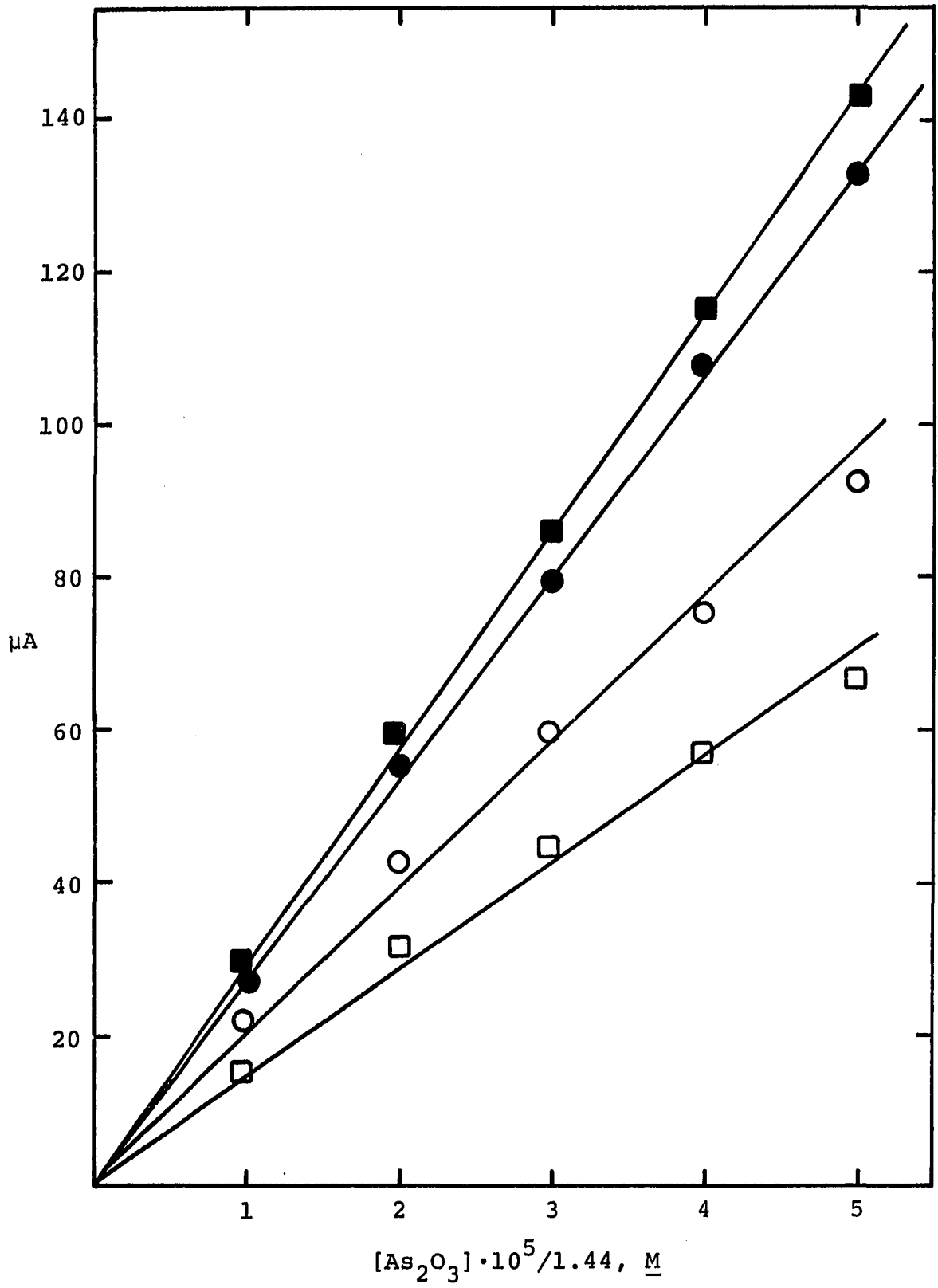


Table III-1. Limiting current produced at Au disk for various concentrations of As(III) in 1.0 M HClO₄

| $C_{As_2O_3}^b$ (M) | V <u>vs.</u> SCE | I_{ℓ} (μ A) |
|-----------------------|------------------|-----------------------|
| 1.44×10^{-5} | 0.90 | 29.0 |
| | 1.20 | 27.5 |
| | 1.30 | 21.5 |
| | 1.50 | 15.0 |
| 2.88×10^{-5} | 0.90 | 58.5 |
| | 1.20 | 55.0 |
| | 1.30 | 42.5 |
| | 1.50 | 31.5 |
| 4.32×10^{-5} | 0.90 | 85.5 |
| | 1.20 | 79.5 |
| | 1.30 | 59.5 |
| | 1.50 | 44.0 |
| 5.76×10^{-5} | 0.90 | 115.0 |
| | 1.20 | 107.5 |
| | 1.30 | 75.5 |
| | 1.50 | 56.5 |
| 7.20×10^{-5} | 0.90 | 143.0 |
| | 1.20 | 133.0 |
| | 1.30 | 92.5 |
| | 1.50 | 66.5 |

when compared to the first term. The oxidation of As(III) is mass transport limited. Once the gold oxide forms, the value of k decreases substantially and the second term in the denominator of Equation III-1 becomes significantly larger. The anodic current is no longer limited by the mass transport process. The slope of the line correlating the limiting current and the concentration of As(III) decreases substantially. For example, the slope at 1.50 V vs. SCE is quite a bit smaller than at 1.20 V vs. SCE. Therefore, for the determination of arsenic in a sample, a

larger change in the current for a given change in the concentration of As(III) in the sample results if the applied potential is less than 1.20 V vs. SCE.

Figure III-3 and Table III-2 illustrate the dependence of the limiting current on the rotation speed. The

Table III-2. Dependence of limiting current on rotation speed of Au disk for As(III) in 1.0 M HClO₄

| $W^{1/2} \left(\frac{\text{rev}}{\text{min}}\right)^{1/2}$ | V <u>vs.</u> SCE | I_l (μA) |
|--|------------------|-------------------------|
| 20 | 0.90 | 47.0 |
| | 1.20 | 46.5 |
| | 1.30 | 47.0 |
| 30 | 0.90 | 71.5 |
| | 1.20 | 70.0 |
| | 1.30 | 70.0 |
| 40 | 0.90 | 97.0 |
| | 1.20 | 93.5 |
| | 1.30 | 89.0 |
| 50 | 0.90 | 123.0 |
| | 1.20 | 117.5 |
| | 1.30 | 105.0 |
| 60 | 0.90 | 149.0 |
| | 1.20 | 140.0 |
| | 1.30 | 115.0 |
| 70 | 0.90 | 173.0 |
| | 1.20 | 160.0 |
| | 1.30 | 125.0 |

rotation speed, W , is given in units of revolutions min^{-1} ($\omega = 2\pi W/60$). The data correlate well with Equation III-1. If the reaction is controlled by the rate of mass transport, a linear relationship between the limiting current and the square root of the rotation speed exists. Prior to the formation of a heavy gold oxide film on the electrode

Figure III-3. Dependence of limiting current on rotation speed of Au disk during positive potential scan for As(III) in 1.0 M HClO₄

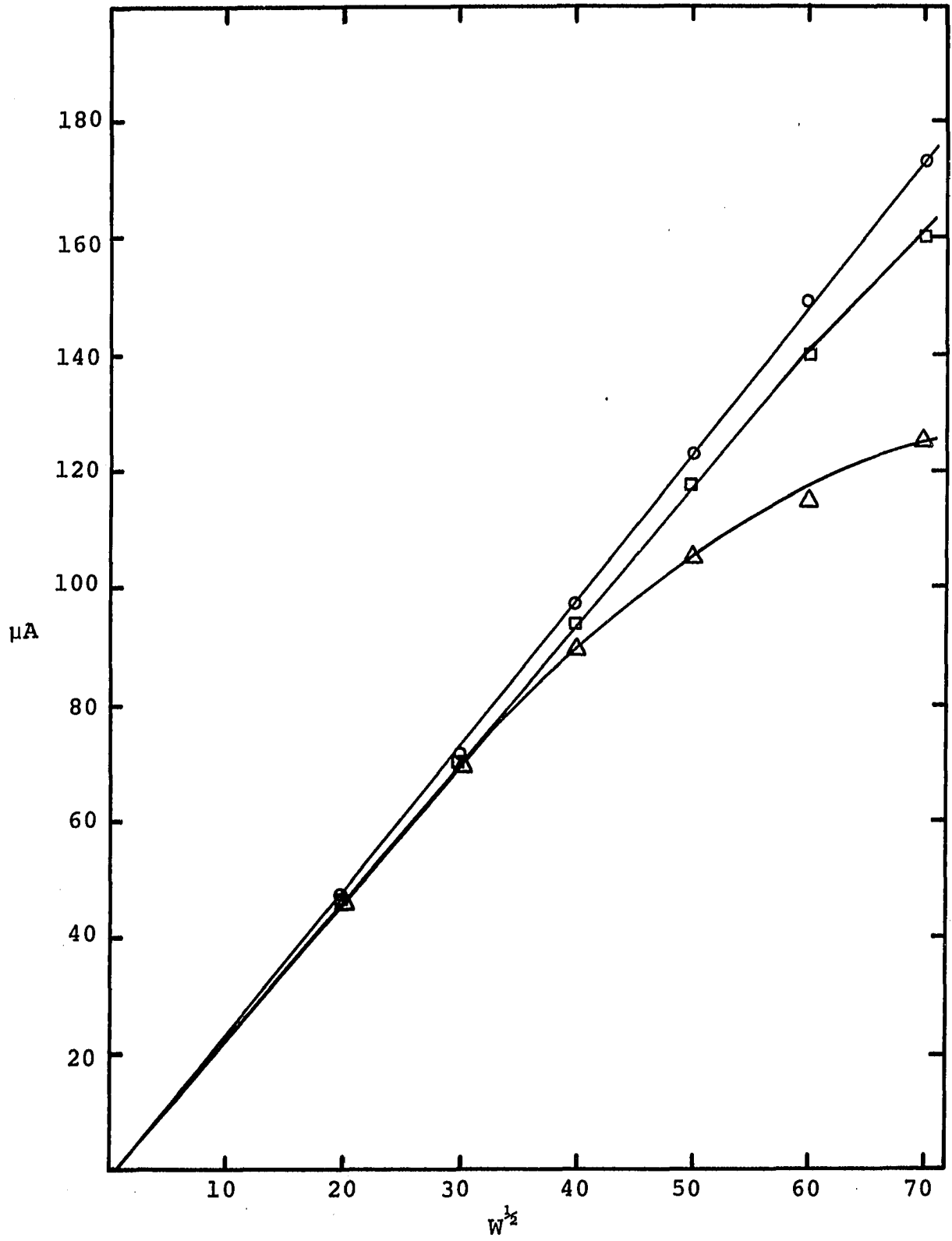
Potential scan rate - 1 V min⁻¹

7.20 x 10⁻⁵ M As₂O₃

○ 0.90 V vs. SCE

□ 1.20 V vs. SCE

△ 1.30 V vs. SCE



surface, the oxidation reaction for As(III) going to As(V) is limited by the rate of mass transport. At 0.9 V vs. SCE, the $I_{\ell} - \omega^{1/2}$ plot is linear. However, once the gold oxide forms, the charge transfer step becomes slower. This results in a decreased dependence on the rotation speed. At 1.3 V vs. SCE, the $I_{\ell} - \omega^{1/2}$ plot deviates from linearity. When $\omega^{1/2}$ is 70 $\text{rev}^{1/2} \text{min}^{-1/2}$, the limiting current changes 28% between 0.90 V vs. SCE and 1.30 V vs. SCE. The denominator of Equation III-1 changed 357% to cause this current change. Therefore, the value of D/k at 1.30 V vs. SCE is about 3.6 times the value of $1.61D_{\text{red}}^{1/3} \nu^{1/6} \omega^{-1/2}$.

The effect of halides on the electrochemistry of As(III) in perchloric acid was investigated. A survey of the literature reveals that halide ions can often exhibit either catalytic or inhibitory effects on the electro-analytical determination of metal species (168-172). The cyclic voltammograms recorded before and after the addition of Cl^- to a solution of As(III) are shown in Figure III-4. If a small amount of chloride is present, the electrochemistry of As(III) at the Au disk is drastically altered. The presence of less than 0.06 ppm NaCl in the solution results primarily in a shift of the $E_{1/2}$ value for the oxidation of As(III). However, by the time the chloride concentration is 0.12 ppm, the oxidation of As(III) can no longer occur. The cyclic voltammogram appears to be very

Figure III-4. Effect of Cl^- on the cyclic voltammetry of As(III) in 1.0 M HClO_4 at a Au disk

Rotation speed - 3600 rev min^{-1}

Potential scan rate - 1 V min^{-1}

..... 3.7×10^{-5} M As_2O_3

1.0 M HClO_4

---- 0.04 ppm NaCl

3.7×10^{-5} M As_2O_3

1.0 M HClO_4

---- 0.06 ppm NaCl

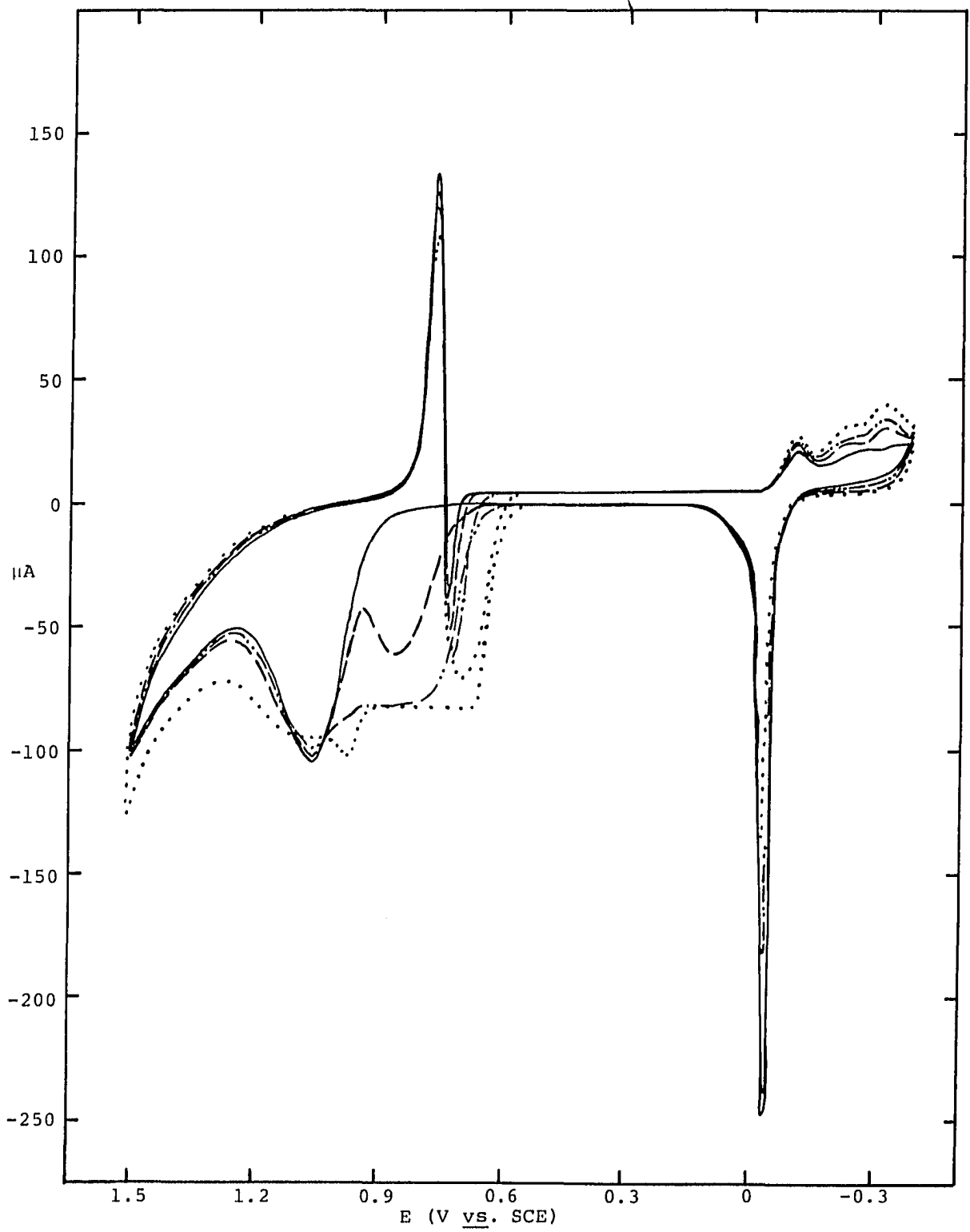
3.7×10^{-5} M As_2O_3

1.0 M HClO_4

—— 0.12 ppm NaCl

3.7×10^{-5} M As_2O_3

1.0 M HClO_4



similar to a cyclic voltammogram obtained at a gold disk for a solution of NaCl in HClO₄. The presence of chloride blocks the oxidation process for As(III). Both NaBr and NaI behave similarly to NaCl. The absorption of halides on the electrode surface apparently prevents the exchange of electrons between the As(III) and the electrode. Realistically, most "real" samples will contain halide ions. A gold electrode can not be used for such samples because of the inhibitory effect of the halides on the electroanalytical determination of As(III).

D. Cyclic Voltammetry of Arsenic at a Platinum Disk

The cyclic voltammograms for various concentrations of As(III) in perchloric acid as well as the cyclic voltammogram for the supporting electrolyte alone are shown in Figure III-5. The characteristics of the residual current-potential curve will be described first.

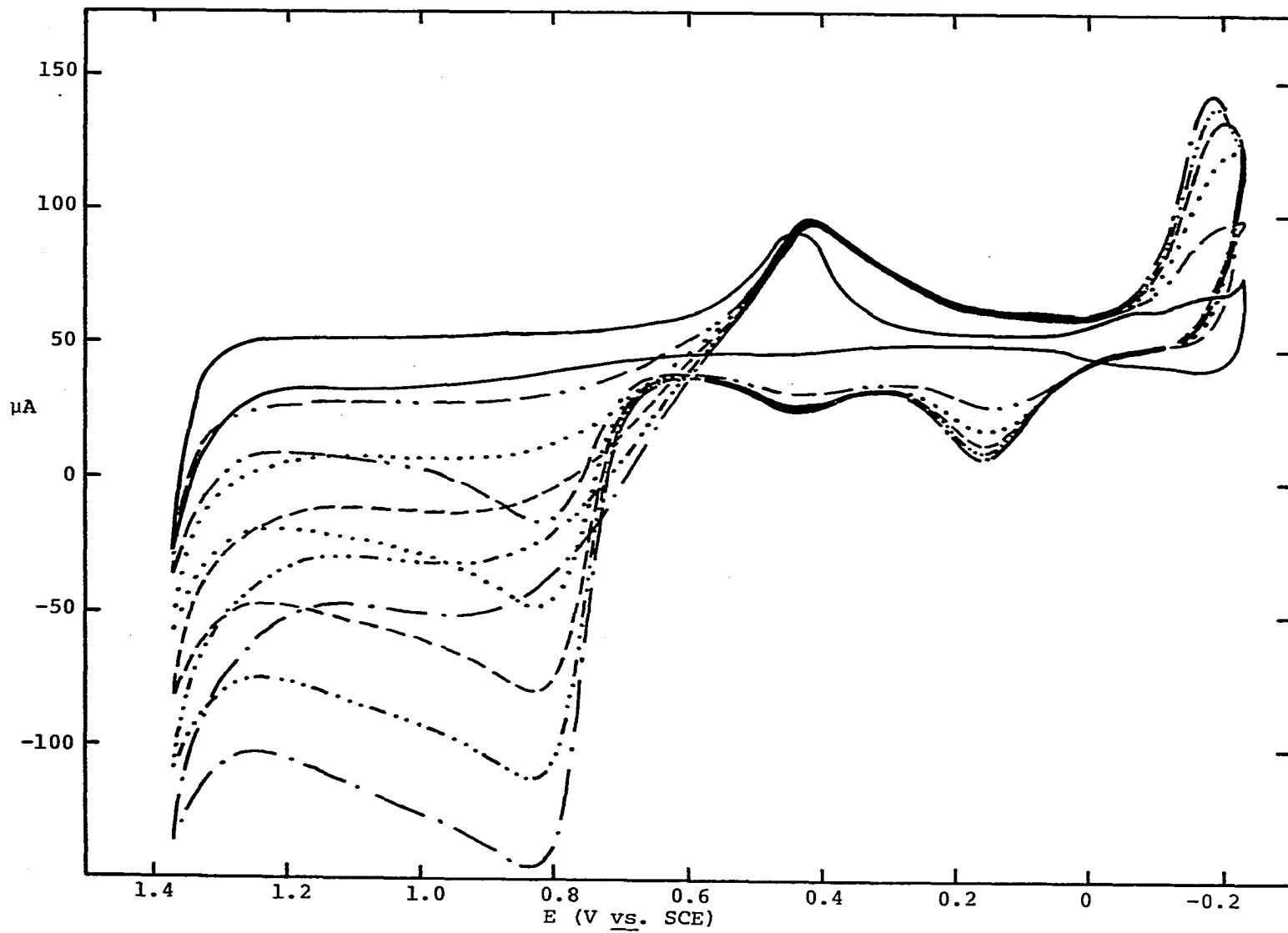
When the potential applied to the platinum disk is scanned in a positive direction starting at 0.1 V vs. SCE, only a negligible amount of current flows until 0.7 V vs. SCE is reached. At 0.7 V vs. SCE, the Pt metal surface undergoes oxidation. The platinum oxide continues to form as the potential increases. The oxide growth is accompanied by a flow of current. At approximately 1.4 V vs. SCE, the potential is positive enough to oxidize some

Figure III-5. Cyclic voltammograms of As(III) in 0.5 M HClO₄ at a Pt disk

Rotation speed - 3600 rev min⁻¹

Potential scan rate - 1 V min⁻¹

———— 0.5 M HClO₄
----- 1.44 x 10⁻⁵ M As₂O₃
 0.5 M HClO₄
..... 2.88 x 10⁻⁵ M As₂O₃
 0.5 M HClO₄
- - - 4.32 x 10⁻⁵ M As₂O₃
 0.5 M HClO₄
-...- 5.76 x 10⁻⁵ M As₂O₃
 0.5 M HClO₄
-...- 7.20 x 10⁻⁵ M As₂O₃
 0.5 M HClO₄



of the water in the solution to oxygen gas. When the direction of the potential scan is reversed, the current rapidly decays to a low level because the driving force for the continued formation of the oxide is diminished as the applied potential decreases. Consequently, no current due to the formation of the oxide is observed. When the potential reaches 0.6 V vs. SCE, the potential is no longer positive enough to sustain an oxide film on the Pt surface. The platinum oxide is reduced to Pt metal. Once the platinum oxide has been removed, virtually no current flows until negative potentials are applied to the disk. At potentials more negative than 0.0 V vs. SCE, the water in the sample is reduced to hydrogen gas. The Pt metal adsorbs the generated hydrogen gas and when the direction of the scan is reversed, the adsorbed hydrogen is oxidized either to hydrogen ions or water (165, 166).

Once As(III) is added to the solution, a very complex looking cyclic voltammogram is recorded. At 0.7 V vs. SCE, As(III) is oxidized to As(V). As the thickness of the oxide film increases, however, the oxidation current for the As(III) decreases. When the applied potential reaches 1.4 V vs. SCE, the water in the sample becomes oxidized. Unlike at the gold disk, the current at the platinum disk does not decay to zero on the reverse scan. The presence of an oxide film on the Pt surface doesn't totally block

the oxidation of As(III). Rather, a limiting plateau results. At 0.6 V vs. SCE, the platinum oxide is reduced to Pt metal. A shoulder appears off the platinum oxide reduction peak. The shoulder is attributed to the reduction of adsorbed As(V) which is produced during the oxidation of As(III). Below 0.0 V vs. SCE, arsenic metal plates out on the Pt surface. When the potential is reversed, stripping peaks appear at 0.15 V vs. SCE and at 0.35 V vs. SCE. The peak at 0.35 V vs. SCE is independent of the As(III) concentration and represents the stripping peak for the first monolayer of arsenic deposited on the Pt metal. The peak at 0.15 V vs. SCE varies with the concentration of the As(III) in the solution and is attributed to the stripping of the bulk arsenic metal (157, 158).

Variation of the negative potential limit (Figure III-6), the positive potential limit (Figure III-7), the rotation speed of the electrode (Figure III-8) and the potential scan rate (Figure III-9) helps to elucidate the reactions occurring in the various regions of the cyclic voltammogram. For example, Figure III-6 illustrates that a correlation exists between the current generated at negative potentials during the negative sweep and the anodic peaks obtained at 0.15 V vs. SCE and 0.35 V vs. SCE. In this region of the cyclic voltammogram there is no dependence of electrode current on rotation speed (Figure III-8), but a strong

Figure III-6. Variation of potential limit applied to Pt disk during negative scan for As(III) in 0.5 M HClO₄

Rotation speed - 3600 rev min⁻¹
Potential scan rate - 1 V min⁻¹
5.4 x 10⁻⁵ M As₂O₃

..... -0.23 V vs. SCE
----- -0.20 V vs. SCE
----- -0.10 V vs. SCE
----- -0.00 V vs. SCE
----- 0.10 V vs. SCE
..... 0.20 V vs. SCE
----- 0.30 V vs. SCE
----- 0.40 V vs. SCE

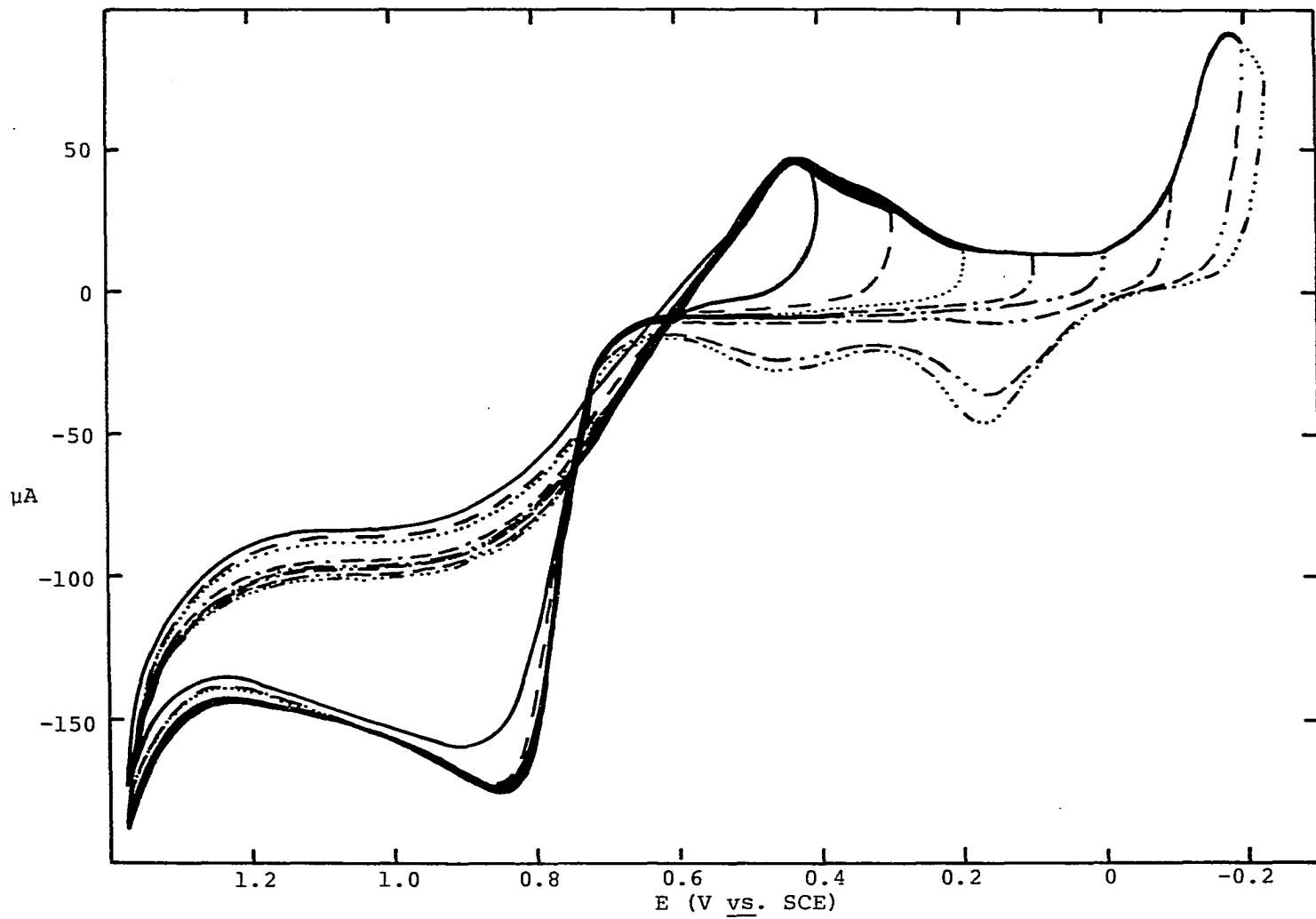


Figure III-7. Variation of potential limit applied to Pt disk during positive

scan for As(III) in 0.5 M HClO₄

Rotation speed - 3600 rev min⁻¹

Potential scan rate - 1 V min⁻¹

1.95 x 10⁻⁵ M As₂O₃

..... 0.70 V vs. SCE
..... 0.80 V vs. SCE
----- 0.90 V vs. SCE
..... 1.00 V vs. SCE
----- 1.10 V vs. SCE
----- 1.20 V vs. SCE
..... 1.30 V vs. SCE
----- 1.40 V vs. SCE

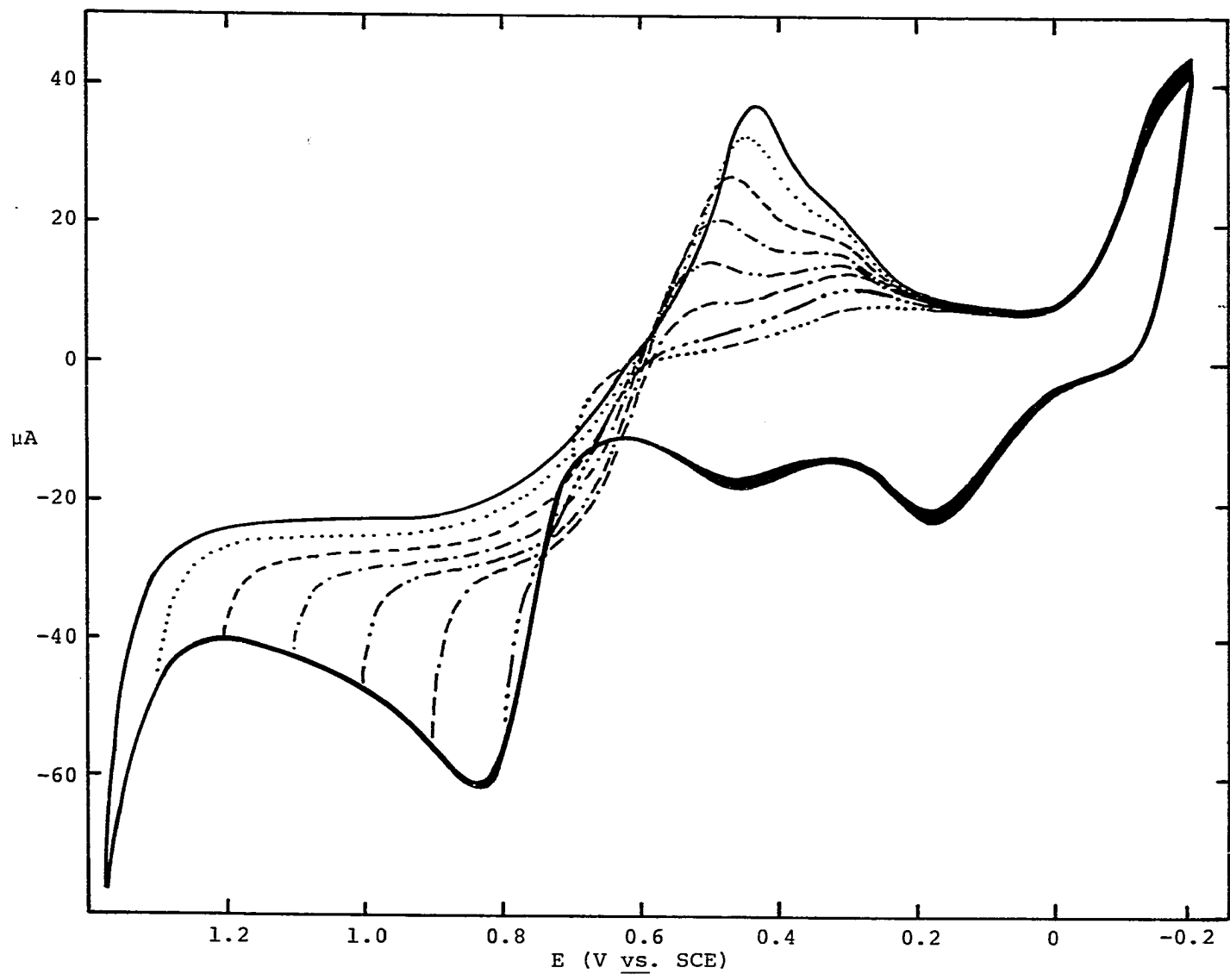


Figure III-8. Variation of rotation speed of Pt disk for As(III) in 0.5 M HClO₄,

Potential scan rate - 1 V min⁻¹
7.17 x 10⁻⁵ M As₂O₃

- 400 rev min⁻¹
- 900 rev min⁻¹
- 1600 rev min⁻¹
- ... 2500 rev min⁻¹
- ... 3600 rev min⁻¹
- 4900 rev min⁻¹

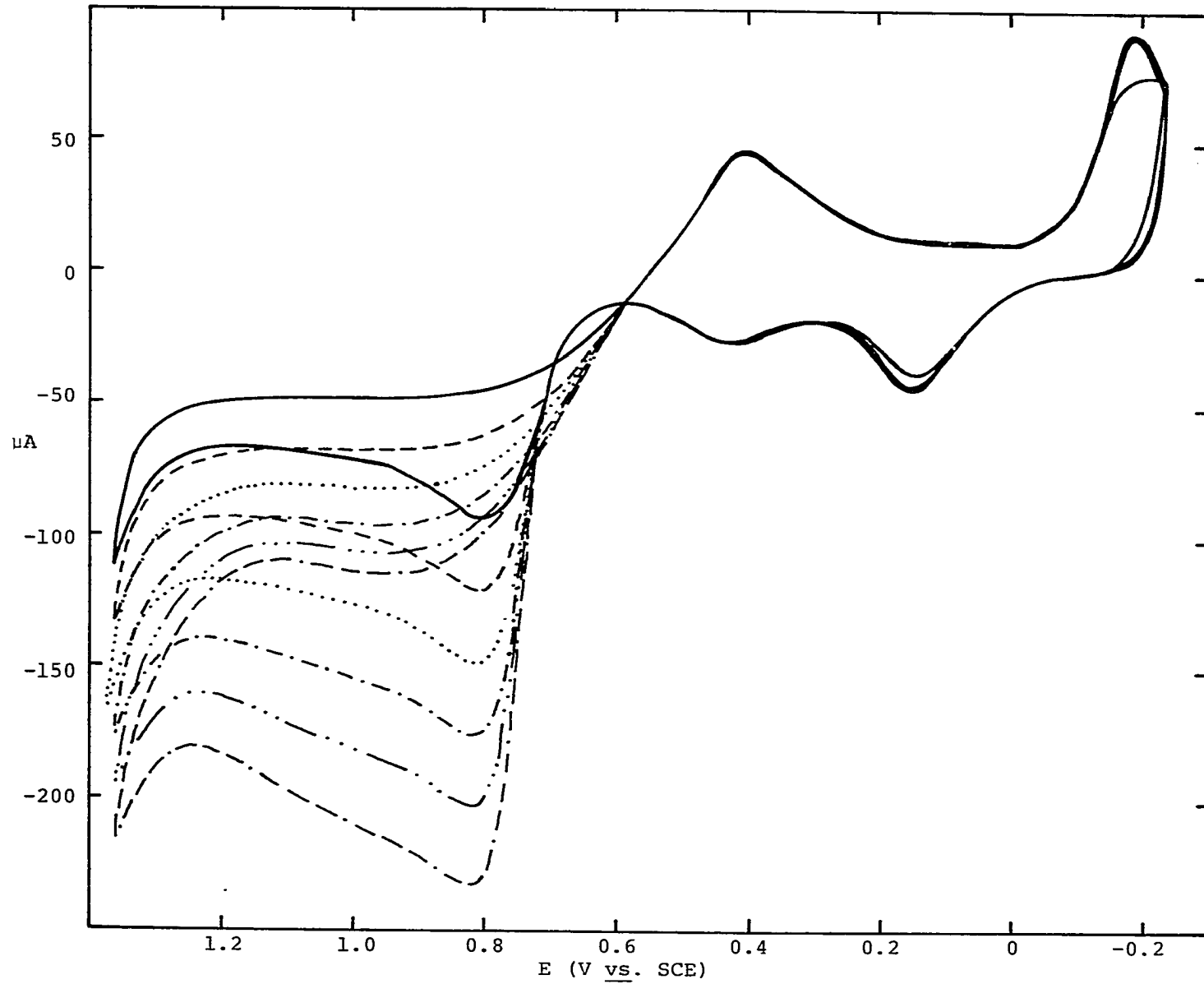
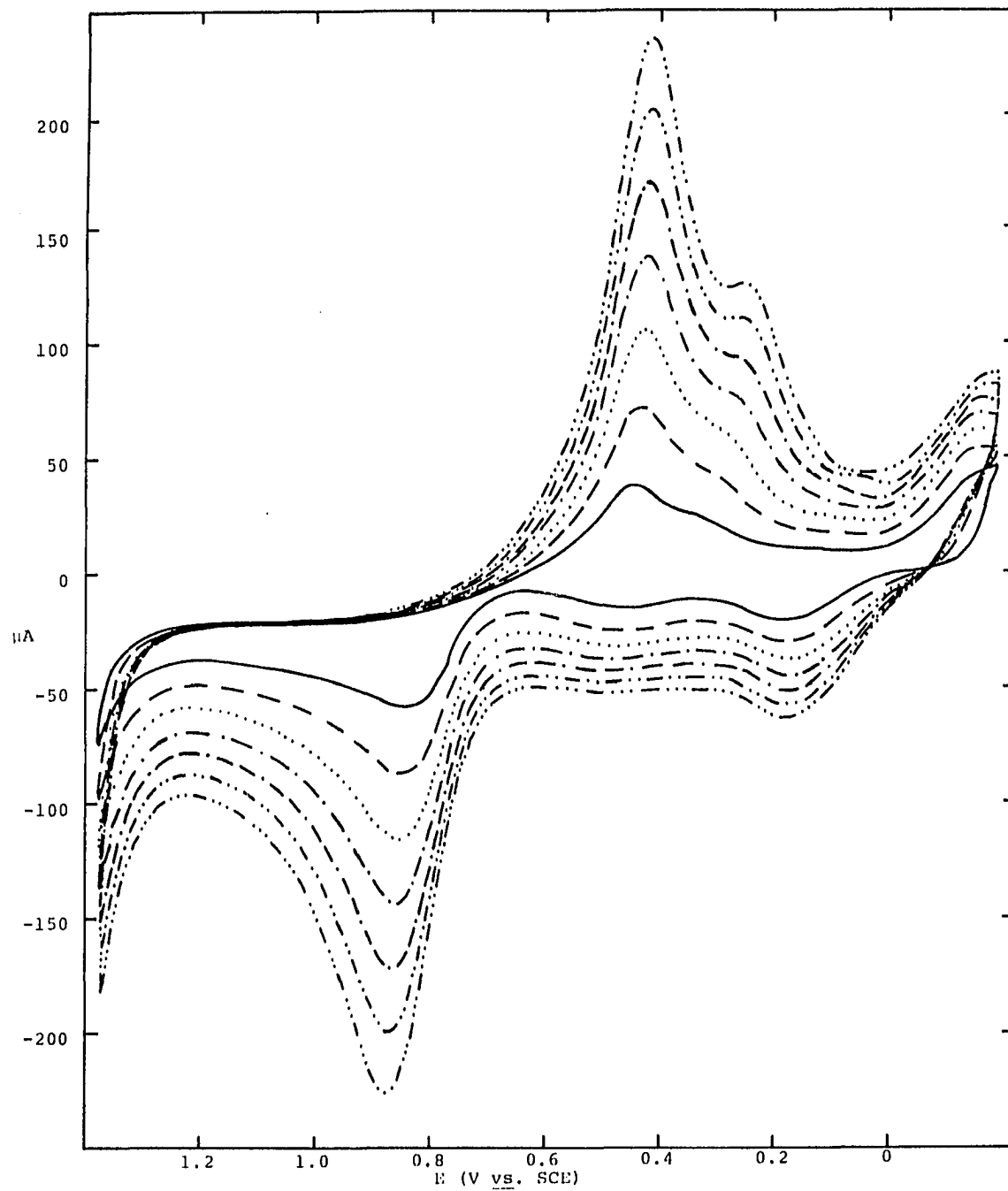


Figure III-9. Variation of potential scan rate of Pt disk
for As(III) in 0.5 M HClO₄

Rotation speed - 3600 rev min⁻¹
1.95 x 10⁻⁵ M As₂O₃

—— 1 V min⁻¹
----- 2 V min⁻¹
..... 3 V min⁻¹
-.-.- 4 V min⁻¹
--- 5 V min⁻¹
... 6 V min⁻¹
....- 7 V min⁻¹



dependence on the potential scan rate exists (Figure III-9). These facts indicate that a surface controlled reaction is involved and can be explained quite readily if arsenic metal is deposited during the negative sweep and stripped during the positive sweep. The size of the stripping peaks is dependent upon the amount of arsenic metal deposited on the platinum surface. The deposition and stripping process is consistent with the fact that the reaction is surface controlled.

The size of the shoulder off the platinum oxide reduction peak is dependent upon the limiting potential for the positive scan as shown in Figure III-7. The current in this region of the cyclic voltammogram is produced by a surface controlled reaction. The current is independent of the rotation speed of the platinum disk (Figure III-8), but is dependent on the potential scan rate (Figure III-9). The data can be readily explained if the shoulder is the result of the reduction of adsorbed As(V). The current produced by the oxidation of an adsorbed species has no dependence on the rotation speed. When the potential limit is shifted in a positive direction, more As(V) forms during the anodic sweep. Subsequently, the size of the reduction peak for the reaction involving As(V) going to As(III) increases as the potential limit increases.

The limiting current produced as a result of the oxidation of As(III) to As(V) is described by Equation III-1. A plot of the limiting current vs. the bulk concentration of As(III) should be linear with a zero intercept. The plot is linear, but the intercept is not zero as shown in Figure III-10 and Table III-3. The data are from Figure III-5.

Table III-3. Limiting current produced at Pt disk for various concentrations of As(III) in 0.5 M HClO_4

| $C_{\text{As}_2\text{O}_3}^b$ (M) | V <u>vs.</u> SCE | $I_{\ell,p}$ (μA) | $I_{\ell,n}$ (μA) |
|-----------------------------------|------------------|--------------------------------|--------------------------------|
| 1.43×10^{-5} | 0.80 | 55.0 | 23.0 |
| | 1.0 | 30.0 | 24.0 |
| 2.86×10^{-5} | 0.80 | 84.5 | 41.5 |
| | 1.0 | 62.5 | 45.0 |
| 4.29×10^{-5} | 0.80 | 115.0 | 58.5 |
| | 1.0 | 94.0 | 65.0 |
| 5.72×10^{-5} | 0.80 | 145.0 | 75.0 |
| | 1.0 | 126.0 | 84.0 |
| 7.15×10^{-5} | 0.80 | 175.0 | 91.0 |
| | 1.0 | 159.0 | 102.5 |

The data used for the limiting current were corrected by subtracting the current obtained when the supporting electrolyte alone was in the solution. Unfortunately, this correction is not satisfactory. Experimental data indicate that the residual current obtained in the absence of As(III) is not identical with the residual current obtained in the presence of As(III). This is shown in Figure III-11. In the absence of As(III), the

Figure III-10. Limiting current produced at Pt disk for various concentrations of As(III) in 0.5 M HClO₄

Rotation speed - 3600 rev min⁻¹

Potential scan rate - 1 V min⁻¹

7.20 x 10⁻⁵ M As₂O₃

- 0.80 V vs. SCE (positive potential scan)
- 1.00 V vs. SCE (positive potential scan)
- △ 1.00 V vs. SCE (negative potential scan)
- ◇ 0.80 V vs. SCE (negative potential scan)

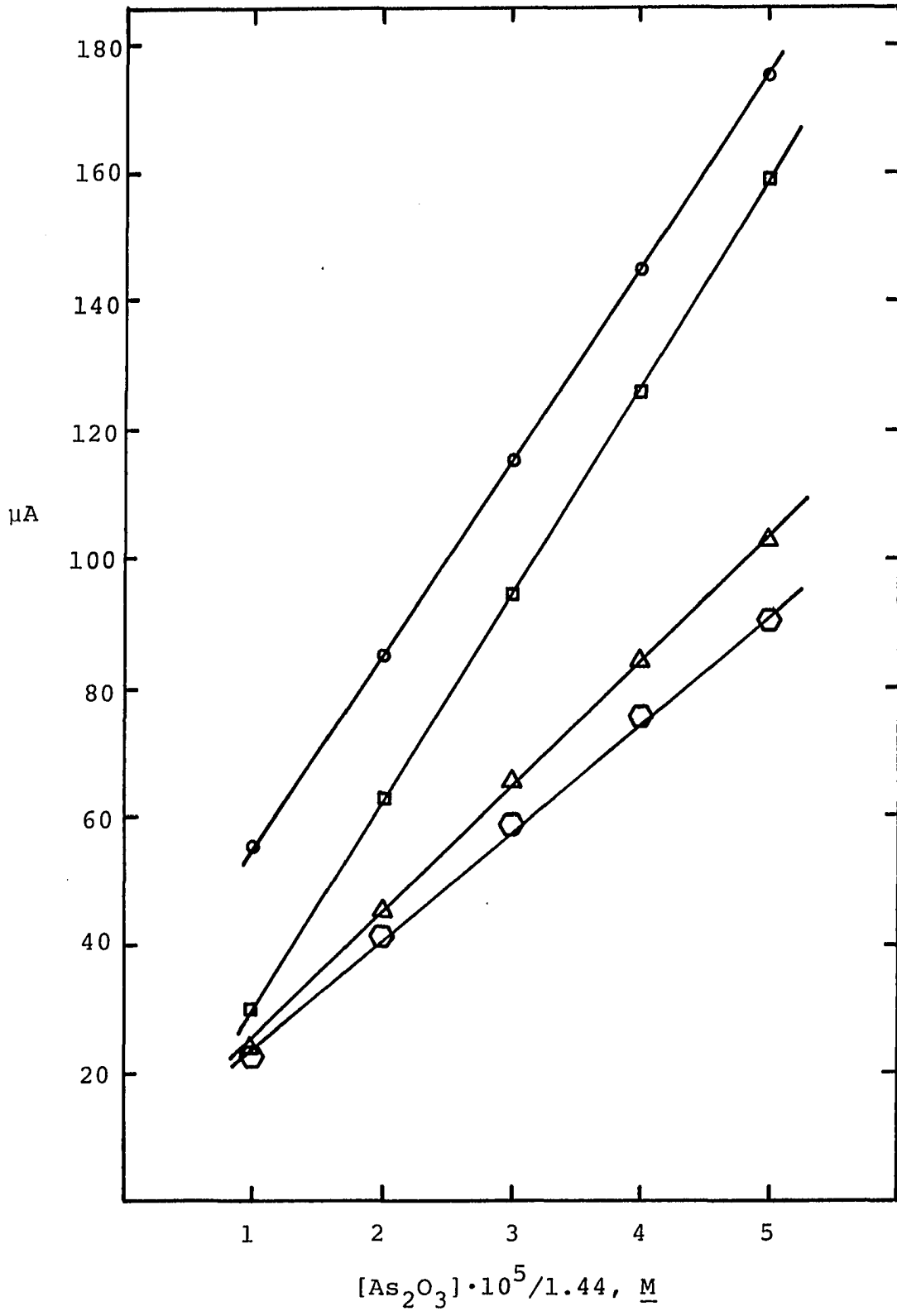
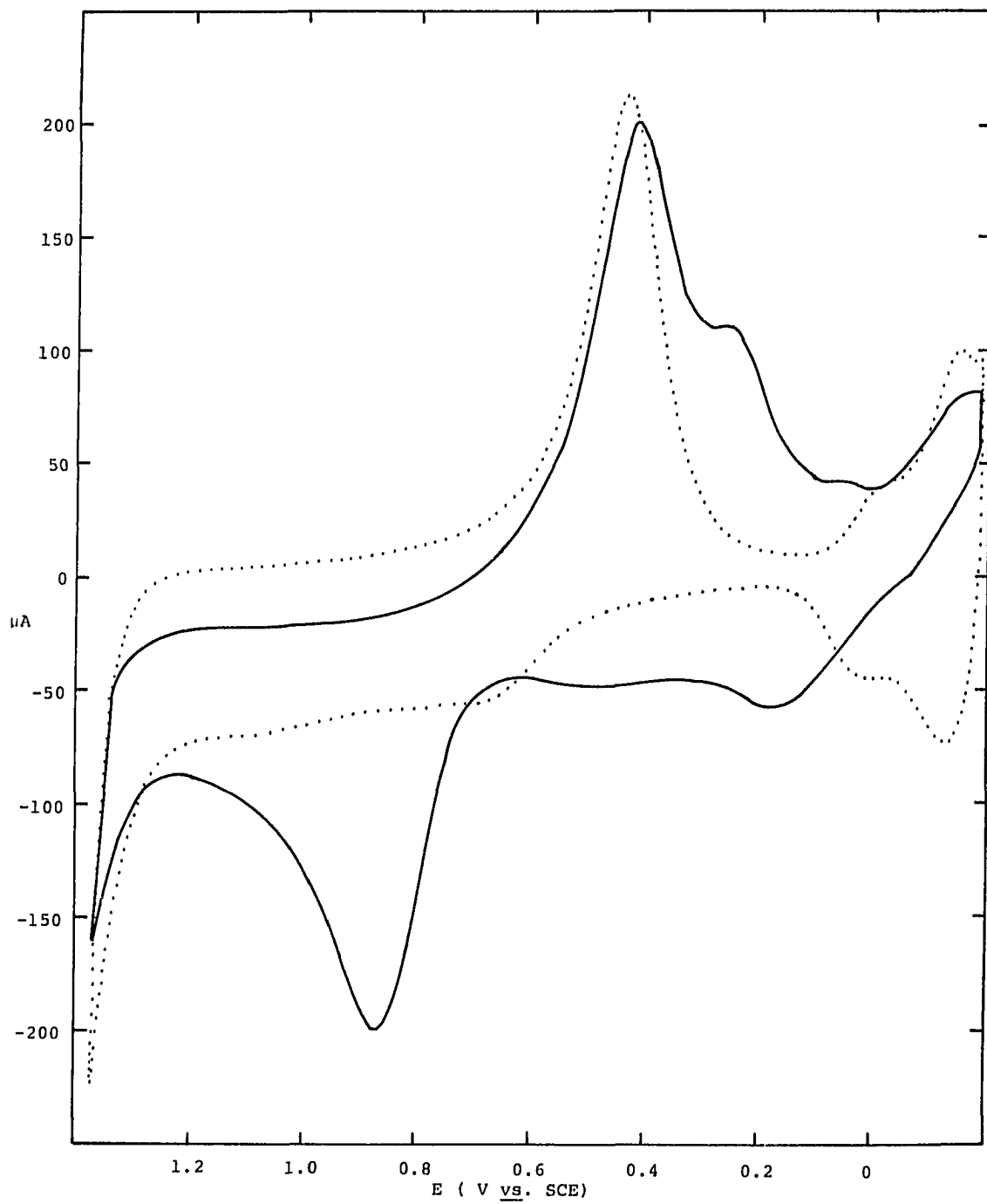


Figure III-11. Change in onset of formation of Pt oxide
in the presence of As(III)

Rotation speed - $3600 \text{ rev min}^{-1}$
Potential scan rate - 6 V min^{-1}

..... 0.5 M HClO_4
——— $1.95 \times 10^{-5} \text{ M As}_2\text{O}_3$
 0.5 M HClO_4



platinum oxide begins to form at lower potentials. The presence of arsenic on the electrode surface inhibits the onset of the platinum oxidation process. Once the potential becomes positive enough to oxidize the As(III), however, the platinum surface undergoes oxidation. Because of this change in the characteristics of the oxide formation when As(III) is present, an accurate correction for the residual current is impossible when dealing with data procured during cyclic voltammetry.

Prior to the formation of a thick oxide film on the electrode surface, the oxidation of As(III) to As(V) is mass transport limited. This is shown in Figure III-12 and Table III-4 by the linear relationship between the limiting current and the square root of the rotation speed at 0.80 V vs. SCE and 1.00 V vs. SCE during the positive potential sweep. As the thickness of the platinum oxide layer increases, however, the heterogeneous rate constant for the oxidation reaction decreases. A decrease in the heterogeneous rate constant causes the current to be less dependent upon the rotation speed of the electrode. Deviations from linearity are seen at 1.3 V vs. SCE during the positive scan and for all the potentials plotted during the negative scan. Because of the small heterogeneous rate constant, the charge transfer step becomes the rate limiting step at high rotation speeds.

Figure III-12. Dependence of limiting current on rotation speed of Pt disk for As(III) in 0.5 M HClO₄

Potential scan rate - 1 V min⁻¹

7.17 x 10⁻⁵ M As₂O₃

- 0.80 V vs. SCE (positive potential scan)
- 1.00 V vs. SCE (positive potential scan)
- △ 1.30 V vs. SCE (positive potential scan)
- 1.00 V vs. SCE (negative potential scan)
- 0.80 V vs. SCE (negative potential scan)

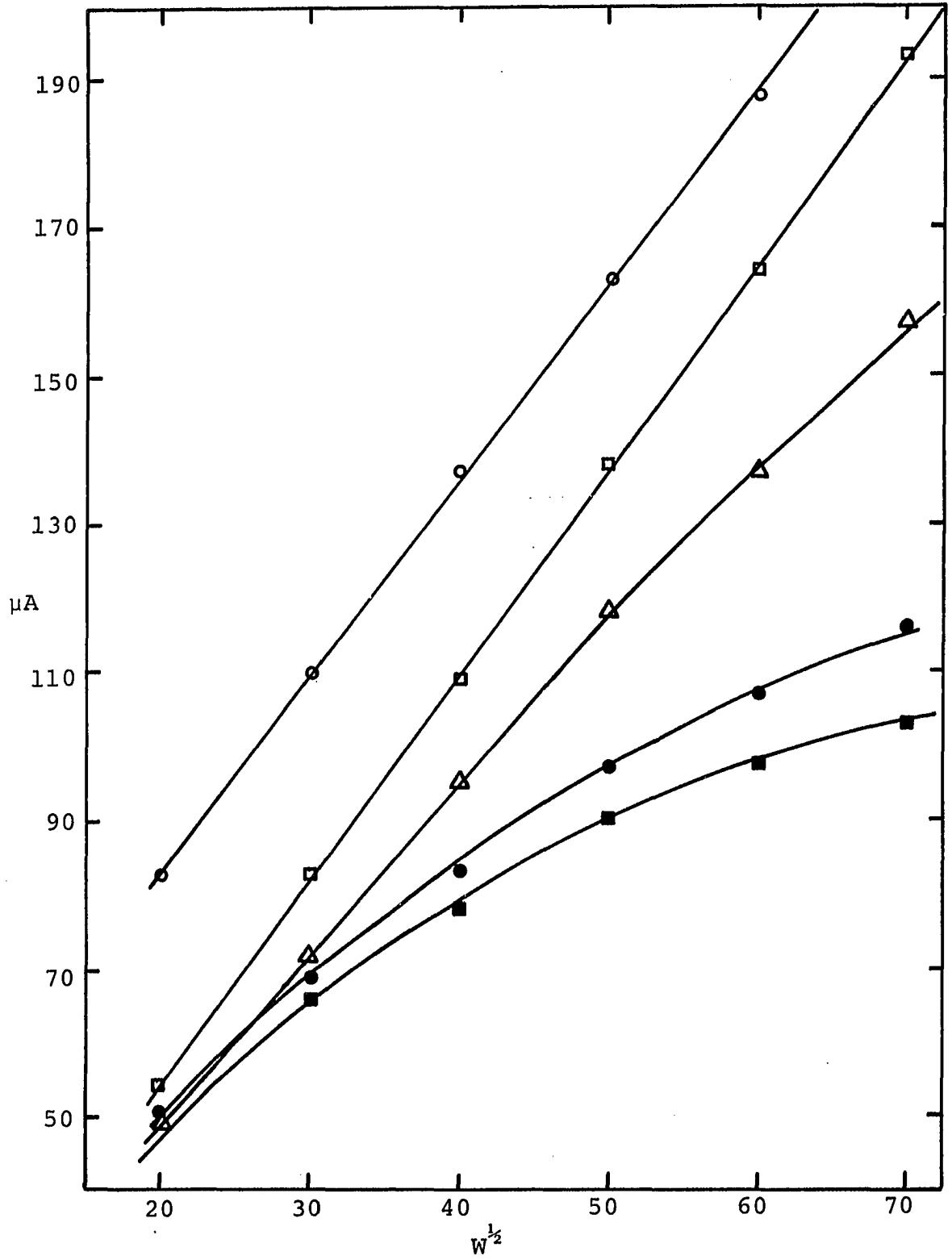


Table III-4. Dependence of limiting current on rotation speed of Pt disk for As(III) in 0.5 M HClO₄

| $W^{1/2}$ ($\frac{\text{rev}}{\text{min}}$) ^{1/2} | V <u>vs.</u> SCE | $I_{l,p}$ (μA) | $I_{l,n}$ (μA) |
|--|------------------|-----------------------------|-----------------------------|
| 20 | 0.8 | 82.5 | 50.5 |
| | 1.0 | 54.0 | 66.0 |
| | 1.3 | 48.5 | |
| 30 | 0.8 | 110.0 | 69.0 |
| | 1.0 | 83.0 | 66.0 |
| | 1.3 | 72.0 | |
| 40 | 0.8 | 137.0 | 83.5 |
| | 1.0 | 109.0 | 78.0 |
| | 1.3 | 95.0 | |
| 50 | 0.8 | 163.0 | 97.5 |
| | 1.0 | 138.0 | 90.0 |
| | 1.3 | 118.0 | |
| 60 | 0.8 | 187.5 | 107.5 |
| | 1.0 | 164.0 | 97.5 |
| | 1.3 | 137.5 | |
| 70 | 0.8 | 215.5 | 115.5 |
| | 1.0 | 194.0 | 103.0 |
| | 1.3 | 157.0 | |

The effect of chloride on the cyclic voltammetry of As(III) in 0.5 M HClO₄ at a Pt disk is depicted in Figure III-13. The value for $E_{1/2}$ shifts in a positive direction when chloride is present. Also, the oxidation wave obtained during the negative sweep is more irreversible in the presence of chloride. The current contributed by the oxidation of As(III) to As(V) decreases during the positive scan as the chloride concentration increases. For example, at 1.0 V vs. SCE the current produced by a 1.1×10^{-4} M As₂O₃ solution decreases by 13% when the Cl⁻ concentration is 8.5×10^{-4} M. Although the sensitivity for the

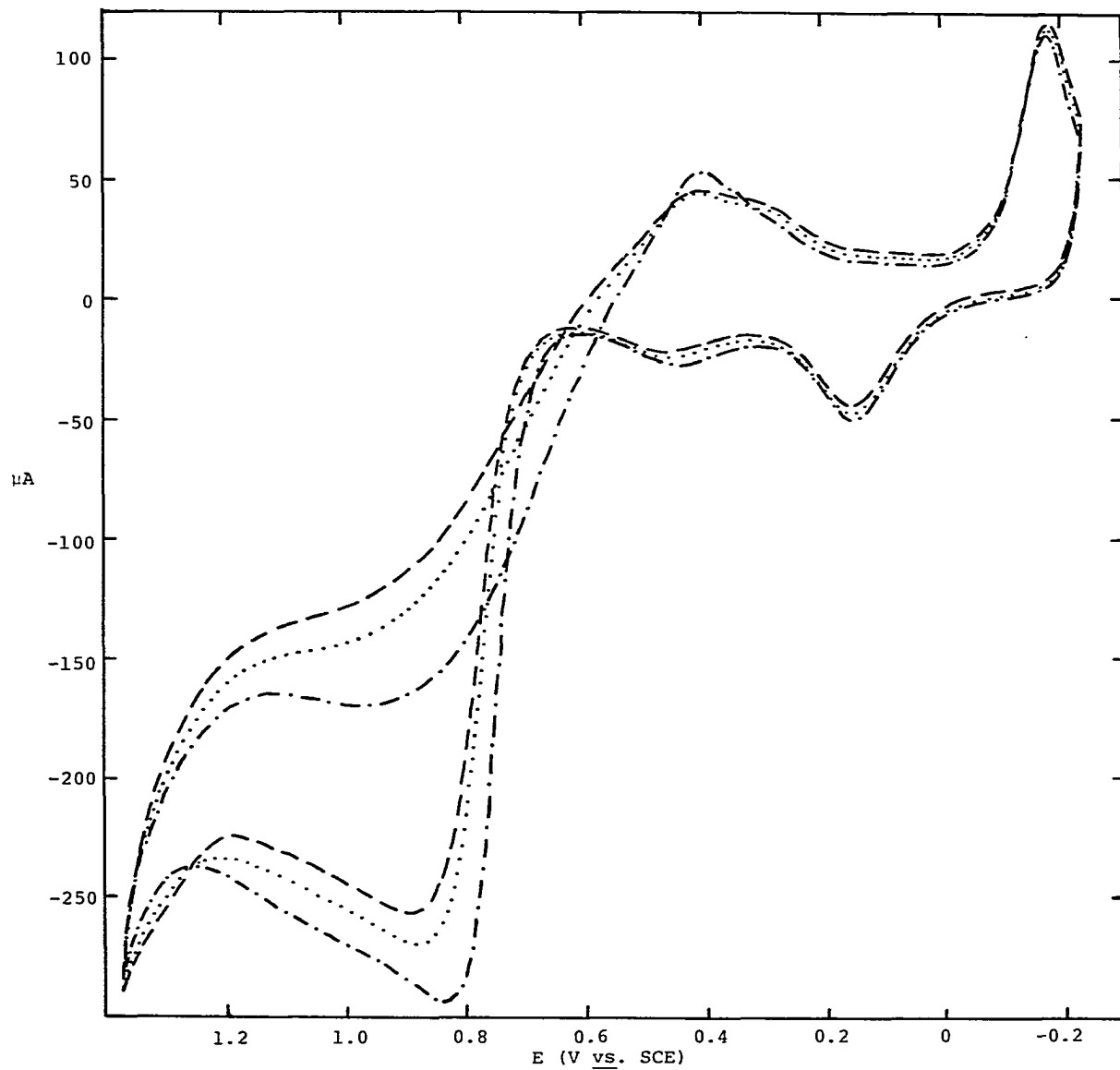
Figure III-13. Effect of Cl^- on the cyclic voltammetry at a Pt disk for As(III)
in 0.5 M HClO_4

Rotation speed - 3600 rev min^{-1}
Potential scan rate - 1 V min^{-1}

----- 1.08 x 10⁻⁴ M As_2O_3
0.5 M HClO_4

..... 20 ppm NaCl
1.08 x 10⁻⁴ M As_2O_3
0.5 M HClO_4

----- 40 ppm NaCl
1.08 x 10⁻⁴ M As_2O_3
0.5 M HClO_4



detection of As(III) diminishes in the presence of chloride, the chloride does not drastically alter the electrochemistry occurring at the Pt surface. A similar chloride concentration would have prevented the oxidation of As(III) on a Au surface.

All the cyclic voltammograms shown so far were obtained for solutions of As(III) in perchloric acid. However, in nature most of the arsenic is present in the pentavalent form. Figure III-14 illustrates the cyclic voltammetry of As(V) in perchloric acid at a Pt disk. Unfortunately, the currents produced are not dependent upon the concentration of As(V) in the solution. Identical cyclic voltammograms were obtained for all the solutions tested in which the As(V) concentration was varied from 1×10^{-4} M to 1×10^{-6} M. The entire cyclic voltammogram is independent of rotation speed but is dependent upon the potential scan rate. The currents observed are concluded to be due to the reduction or oxidation of arsenic species adsorbed on the platinum surface. The shoulder off the platinum oxide reduction peak during the positive potential sweep is attributed to the reduction of surface adsorbed As(V) to As(III). As the potential applied to the platinum disk becomes more negative, some of the As(III) produced can be reduced to arsenic metal. Two small stripping peaks appear during the anodic scan corresponding to the oxidation of the

Figure III-14. Cyclic voltammetry of As(V) in 0.5 M HClO₄ at Pt disk

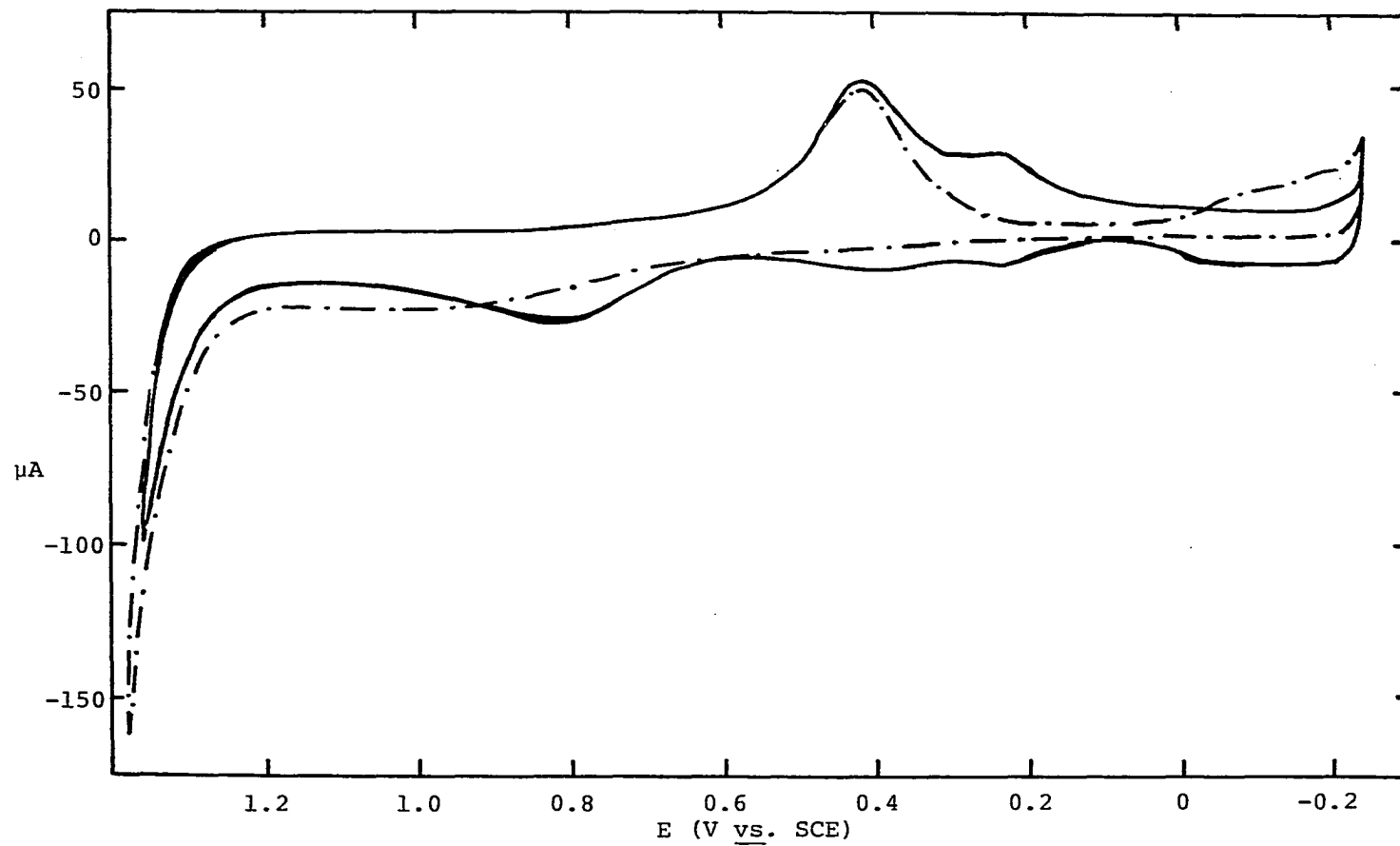
Rotation speed - 3600 rev min⁻¹

Potential scan rate - 1 V min⁻¹

-·- 0.5 M HClO₄

— 1 x 10⁻⁴ M As₂O₅

0.5 M HClO₄



deposited arsenic metal to As(III). The As(III) produced can then be oxidized to As(V) at 0.80 V vs. SCE.

E. Conclusions

Platinum is a better electrode material for the electroanalytical determination of arsenic than gold. The presence of chloride in a solution seriously alters the electrochemical behavior of As(III) in perchloric acid at a gold disk. The arsenic must be converted to the trivalent form prior to the analysis because the current signal produced by pentavalent arsenic is independent of the arsenic concentration.

IV. EVALUATION OF THE Pt FLOW-THROUGH DETECTOR

A. Introduction

A flow-through system with an electrochemical detector has three distinct advantages over cyclic voltammetry for the electroanalytical determination of arsenic. First of all, by placing a chromatographic column in the eluent stream, arsenic can be separated from other electroactive species. This is particularly advantageous for the case at hand because the As(V) in the sample must be reduced to As(III) prior to the analysis. Almost any species which is capable of reducing the pentavalent arsenic quantitatively would also be electroactive. By the proper choice of column material and eluent, the reducing agent can be separated from the As(III). The second advantage of flow-through detectors is that the residual current can easily be determined. The residual current, due to surface controlled processes such as double layer charging, must be subtracted from the total current to yield the net faradaic current for reaction of the analyte. As shown in Chapter III for the process involving the oxidation of As(III) at a Pt disk, the value of the residual current is difficult to measure from cyclic voltammograms. The third advantage of the flow-through system is that the method can easily be automated.

Flow-through electrochemical detectors have been utilized in the past for the determination of many metal ions including Fe(III), Au(III), Cu(II), Cd(II), Hg(II), Zn(II), Ni(II), Pb(II), Co(II), Sb(III), Cr(VI) and Se(IV) (173-180). Detection of ng quantities has been reported.

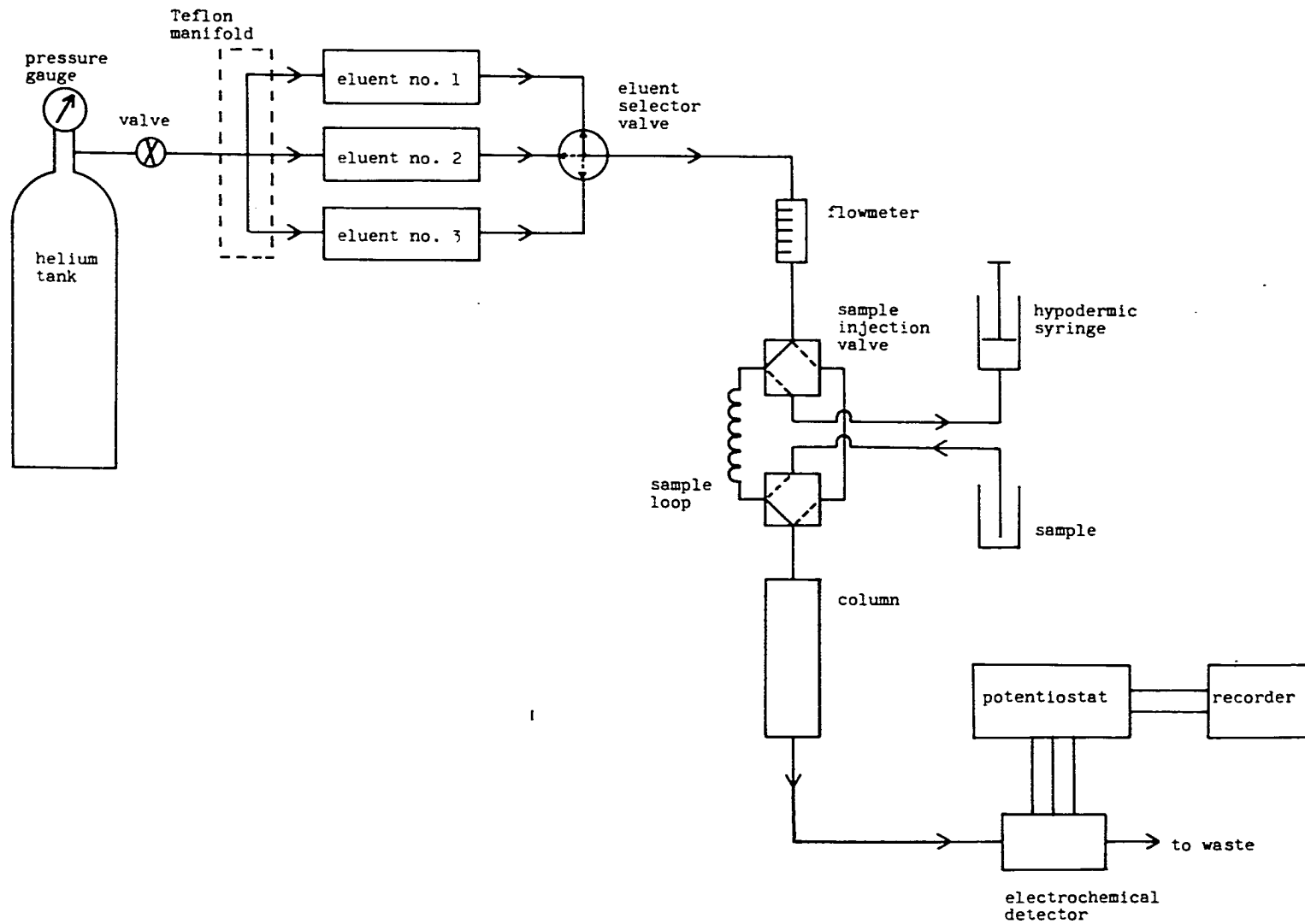
This chapter describes the flow-through system used for the electroanalytical determination of arsenic. The detector response was studied as a function of flow rate, time and potential applied to the detector. A calibration curve was obtained and the detection limit is reported.

B. Experimental

1. Description of the flow system

The flow system utilized is shown schematically in Figure IV-1. The design is a modified version of the system described by Seymour, Sickafoose and Fritz (181). Compressed He, available from Air Products, Inc., supplied the necessary pressure within the eluent reservoirs to cause fluid flow. The eluent reservoirs were 2 l acid bottles. The cap design for the eluent bottles is described in reference 182. The Teflon tubing, Kel-F valves, chromatographic columns and polypropylene fittings are available from Larry Bell Associates of Hopkins, MN. The flow rate control valves as well as the flowmeters were obtained from Roger Gilmont Instruments, Inc., of Great

Figure IV-1. Schematic diagram of flow-through system used for determination of As(III)



Neck, NY. The ion-exchange resin, placed in the chromatographic columns, was purchased from Bio-Rad Laboratories in Richmond, CA. The strong-acid, cation-exchange resin AG50W-X8 was used. The mesh size of the resin was 100-200.

The procedure used for the calibration of the sample loop and for the measurement of the flow rate is described in reference 182.

2. Detector and instrumentation

A cross-sectional diagram of the Pt wire detector used in the studies is shown in Figure IV-2. The detector was designed by R. Koile and modified by B. Snider. Sixteen gauge Pt wire was used for both the counter and working electrodes. The channel containing the working electrode had an internal diameter of 0.152 cm and a length of 2.1 cm. The detector was built by the Chemistry Department Machine Shop at Iowa State University. The reference electrode was a miniature saturated calomel electrode with a saturated solution of NaCl rather than KCl.


The three electrode potentiostat was the Polarographic Analyzer, Model 174A, from the Princeton Applied Research Corp. of Princeton, NJ. The strip-chart recorder was from the Heath-Schlumberger Co. of Benton Harbor, MI. A digital multimeter from Systron-Donner, Inc. of Culver City, CA, was used to monitor the potential applied to the detector with respect to the reference electrode.


Figure IV-2. Pt wire flow-through electrochemical detector

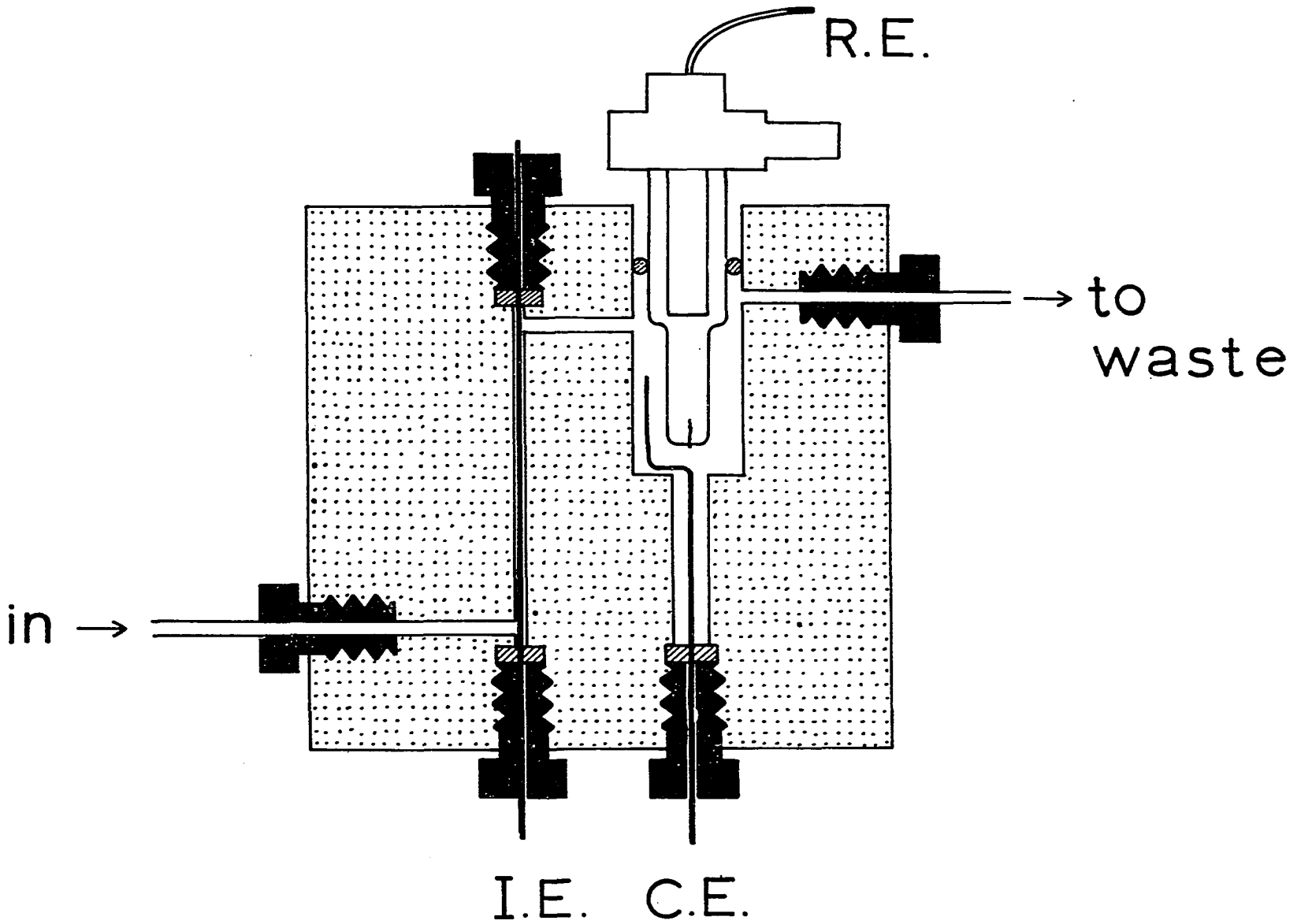
R.E. Reference electrode

C.E. Counter electrode

I.E. Indicating or working electrode

 Si-teflon

 Fette washers



C. Detector Response

1. Current as a function of time for As(III)

In an acidic environment, trivalent arsenic exists as the neutral species HAsO_2 or H_3AsO_3 . The pK_a value for arsenious acid is 9.2 (183). Consequently, if As(III) is injected into a flowing stream of 0.5 M HClO_4 , the As(III) will not be retained on a cation-exchange resin placed in a column located between the injection chamber and the flow-through detector. However, many other cationic species, which could interfere with the electroanalytical determination of arsenic, can be retained on the cation-exchange resin.

The electrochemical detector is maintained at a fixed potential. Prior to the injection of the sample, a background signal is obtained on the recorder for the eluent passing through the detector. When the sample is injected, a chromatographic peak appears on top of the background signal current. The peak is attributed to the oxidation of As(III) to As(V) as the arsenic passes through the Pt wire detector. The size of the chromatographic peak is proportional to the concentration of As(III) in the sample.

In order to maximize the current signal obtained when arsenic passes through the electrochemical detector, the optimum potential applied to the working electrode had to

be determined. A solution containing 1.4×10^{-4} M As(III) in 0.5 M HClO₄ was passed through the detector for a 2 hour time span while the potential applied to the detector was held constant. The current was monitored with a strip-chart recorder as a function of time. Successive experiments were performed in which the potential difference between the working electrode and the reference electrode was varied from 0.60 V vs. SCE to 1.30 V vs. SCE by 0.10 V increments. A constant flow rate of 1.15 ml/min was maintained. Prior to each experiment, the potential was cycled linearly 10 times between -0.20 V vs. SCE and 1.30 V vs. SCE. As shown in Chapter III, a layer of platinum oxide forms on the electrode surface when the applied potential is above 0.70 V vs. SCE and the oxide layer is reduced below 0.60 V vs. SCE. The alternate electrochemical formation and dissolution of an oxide layer has traditionally been used for the removal of adsorbed impurities from electrode surfaces. The entire set of experiments was repeated passing only 0.5 M HClO₄ through the detector. The current obtained for the HClO₄ solution was subtracted from the current obtained for the solution containing both As(III) and HClO₄. The current difference is plotted as a function of time in Figure IV-3 for 0.80, 1.00 and 1.20 V vs. SCE. The data obtained at all the

Figure IV-3. Current as a function of time for As(III) in
0.5 M HClO₄ passing through Pt flow-through
electrochemical detector held at various
potentials

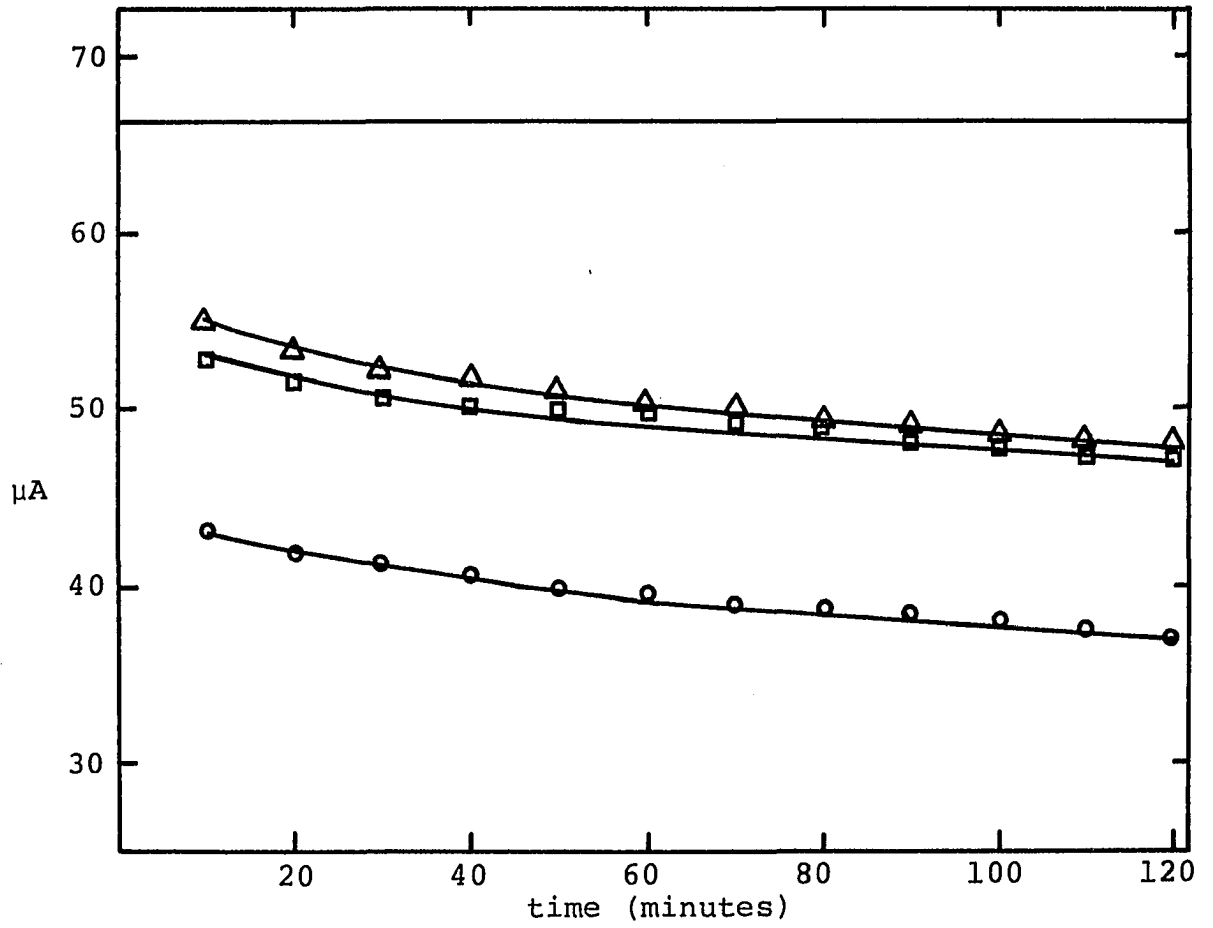
flow rate - 1.5 ml min⁻¹

1.4 x 10⁻⁴ M As₂O₃

△ 1.20 V vs. SCE

□ 1.00 V vs. SCE

○ 0.80 V vs. SCE



potentials studied are in Table IV-1. The magnitude of the current decreased continuously during the 2 hour period.

The theoretical mass-transport limited current for As(III) in Figure IV-3 was calculated from data obtained for the anodic detection of Br^- . Johnson and Bruckenstein (184) reported that the oxidation of Br^- at a rotating Pt disk electrode is not hindered by the presence of a layer of platinum oxide on the electrode surface. Repetitive injections of 0.226 ml of $3.90 \times 10^{-4} \text{ M}$ NaBr were made into a flowing stream of 0.1 M HClO_4 to test further the conclusions of Johnson and Bruckenstein. For 9 injections over a period of 2.5 hours into a stream flowing at a rate of 1.30 ml min^{-1} , the peak area for Br^- was 2.03 mC with a relative standard deviation of 0.88%. The small relative standard deviation is verification that the oxide layer formed on the Pt wire in the flow-through detector does not inhibit Br^- oxidation.

The steady-state, mass-transport limited current (I_{ss}) for the continuous flow of a homogeneous solution of analyte can be predicted from the peak signals obtained for injections of the same solution into a stream of the supporting electrolyte. P. L. Meschi, of this laboratory, has obtained experimental verification that the area of the detection peak is the same whether or not dispersion has

Table IV-1. Current as a function of time for As(III) in 0.5 M HClO₄ passing through Pt flow-through electrochemical detector

| V vs. SCE | time | I (μA) | V vs. SCE | time | I (μA) |
|-----------|------|--------|-----------|------|--------|
| 0.8 | 10 | 43.1 | 1.1 | 10 | 52.5 |
| | 20 | 41.9 | | 20 | 50.8 |
| | 30 | 41.3 | | 30 | 50.1 |
| | 40 | 40.7 | | 40 | 50.0 |
| | 50 | 39.8 | | 50 | 50.0 |
| | 60 | 39.4 | | 60 | 49.8 |
| | 70 | 39.0 | | 70 | 49.6 |
| | 80 | 38.8 | | 80 | 49.3 |
| | 90 | 38.5 | | 90 | 48.8 |
| | 100 | 38.0 | | 100 | 48.3 |
| | 110 | 37.4 | | 110 | 47.8 |
| | 120 | 37.0 | | 120 | 47.7 |
| 0.9 | 10 | 52.3 | 1.2 | 10 | 54.8 |
| | 20 | 50.7 | | 20 | 53.2 |
| | 30 | 49.2 | | 30 | 52.1 |
| | 40 | 48.8 | | 40 | 51.7 |
| | 50 | 48.3 | | 50 | 50.9 |
| | 60 | 47.9 | | 60 | 50.2 |
| | 70 | 46.2 | | 70 | 49.9 |
| | 80 | 45.1 | | 80 | 49.4 |
| | 90 | 44.9 | | 90 | 48.9 |
| | 100 | 44.8 | | 100 | 48.3 |
| | 110 | 44.6 | | 110 | 48.0 |
| | 120 | 44.2 | | 120 | 48.0 |
| 1.0 | 10 | 52.7 | 1.3 | 10 | 51.1 |
| | 20 | 51.5 | | 20 | 50.0 |
| | 30 | 50.7 | | 30 | 49.2 |
| | 40 | 50.1 | | 40 | 48.6 |
| | 50 | 49.9 | | 50 | 47.7 |
| | 60 | 49.6 | | 60 | 46.9 |
| | 70 | 49.1 | | 70 | 46.0 |
| | 80 | 48.7 | | 80 | 45.6 |
| | 90 | 48.0 | | 90 | 45.3 |
| | 100 | 47.6 | | 100 | 45.0 |
| | 110 | 47.1 | | 110 | 44.8 |
| | 120 | 47.0 | | 120 | 44.7 |

taken place (185). For a sample plug that does not experience dispersion, the number of coulombs, Q , under the signal peak is given by Equation IV-1. In Equation IV-1,

$$Q = I_{ss} t_w \quad (\text{IV-1})$$

the symbol t_w refers to the time it takes for the sample plug to pass through the detector for the case in which dispersion does not occur. For a sample of volume V_s injected into a stream flowing at a constant flow rate v_f ,

$$t_w = V_s/v_f. \quad (\text{IV-2})$$

Regardless of dispersion, I_{ss} can be predicted from measurement of the peak area. Based on the data obtained for the

$$I_{ss} = Qv_f/V_s \quad (\text{IV-3})$$

oxidation of Br^- , the value of I_{ss} for Br^- is 0.195 mA.

The theoretical value of I_{ss} for the oxidation of As(III) can be calculated from the steady-state current obtained for the oxidation of Br^- . The current produced by an electroactive species in a flowing stream is described in Equation IV-2 (186, 187).

$$I_l = knAFD^{2/3} v_f^\alpha C^b \quad (\text{IV-4})$$

In Equation IV-4,

k = proportionality constant;

n = number of electrons involved (equivalents mole^{-1});

F = Faraday's constant (coulombs equivalent $^{-1}$);

D = diffusion coefficient ($\text{cm}^2/\text{s}^{-1}$);

A = electrode surface area (cm^2);

v_f = fluid flow rate ($\text{cm}^3 \text{s}^{-1}$);

C^b = bulk concentration of the electroactive species
(moles l^{-1}).

For a sample plug that is not dispersed, $I = I_{ss}$. For the flow rates used during this study, the value of α in Equation IV-4 is 0.58. The determination of the value for α will be presented later in this chapter for the Pt wire electrode. The current for the oxidation of Br^- can be described by Equation IV-5. Likewise, the current for

$$I_{\text{Br}} = kn_{\text{Br}} D_{\text{Br}}^{2/3} F A C_{\text{Br}}^b v_{f,\text{Br}}^{0.58} \quad (\text{IV-5})$$

the oxidation of As(III) is given by Equation IV-6. If

$$I_{\text{As}} = kn_{\text{As}} D_{\text{As}}^{2/3} F A C_{\text{Br}}^b v_{f,\text{As}}^{0.58} \quad (\text{IV-6})$$

both Equations IV-5 and IV-6 are solved for $knFA$ and the two resulting expressions are equated, Equation IV-7 results

$$I_{\text{As}} = \frac{I_{\text{Br}} n_{\text{As}} D_{\text{As}}^{2/3} C_{\text{As}}^b v_{f,\text{As}}^{0.58}}{n_{\text{Br}} D_{\text{Br}}^{2/3} C_{\text{Br}}^b v_{f,\text{Br}}^{0.58}} \quad (\text{IV-7})$$

after rearrangement. In Equation IV-7, $n_{\text{As}} = 2$, $n_{\text{Br}} = 1$, $D_{\text{As}} = 0.94 \times 10^{-5} \text{ cm}^2 \text{ s}^{-1}$ (188), $D_{\text{Br}} = 1.58 \times 10^{-5} \text{ cm}^2 \text{ s}^{-1}$ (184), $v_{f,\text{As}} = 1.15 \text{ ml min}^{-1}$, $v_{f,\text{Br}} = 1.30 \text{ ml min}^{-1}$, $C_{\text{As}}^b = 1.44 \times 10^{-4} \text{ M}$ and $C_{\text{Br}}^b = 3.90 \times 10^{-4} \text{ M}$. Consequently, the

steady-state current for the arsenic oxidation process should be 95.3 μA . However, the sensitivity of the detector had decreased by a factor of 1.44 between the time the data for the oxidation of Br^- were obtained and the time when the current-time curves shown in Figure IV-3 were obtained. The change in the sensitivity is attributed to the fact that the surface of the working electrode was sanded after the data for the As(III) was procured. The diameter of the wire had decreased appreciably. Therefore, the calculated steady-state current of the As(III) is 66.2 μA . The steady-state current that was calculated is also shown in Figure IV-3. At 1.0 V vs. SCE, the experimental current value is 71% of the calculated value after 2 hours.

2. Relationship between oxide growth on Pt electrode and current decay for oxidation of As(III)

Cyclic voltammetry at a rotating Pt disk electrode was used to further investigate the current decay for the oxidation of As(III) as a function of time at constant potential. A 2.2×10^{-4} M solution of As(III) in 0.5 M HClO_4 was placed in the cell described in Chapter III for studies involving cyclic voltammetry. The potential applied to the Pt disk was cycled between -0.30 V vs. SCE and 1.35 V vs. SCE and the potential scan was stopped at 1.35 V vs. SCE. The time during which the potential was held at

1.35 V vs. SCE was varied from 0 to 20 minutes. The resulting cyclic voltammograms are shown in Figure IV-4. The current obtained at 1.0 V vs. SCE on the negative sweep is plotted in Figure IV-5 as a function of the time during which the potential was held at 1.35 V vs. SCE. The data are also presented in Table IV-2. The longer the potential

Table IV-2. Current at 1.0 V vs. SCE on negative potential sweep vs. time potential of Pt disk held at 1.35 V vs. SCE for As(III) in 0.5 M HClO₄

| Time (min) | Current (μ A) |
|------------|--------------------|
| 0 | 171 |
| 1 | 126 |
| 5 | 81 |
| 10 | 60 |
| 15 | 49 |
| 20 | 41 |

was held at 1.35 V vs. SCE, the smaller is the current recorded at 1.0 V vs. SCE during the negative scan. The magnitude of the current at 1.0 V vs. SCE after the potential was held at 1.35 V vs. SCE for 20 minutes is only 24% of the current obtained when the potential scan was not stopped at 1.35 V vs. SCE. At 1.35 V vs. SCE, there is a considerable amount of Pt oxide forming on the electrode surface. The data seem to indicate that the oxide layer grows rapidly initially and then the rate of formation decreases. The thicker the oxide on the Pt electrode,

Figure IV-4. Cyclic voltammograms of As(III) in 0.5 M HClO₄ at Pt disk as varied time potential held at 1.35 V vs. SCE

Rotation speed - 3600 rev min⁻¹

Potential scan rate - 1 V min⁻¹

1.08 x 10⁻⁴ M As₂O₃

———— 0 min

----- 1 min

..... 5 min

-.-.-.- 10 min

-.-.-.- 15 min

----. 20 min

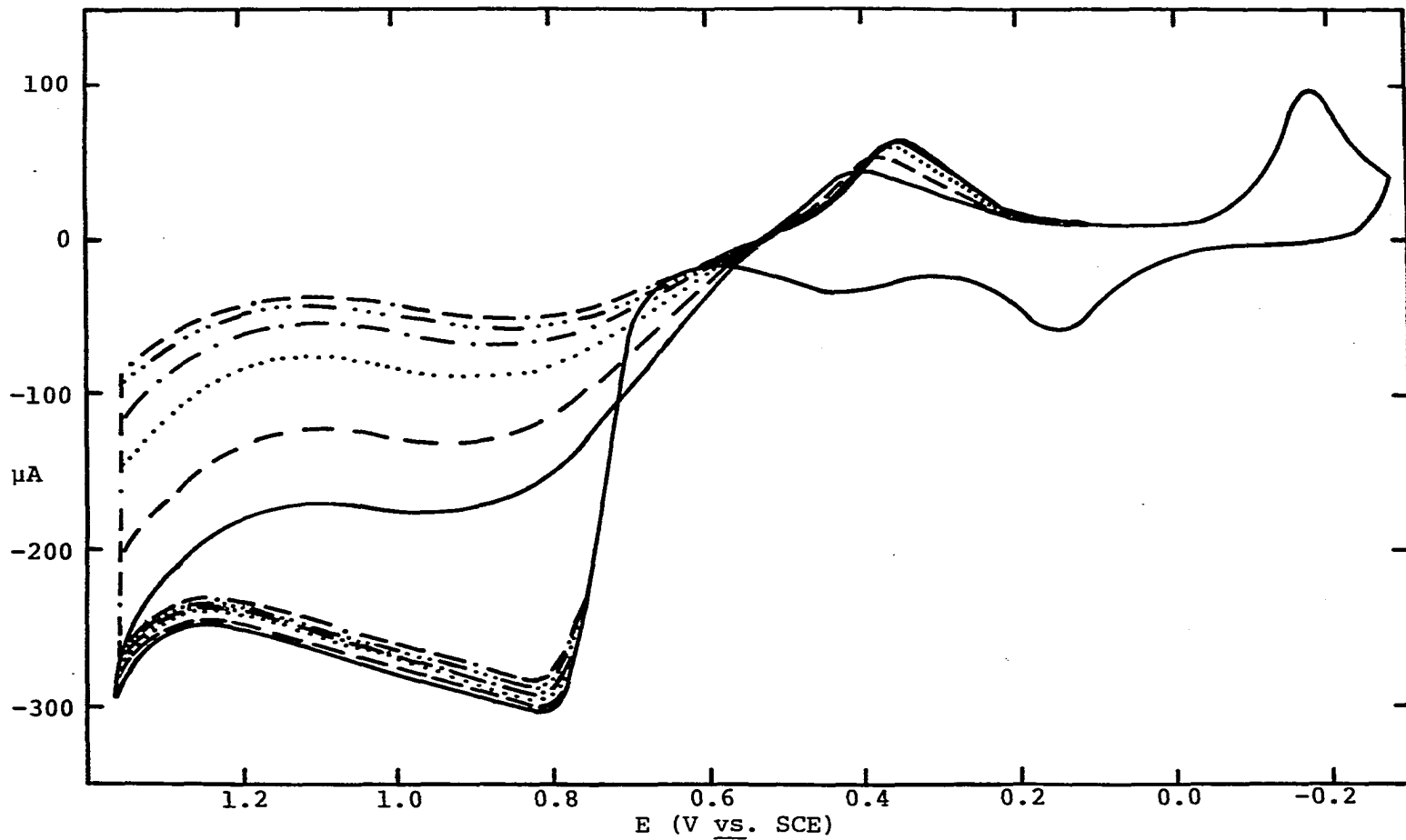
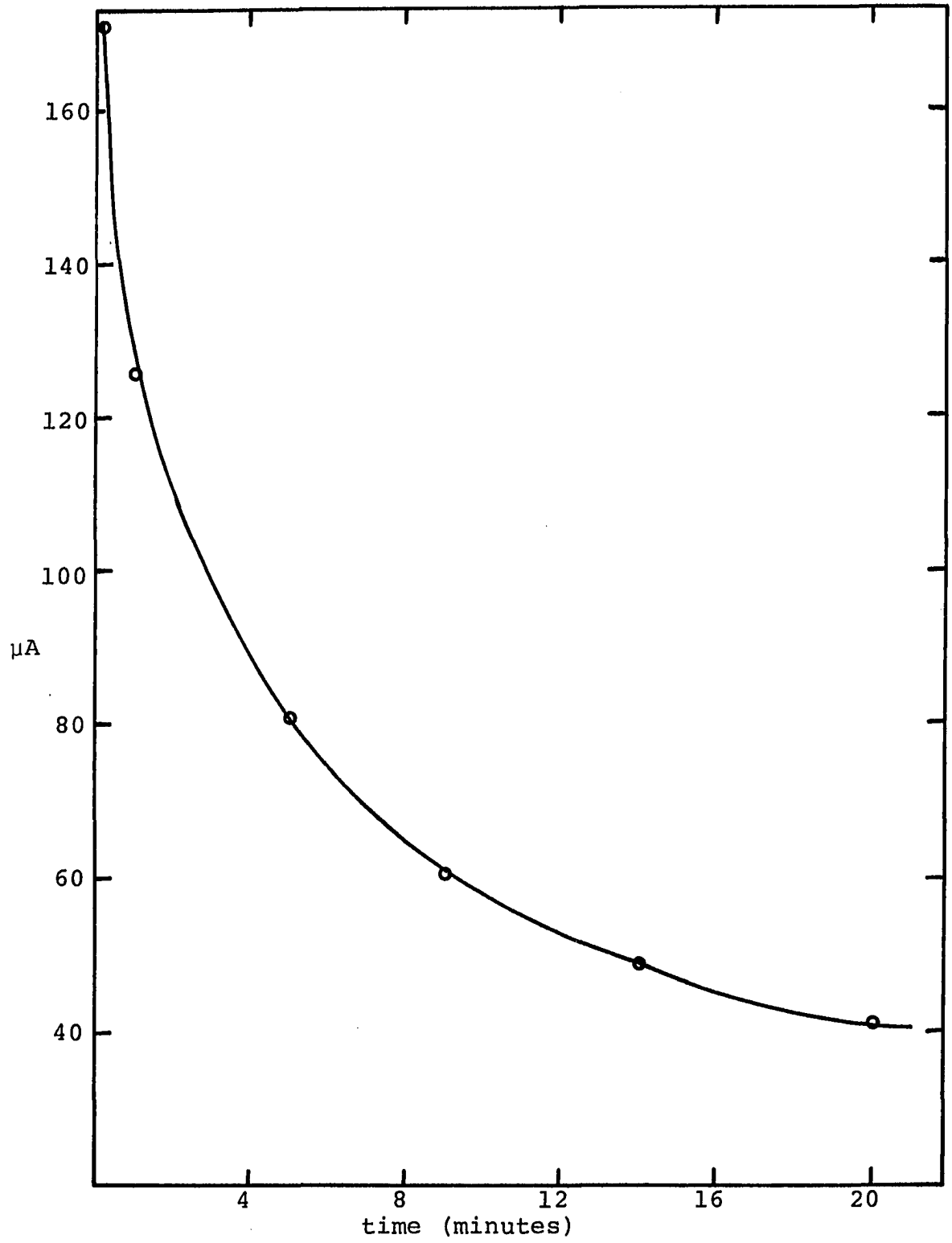


Figure IV-5. Current at 1.0 V vs. SCE during negative potential scan vs. time potential of Pt disk held at 1.35 V vs. SCE for As(III) in 0.5 M HClO₄

Rotation speed - 3600 rev min⁻¹

Scan rate - 1 V min⁻¹

1.08 x 10⁻⁴ M As₂O₃



the smaller is the current that passes as a result of the oxidation of As(III) to As(V).

Although the oxide layer continues to grow, the growth rate after 1 hour is too low to create any analytical problems. For example, the current produced at 1.0 V vs. SCE for a solution containing 8.2×10^{-5} M As(III) in 0.5 M HClO₄ flowing through the Pt wire electrochemical detector for a span of 7 hours is shown in Figure IV-6 and Table IV-3. The steady-state current, as calculated from

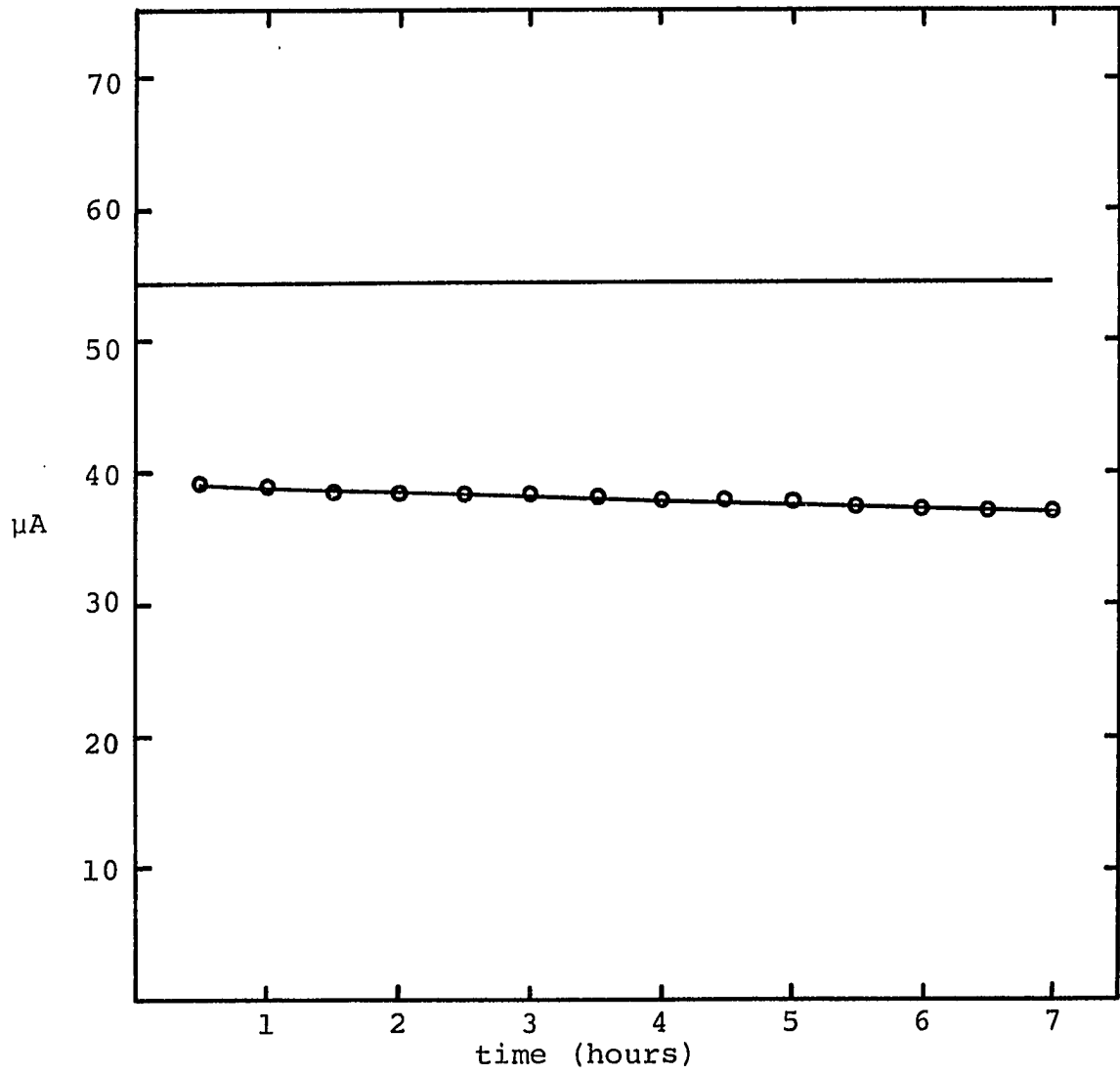
Table IV-3. Current vs. time for As(III) in 0.5 M HClO₄ flowing through Pt wire electrochemical detector held at 1.0 V vs. SCE for 7 hours

| Time (hours) | Current (μ A) |
|--------------|--------------------|
| 0.5 | 39.0 |
| 1.0 | 38.8 |
| 1.5 | 38.7 |
| 2.0 | 38.6 |
| 2.5 | 38.5 |
| 3.0 | 38.3 |
| 3.5 | 38.1 |
| 4.0 | 37.9 |
| 4.5 | 37.8 |
| 5.0 | 37.7 |
| 5.5 | 37.5 |
| 6.0 | 37.4 |
| 6.5 | 37.3 |
| 7.0 | 37.1 |

Equation IV-5, is 54.3 μ A. The current produced after 1 hour is 71.5% of the calculated steady-state current. The current produced after 7 hours is 68.3% of the calculated steady-state current. The current changed only 3.2% between 1 and

Figure IV-6. Current vs. time for As(III) in 0.5 M HClO₄
flowing through Pt wire electrochemical
detector held at 1.0 V vs. SCE for 7 hours

8.2×10^{-5} M As₂O₃
flow rate = 1.30 ml min⁻¹



7 hours. Consequently, as long as the system runs for about 30 minutes prior to the beginning of an analysis, reproducibility in the data is no problem. A calibration is generally made at the same time the samples are analyzed.

3. Pseudo I-E curve for As(III) in 0.5 M HClO₄

The pseudo current-voltage curve is shown in Figure IV-7 for As(III) in 0.5 M HClO₄ flowing through a Pt wire detector. The currents obtained after 2 hours as shown in Figure IV-3 were plotted vs. the applied potential. Table IV-4 also contains the data. Any potential above 0.90 V

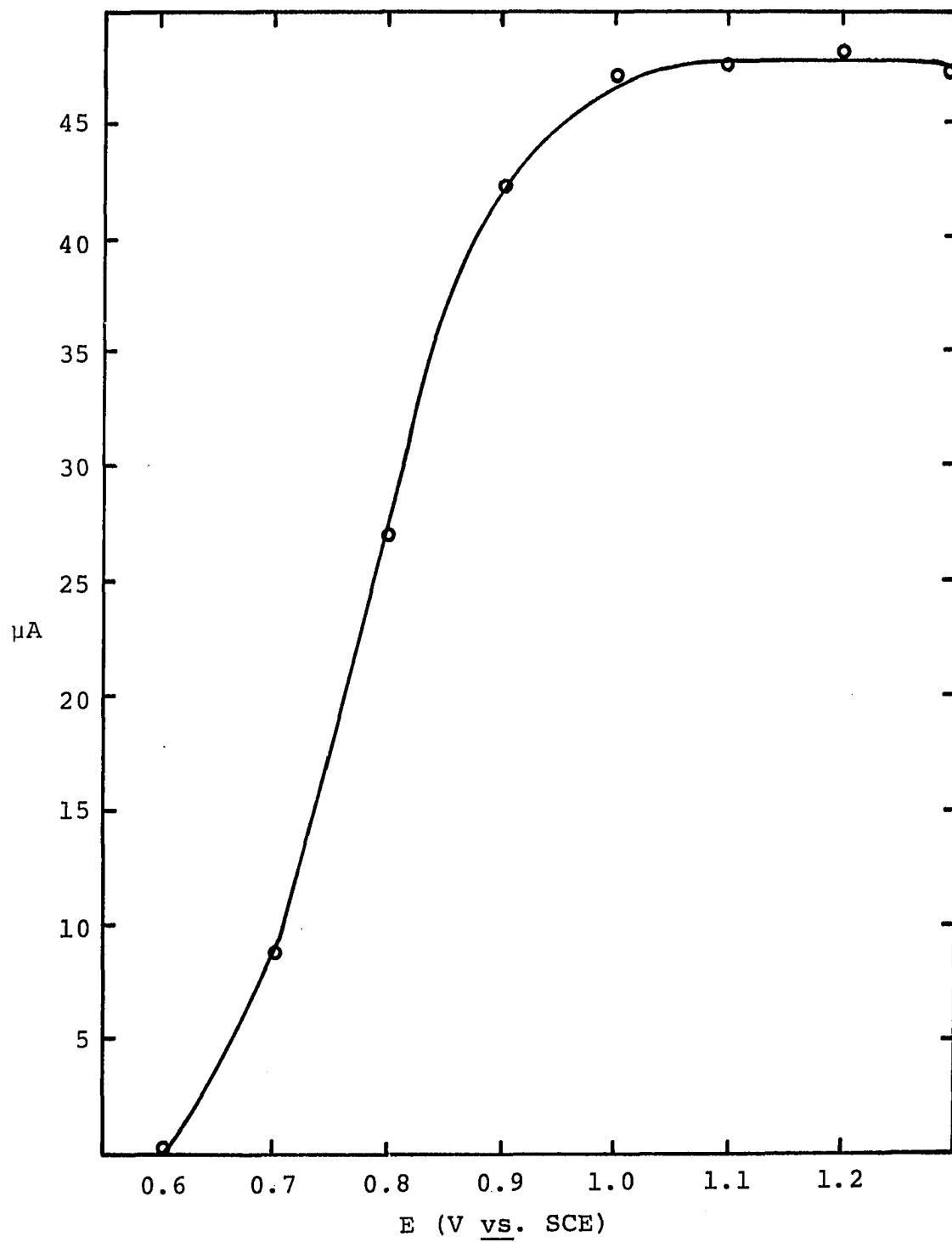
Table IV-4. Pseudo current-voltage curve for As(III) in 0.5 M HClO₄ through Pt wire flow-through detector

| Potential (<u>vs.</u> SCE) | Current (μA) |
|-----------------------------|--------------|
| 0.60 | 0.1 |
| 0.70 | 8.7 |
| 0.80 | 37.0 |
| 0.90 | 44.2 |
| 1.00 | 47.0 |
| 1.10 | 47.6 |
| 1.20 | 48.0 |
| 1.30 | 47.2 |

vs. SCE is satisfactory for the determination of arsenic. For the remainder of the work, an applied potential of 1.0 V vs. SCE was used.

Figure IV-7. Pseudo current-voltage curve for As(III) in
0.5 M HClO₄ through Pt wire flow-through
detector

flow rate = 1.15 ml min⁻¹
1.4 x 10⁻⁴ M As₂O₃



4. Dependence of current on flow rate

The dependence of the current on the flow rate was studied. For a cylindrical electrode placed in a flowing stream, the value of α in Equation IV-4 was reported to be 0.33 under conditions which resulted in laminar fluid flow and 0.58 under conditions which resulted in turbulent flow (188). For the Pt wire electrode used for the electro-analytical determination of As(III), however, the situation is more complex because of the 90 degree bends in the fluid flow directly before and after passage by the working electrode.

To evaluate the value of α , the following experiment was performed. Injections of As(III) into a stream of 0.5 M HClO_4 were made. The detector was potentiostated at 1.0 V vs. SCE. The flow rate was varied from 0.15 ml min^{-1} to 1.62 ml min^{-1} . The coulombs of electricity which passed was determined by measuring the area under the signal.

The number of coulombs passed, Q , is defined by Equation IV-8.

$$Q = \int I dt \quad (\text{IV-8})$$

The combination of Equations IV-8 and IV-4 results in Equation IV-9.

$$Q = knFAD^{2/3} v_f^\alpha \int C^b dt \quad (\text{IV-9})$$

However,

$$\text{moles} = v_f \int C^b dt \quad (\text{IV-10})$$

If Equation IV-10 is substituted into Equation IV-9 the result is Equation IV-11. Equation IV-12 is the logarithm

$$Q = knFAD^{2/3} v_f^{\alpha-1} \quad (\text{moles}) \quad (\text{IV-11})$$

$$\log Q = \text{constant} + (\alpha-1)\log v_f \quad (\text{IV-12})$$

of Equation IV-11. If $\log Q$ is plotted vs. $\log v_f$, the slope of the line should be $\alpha-1$. This is plotted in Figure IV-8. The data also appear in Table IV-5. A line of slope -0.67 is shown drawn through the data obtained between a flow rate of 3.2×10^{-3} ml/sec ($\log = -2.5$) and 1.0×10^{-2} ml/sec ($\log v_f = -2.0$). A slope of -0.67 means that the value of α is 0.33 . Below a flow rate of 1.0×10^{-2} ml/sec, the flow is laminar in nature through the Pt wire electrode. Above a flow rate of 1.0×10^{-2} ml/sec, the current is larger than would be expected under conditions of laminar flow. The flow is more turbulent and the efficiency of electrolysis is greater. A line with a slope of -0.42 is shown drawn through the data collected for flow rates between 1.5×10^{-2} ml/sec ($\log v_f = -1.82$) and 2.7×10^{-2} ml/sec ($\log v_f = -1.57$). Therefore, the value for α at the higher flow rates is 0.58 . This corresponds to the theoretical value for α reported under conditions

Figure IV-8. Dependence of current on flow rate of As(III)
in 0.5 M HClO₄ through Pt wire detector

0.226 ml

1.0 V vs. SCE

1.43 x 10⁻⁵ M As₂O₃

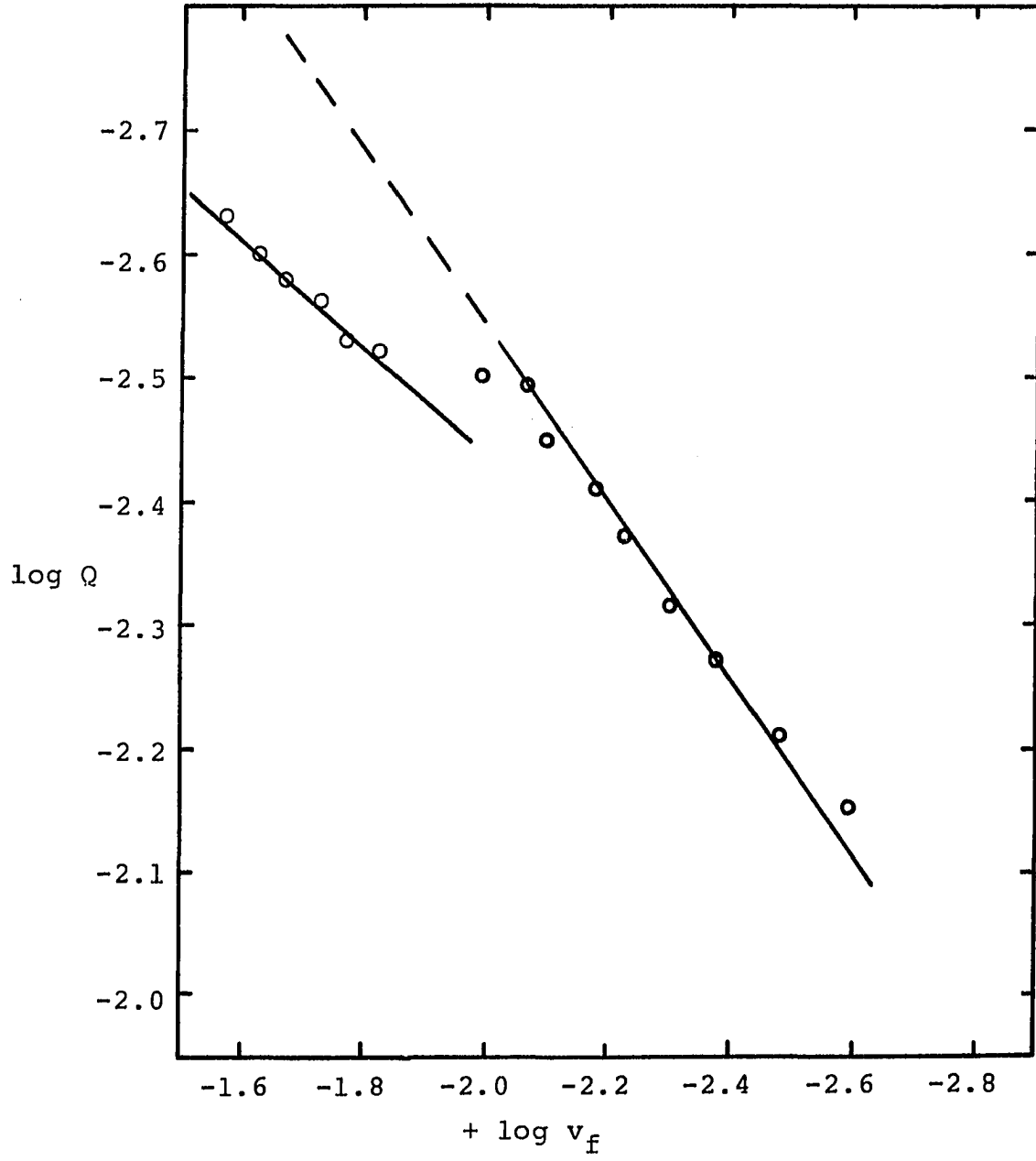


Table IV-5. Dependence of current on flow rate of As(III) in 0.5 M HClO_4 through Pt wire detector

| Flow rate ml/min | Flow rate, v_f ml/sec | $\log v_f$ | $\log Q$ |
|---------------------|----------------------------|------------|----------|
| 0.15 | 2.51×10^{-3} | -2.60 | -2.15 |
| 0.20 | 3.31×10^{-3} | -2.48 | -2.21 |
| 0.25 | 4.17×10^{-3} | -2.38 | -2.27 |
| 0.30 | 5.01×10^{-3} | -2.30 | -2.31 |
| 0.35 | 5.89×10^{-3} | -2.23 | -2.37 |
| 0.40 | 6.61×10^{-3} | -2.18 | -2.41 |
| 0.48 | 7.94×10^{-3} | -2.10 | -2.45 |
| 0.65 | 1.07×10^{-2} | -1.97 | -2.49 |
| 0.77 | 1.29×10^{-2} | -1.89 | -2.50 |
| 0.90 | 1.51×10^{-2} | -1.82 | -2.52 |
| 1.03 | 1.70×10^{-2} | -1.77 | -2.53 |
| 1.15 | 1.90×10^{-2} | -1.72 | -2.56 |
| 1.30 | 2.19×10^{-2} | -1.66 | -2.58 |
| 1.45 | 2.40×10^{-2} | -1.62 | -2.60 |
| 1.62 | 2.69×10^{-2} | -1.57 | -2.63 |

of turbulent flow. The experiment was repeated using Br^- in place of As(III) . The data are plotted in Figure IV-9 and shown in Table IV-6. The Br^- system confirms the theory that there are two regions of fluid flow: laminar and turbulent. The data obtained in the region corresponding to the transition between laminar and turbulent flow conditions are difficult to reproduce. The scatter in the data at low flow rates is attributed to difficulties maintaining a constant flow rate.

The fluid flow becomes turbulent at lower flow rates in the Pt wire detector than in a tubular detector. Blaedel, Olson and Sharma have reported that the flow rate in a tube is laminar until approximately 10 ml/min (189). The Pt wire electrode is not laminar above 0.6 ml/min. It is important to note that the detector response changes with a change in the fluid flow rate. However, at a fixed flow rate the signal is still proportional to the concentration of As(III) in a sample. Also, it is undesirable to work at a flow rate corresponding to the transition between turbulent and laminar flow conditions.

5. Calibration curve for As(III) in 0.1 M HClO_4

To verify the linear relationship between the current signal and the amount of As(III) in the sample, a calibration curve was prepared. Samples varying in concentration

Figure IV-9. Dependence of current on flow rate for Br^-
in 0.5 M HClO_4 through Pt wire detector

2×10^{-5} M NaBr

1.0 V vs. SCE

0.226 ml

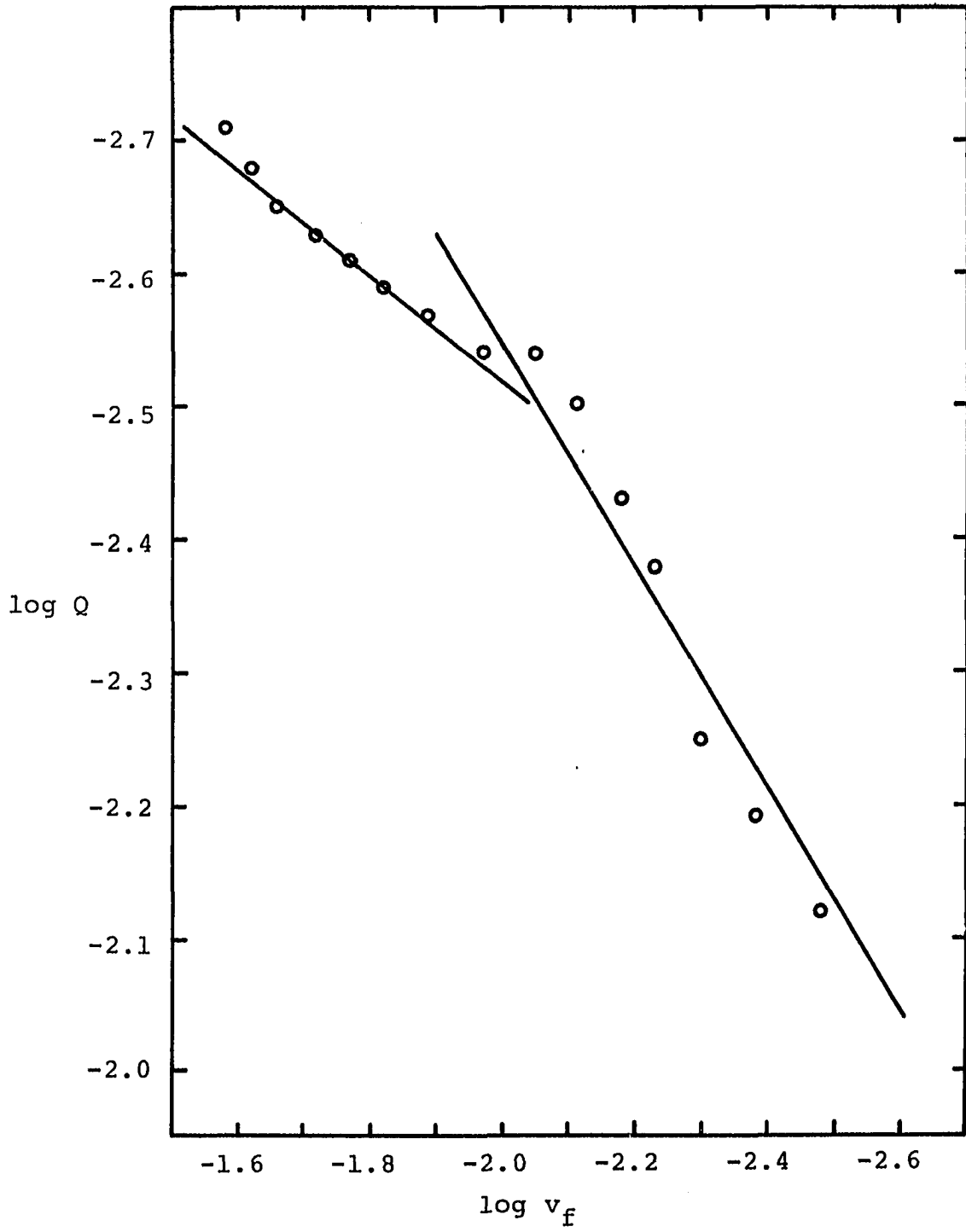


Table IV-6. Dependence of current on flow rate for Br^- in 0.5 M HClO_4 through Pt wire detector

| Flow rate ml/min | Flow rate, v_f ml/sec | $\log v_f$ | $\log Q$ |
|---------------------|----------------------------|------------|----------|
| 0.15 | 2.50×10^{-3} | -2.60 | -2.05 |
| 0.20 | 3.33×10^{-3} | -2.48 | -2.12 |
| 0.25 | 4.17×10^{-3} | -2.38 | -2.19 |
| 0.30 | 5.00×10^{-3} | -2.30 | -2.25 |
| 0.35 | 5.83×10^{-3} | -2.23 | -2.38 |
| 0.40 | 6.67×10^{-3} | -2.18 | -2.43 |
| 0.47 | 7.83×10^{-3} | -2.11 | -2.50 |
| 0.53 | 8.83×10^{-3} | -2.05 | -2.54 |
| 0.65 | 1.08×10^{-2} | -1.97 | -2.54 |
| 0.77 | 1.28×10^{-2} | -1.89 | -2.57 |
| 0.90 | 1.50×10^{-2} | -1.82 | -2.59 |
| 1.03 | 1.72×10^{-2} | -1.77 | -2.61 |
| 1.15 | 1.92×10^{-2} | -1.72 | -2.63 |
| 1.30 | 2.17×10^{-2} | -1.66 | -2.65 |
| 1.43 | 2.38×10^{-2} | -1.62 | -2.68 |
| 1.57 | 2.62×10^{-2} | -1.58 | -2.71 |

from 2.08×10^{-8} M As_2O_3 in 0.1 M HClO_4 to 1.25×10^{-3} M As_2O_3 in 0.1 M HClO_4 were prepared. The samples were injected into a flowing stream of 0.1 M HClO_4 . The flow rate was held constant at 1.15 ml/min. The electrochemical detector was potentiostated at 1.0 V vs. SCE. The volume of the sample loop was 0.226 ml. The peak area was determined by triangulation. Three injections were made for each sample. The relative standard deviation for each sample is reported in Table IV-7.

The calibration curve is shown in Figure IV-10. The curve is linear over at least 3 orders of magnitude. The detection limit is 3×10^{-10} grams As(III) or 0.1 ppb. The detection limit is not limited by noise from the electronics but by an injection artifact. That is, when a solution of the eluent was injected into the fluid stream, a small signal resulted. This peak was probably due to poor alignment of the valves in the injection chamber. In spite of this injection artifact, however, a low detection limit could be attained with a minimum amount of effort. Typical signal peaks are illustrated in Figure IV-11.

D. Conclusion

Reproducible chromatographic peaks can be obtained during the electroanalytical determination of As(III) provided the oxide on the Pt surface has been forming for

Table IV-7. Calibration curve for As(III) in 0.1 M HClO₄ at Pt wire detector

| Concentration <u>M</u> As ₂ O ₃ | -Log grams | Q (mc) | RSD (%) | +Log Q |
|--|------------|-------------------------|---------|--------|
| 2.08 x 10 ⁻⁸ | 10.10 | 1.20 x 10 ⁻³ | 13.1 | -2.92 |
| 4.15 x 10 ⁻⁸ | 9.80 | 1.31 x 10 ⁻³ | 6.1 | -2.88 |
| 8.30 x 10 ⁻⁸ | 9.50 | 2.16 x 10 ⁻³ | 1.5 | -2.67 |
| 1.25 x 10 ⁻⁷ | 9.32 | 2.34 x 10 ⁻³ | 1.9 | -2.63 |
| 2.08 x 10 ⁻⁷ | 9.10 | 4.30 x 10 ⁻³ | 3.0 | -2.37 |
| 4.15 x 10 ⁻⁷ | 8.80 | 7.96 x 10 ⁻³ | 0.4 | -2.10 |
| 8.30 x 10 ⁻⁷ | 8.50 | 1.51 x 10 ⁻² | 1.6 | -1.82 |
| 1.25 x 10 ⁻⁶ | 8.32 | 2.03 x 10 ⁻² | 0.5 | -1.69 |
| 2.08 x 10 ⁻⁶ | 8.10 | 3.14 x 10 ⁻² | 0.0 | -1.50 |
| 4.15 x 10 ⁻⁶ | 7.80 | 6.66 x 10 ⁻² | 5.6 | -1.18 |
| 8.30 x 10 ⁻⁶ | 7.50 | 1.24 x 10 ⁻¹ | 0.4 | -0.91 |
| 1.25 x 10 ⁻⁵ | 7.32 | 1.81 x 10 ⁻¹ | 0.0 | -0.74 |
| 2.08 x 10 ⁻⁵ | 7.10 | 2.99 x 10 ⁻¹ | 0.0 | -0.52 |
| 4.15 x 10 ⁻⁵ | 6.80 | 5.84 x 10 ⁻¹ | 0.4 | -0.23 |
| 8.30 x 10 ⁻⁵ | 6.50 | 1.10 | 0.5 | 0.04 |
| 1.25 x 10 ⁻⁴ | 6.32 | 1.62 | 0.4 | 0.21 |
| 2.08 x 10 ⁻⁴ | 6.10 | 2.21 | 5.1 | 0.34 |
| 4.15 x 10 ⁻⁴ | 5.80 | 3.18 | 0.4 | 0.50 |
| 8.30 x 10 ⁻⁴ | 5.50 | 4.34 | 0.4 | 0.64 |
| 1.25 x 10 ⁻³ | 5.32 | 5.19 | 0.7 | 0.71 |

Figure IV-10. Calibration curve for As(III) in 0.1 M
HClO₄ at Pt wire flow-through detector

flow rate = 1.15 ml min⁻¹

1.0 V vs. SCE

0.226 ml

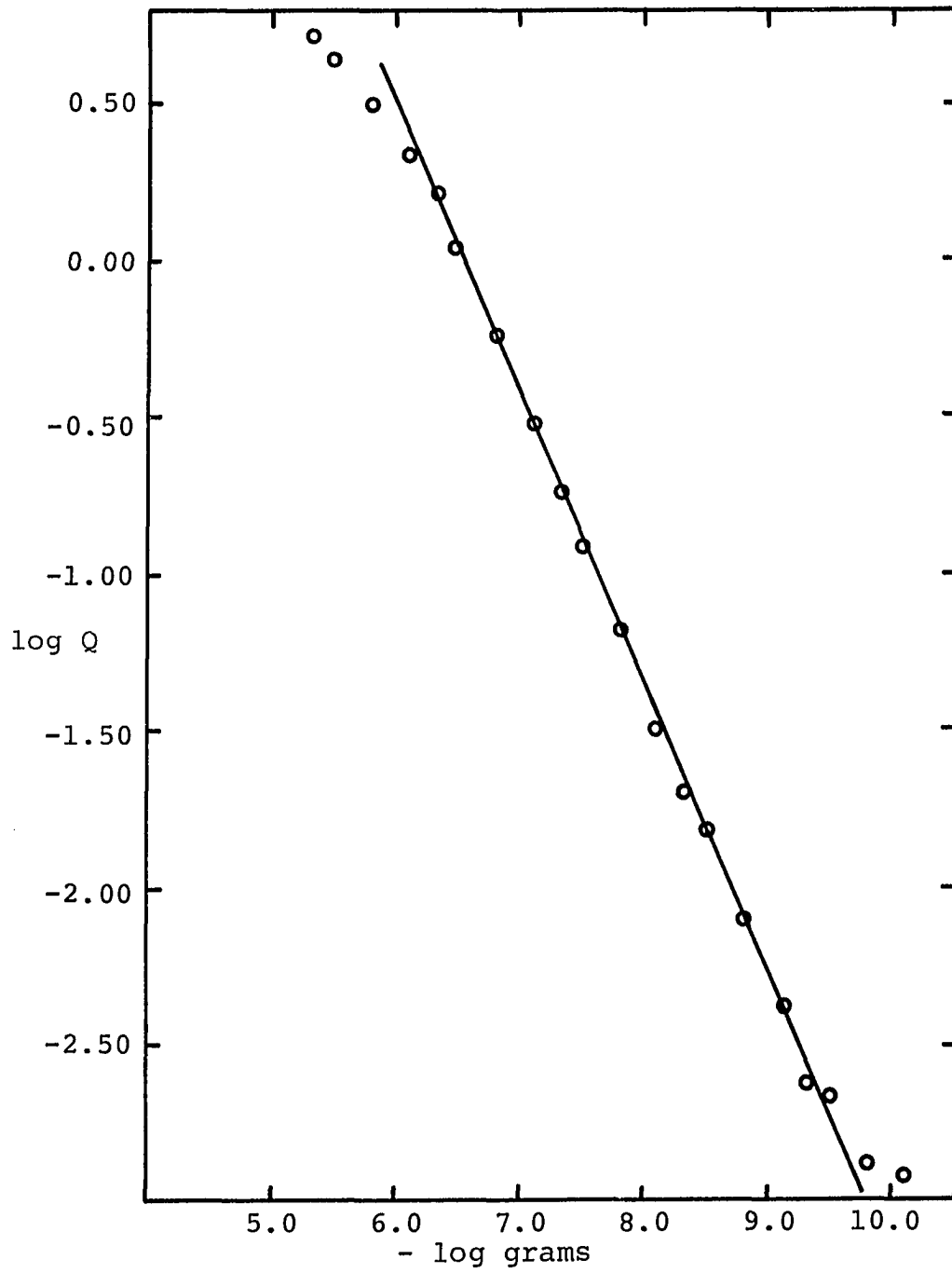


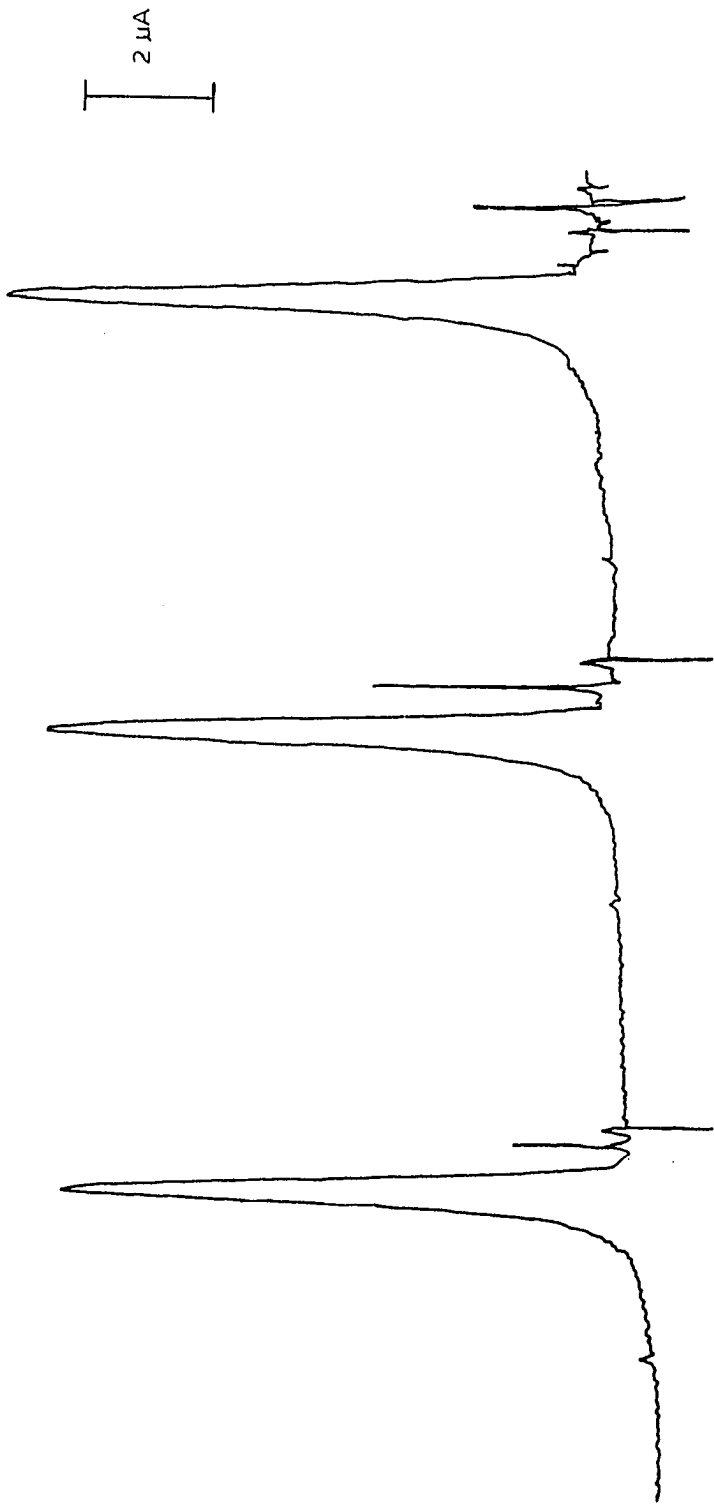
Figure IV-11. Typical signal peak for As(III) in 0.1 M HClO₄ at Pt flow-through detector

flow rate = 1.15 ml min⁻¹

1.0 V vs. SCE

0.226 ml

1.25 x 10⁻⁷ M As₂O₃



at least 30 minutes prior to the analysis. The detection potential must be above 0.90 V vs. SCE. The flow-through detector is laminar below a flow rate of 0.60 ml/min. A linear calibration curve is obtained over at least 3 orders of magnitude. Detection in the sub-nanogram region is possible.

V. CHOICE OF REDUCING AGENT FOR As(V)

A. Introduction

The electrode current observed for the reduction of As(V) at a Pt electrode in perchloric acid is not a linear function of the bulk concentration of As(V). Hence, the electroinactive form of arsenic, As(V), must be chemically converted to As(III). The reducing agent used must quantitatively convert the As(V) to As(III). Also, if the reducing agent is electroactive at the value of electrode potential used for detecting As(III), a means must be found to separate the As(III) from the reducing agent prior to the detection of As(III) in the sample.

The standard reduction potential for the As(V)-As(III) couple in an acidic medium is +0.314 V vs. SCE. Consequently, any reducing agent used must have a standard reduction potential less than +0.314 V vs. SCE. This chapter describes the study of a wide range of reducing agents in an attempt to find one that rapidly and quantitatively reduces As(V). Hydrazine sulfate proved to be the most suitable reducing agent.

B. Experimental

1. Procedure

An aliquot of a standard solution of As(V) was subjected to the reducing agent under study. The completeness of

the reaction was judged by injecting the solution into a flowing solution of acid. The area of the chromatographic peak obtained as the arsenic passed through the Pt wire detector was calculated. A calibration curve was prepared by injecting standard solutions of As(III) under the same conditions.

2. Standardization of As(V)

A solution of approximately 4×10^{-3} M As_2O_5 was prepared by dissolving 0.9 g As_2O_5 in 25 ml of 5 M NaOH. Triply distilled water was added to bring the solution volume to 1.00 l. A 15.00 ml aliquot of the As_2O_5 solution, 10 ml of 2 M H_2SO_4 and 1 g KI were placed in a 500 ml erlenmeyer flask. Iodide is a sufficiently powerful reducing agent to convert As(V) to As(III) quantitatively. The solution in the erlenmeyer was heated to boiling. When the sample turned a pale yellow, a few drops of 1 M $\text{Na}_2\text{S}_2\text{O}_3$ were added to make the solution clear. This step converted any I_2 formed back to I^- . The solution was then saturated with NaHCO_3 and transferred to a 100 ml volumetric flask. Triply distilled water was added to bring the total volume of liquid inside the flask to 100 ml.

A coulometric titration was performed using I_2 , electro-generated at a constant current, to determine the amount of arsenic in a 10.00 ml aliquot. The coulometric cell had three compartments interconnected with fritted glass disks.

The I_2 was generated in a solution containing 0.1 M KI, 0.1 M KH_2PO_4 , 0.1 M K_2HPO_4 and the arsenic aliquot. The anode was a cylindrical shaped Pt gauze electrode. The compartment housing the Pt cathode was filled with 0.1 M Na_2SO_4 . The intermediate chamber, separated from the anode and cathode compartments by fritted glass disks, was filled with a saturated solution of Na_2SO_4 . The Sargent Coulometric Source (Model IV), manufactured by the E. H. Sargent Co. in Chicago, IL, was used to electrogenerate the iodine. Starch was the end-point indicator. The time needed to titrate the sample was compared to the time needed to titrate a standard solution of As(III). The concentration of the As_2O_5 , as determined coulometrically, was 3.67×10^{-3} M.

C. Results and Discussion

1. Reducing columns

a. Metals The E° value for the Cd(II)-Cd couple is -0.16 V vs. SCE. Cadmium metal should be capable of reducing As(V) to As(III). A Cd rod was pulverized and the chips were packed into a chromatographic column. The column was placed between the injection port and the detector. A strong-acid, cation-exchange resin column was also placed in the eluent stream after the reducing column. A sample of As(V) was then injected. Unfortunately, the noise in

the detector signal was very large and the peak corresponding to the arsenic could not be distinguished from the noise. The noisy background was attributed to the production of H_2 when the acidic eluents passed through the Cd column. The metal used to pack the column was then amalgamated in an attempt to cut down the amount of H_2 produced. A noisy background was still obtained, however.

Zinc was investigated as a reductant. The E° value for the Zn(II)-Zn couple is -0.53 V vs. SCE. The same problems associated with Cd were evident with Zn, also. Zinc is often used as the reducing agent when atomic absorption spectroscopy is applied for the determination of arsenic. Volatile arsines can be produced under acidic conditions and aspirated directly into the flame.

Columns of copper, silver and nickel also were tried without any success.

b. Redox resins The idea of electron-exchange polymers was first developed by Cassidy and his co-workers (190-193). They prepared and studied various polymers, such as polyvinylhydroquinone, which are capable of reducing certain organic and inorganic species directly. The redox reactions generally proceed very slowly, however. Since then, several researchers have utilized redox systems adsorbed on ion-exchange resins. For example, a stannous chloride complex bound to an anion-exchange resin was used

to reduce Fe(III) to Fe(II) in HCl (194). Chromium(VI) in an acidic solution was reduced to Cr(III) on a cation-exchange resin in the Fe(III) form (195). Also, AsO_4^{-3} or AsO_3^{-3} , adsorbed on an anion-exchange resin, was reduced to arsenic metal when 1 M SnCl_2 was passed through the column (196).

An attempt was made to reduce the As(V) to As(III) on a redox resin placed directly in the flow-through system. Iron(II) adsorbed on a strong-acid cation-exchange resin and Sn(II) adsorbed on both strong-acid, cation and strong-base, anion exchange resins were investigated as reducing systems. The results were not reproducible. The resins are also capable of reducing oxygen in the eluent stream. Consequently, the reducing capacity of the resins diminish with time. If oxygen could be eliminated from the system, exciting in situ reactions would be possible in the eluent stream.

2. Iodide

Many researchers have used KI as the reductant for As(V) in acidic solutions (32, 31, 74-76, 197). The E° value for the $\text{I}_2\text{-I}^-$ couple is 0.29 V vs. SCE. The reaction is quantitative. Unfortunately, I^- is electroactive at 1.0 V vs. SCE, the potential applied to the Pt wire detector to determine As(III). Several attempts were made to separate I^- from As(III) on an ion-exchange resin.

If an anion-exchange resin is placed in a flowing stream of HClO_4 , the ClO_4^- is retained so strongly by the

resin that I^- passes through the chromatographic column unretained. Consequently, I^- can not be separated from As(III) when the eluent is $HClO_4$.

In an eluent of 9 M HCl, As(III) exists as a negatively charged chloride complex. The complex should be retained on an anion-exchange resin while I^- should not be retained. A separation of As(III) and I^- should be feasible in 9 M HCl. The As(III) should elute in 0.1 M HCl (198). This separation scheme was tried. The Pt wire detector was potentiostated at 1.0 V vs. SCE. When the eluent was 9 M HCl, a peak corresponding to I^- was observed. When the eluent was changed to 0.1 M HCl, however, an enormous change in the background current resulted. By the time the background current became established at the new level, the As(III) had passed through the detector. The current corresponding to the oxidation of As(III) could not be distinguished from the change in the background signal. This separation scheme is unsatisfactory.

The effect of the presence of I^- on the electrochemical behavior of As(III) in $HClO_4$ was studied by cyclic voltammetry. The current-potential curves are shown in Figure V-1. The $E_{1/2}$ value for the oxidation of As(III) to As(V) shifts in a positive direction as the concentration of I^- increases. In a flow-through system, I^- must not be allowed to pass through the detector if a constant signal is expected

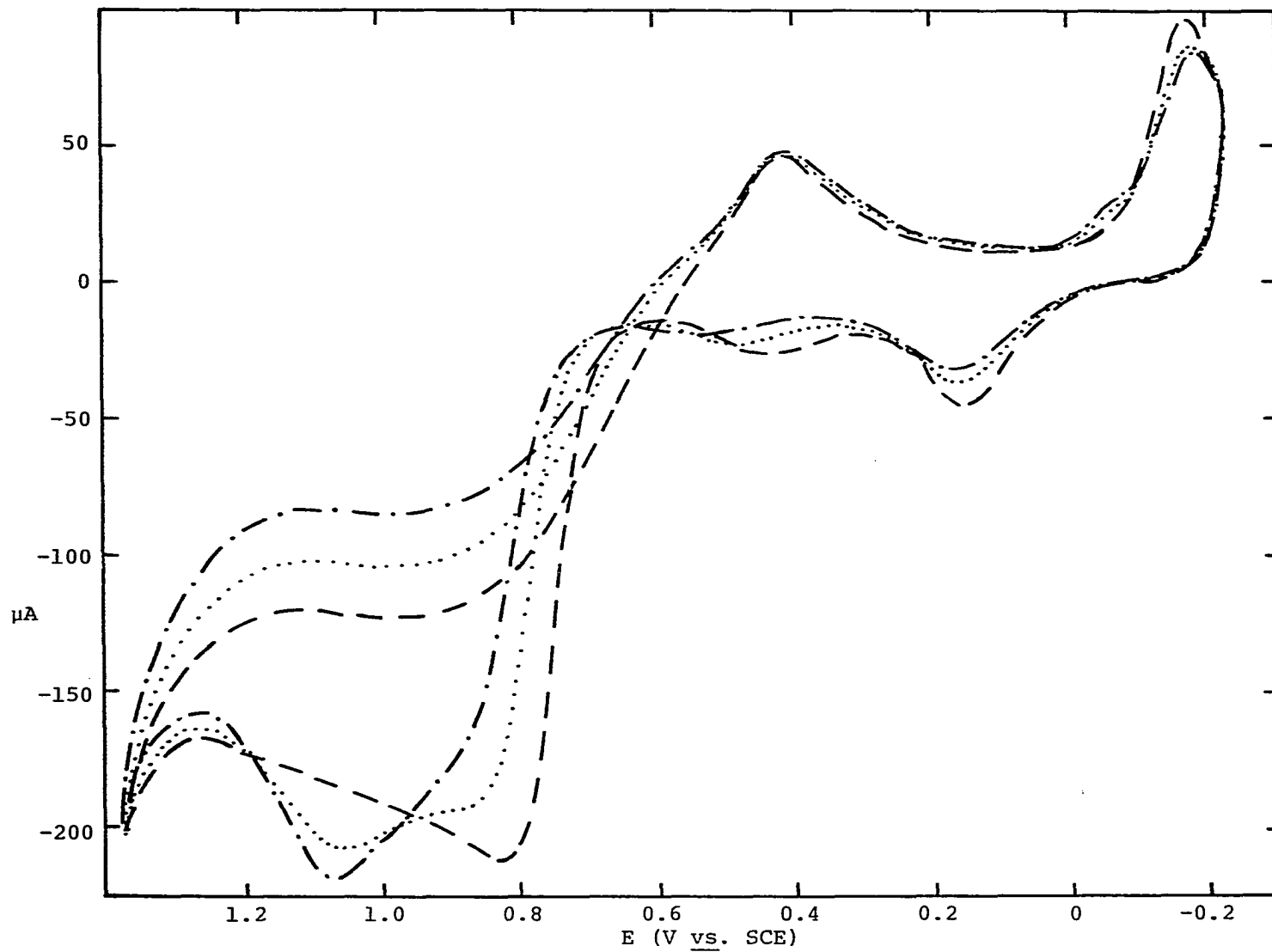
Figure V-1. Effect of I^- on cyclic voltammetry of As(III) in 0.5 M $HClO_4$ at Pt disk

Rotation speed - 3600 rev min⁻¹
Potential scan rate - 1 V min⁻¹

----- 7.17 x 10⁻⁵ M As_2O_3
0.5 M $HClO_4$

..... 0.1 ppm NaI
7.17 x 10⁻⁵ M As_2O_3
0.5 M $HClO_4$

-.-.-.- 0.3 ppm NaI
7.17 x 10⁻⁵ M As_2O_3
0.5 M $HClO_4$



for a given concentration of As(III). No further separation schemes were investigated for As(III) and I^- .

3. Stannous

Pentavalent arsenic has been reduced by $SnCl_2$ in HCl (38, 52, 46). However, Cl^- slightly alters the electrochemistry of As(III) at a Pt disk as shown in Chapter II. Stannous sulfate in $HClO_4$ was investigated as a reducing agent for As(V). The solutions were very cloudy and the reaction did not proceed quantitatively even when the solutions were heated. However, when $SnCl_2$ was substituted for $SnSO_4$, the solutions were clear. A complexing agent, such as Cl^- , must be present in the solution to prevent the hydrolysis of Sn(II). If the Sn(II) is hydrolyzed, no reaction between As(V) and Sn(II) can occur. The evaluation of the completeness of the reaction between the $SnCl_2$ and As(V) was a problem. The samples contained As(III), excess Sn(II) and some Sn(IV) formed during the reduction of As(III). A strong-acid, cation-exchange resin was placed in an eluent stream of 0.5 M $HClO_4$ to retain the cationic tin species. The first samples injected gave sharp chromatographic peaks for the oxidation of As(III). As time progressed, however, the peaks began to spread out. Eventually, no peaks could be obtained when a sample was injected. In order to understand what effect, if any, the various species of tin exerted on the chromatographic

behavior of As(III), three different column packing materials were prepared. The first column was packed with a strong-acid, cation-exchange resin which had equilibrated in a solution of 0.5 M HClO_4 overnight. The second column was packed with strong-acid, cation-exchange resin which had equilibrated overnight in a solution of SnCl_2 in 0.5 M HClO_4 . The third column was packed with a strong-acid, cation-exchange resin which had equilibrated overnight in a solution of SnCl_4 in 0.5 M HClO_4 . Each column was placed in a stream of 0.5 M HClO_4 between the injection port and the Pt wire detector. A standard solution of As(III) in 0.5 M HClO_4 was injected. Sharp chromatographic peaks were obtained when the first and second columns were placed in the eluent stream. No arsenic was detected when the third column was in the stream. Flushing the resin with 4 M HClO_4 had no effect on the behavior of the third column. When the first column was replaced in the eluent stream, sharp peaks were obtained for the oxidation of As(III). This verified that the problem was indeed in the third column and not the detector. The Sn(IV), which is strongly retained on the cation-exchange resin in the third column, acts like a gathering agent for As(III). When only a small amount of Sn(IV) is on the resin, the peak for As(III) spreads out. However, when the amount of Sn(IV) on the resin is high, no As(III) can pass through the column.

There are too many variables involved when Sn(II) is used as a reducing agent for As(V) so the search for a suitable reducing agent continued.

4. Copper(I)

The cuprous ion has been successfully used for the reduction of As(V) in solutions with a high concentration of Cl^- . When Cl^- is present in the solution, the E° value for the Cu(II)-Cu(I) couple is 0.29 V vs. SCE. When the arsenic in the sample is distilled as AsCl_3 , Cu_2Cl_2 is a common reductant (30, 125, 152). The large halide concentrations needed for the reductions are not compatible with the electrochemical determination of As(III) at the Pt wire electrode. Therefore, the cuprous ion was not given further consideration as a reducing agent.

5. Titanium(III)

The Ti(III)-TiO(II) couple has an E° value of -0.15 V vs. SCE. Titanous sulfate can be prepared by dissolving Ti metal in H_2SO_4 and storing the solution under H_2 . The solution is not stable and would not be a practical reducing agent for routine analysis.

6. Sulfur(IV)

The use of S(IV) as a reducing agent for As(V) has been reported (35, 156). Both sulfite and meta-bisulfite

have been used. The E° values for the half-reaction involving sulfite is +0.074 V vs. SCE. The E° value for the meta-bisulfite half reaction is 0.11 V vs. SCE. The products of the reduction reaction are As(III) and $\text{SO}_4^{=}$. Sulfate is not electroactive so no separation step is required to remove the $\text{SO}_4^{=}$ from the As(III). The excess $\text{SO}_3^{=}$ and $\text{S}_2\text{O}_5^{=}$ can be removed by boiling the solution to expel SO_2 . Nitrogen gas generally must be bubbled through the solution to remove the last traces of SO_2 . Forsberg and co-workers reported an average percent reduction of 97.6 with a relative standard deviation of 6.9% when the reaction was performed in 2 M HClO_4 using Na_2SO_3 (156). The solutions were heated for 1 hour between 80°C and 100°C. The value reported by Forsberg could not be reproduced in this laboratory. The average percent reduction was 39.5 with a relative standard deviation of 3.4% when Na_2SO_3 was the reducing agent. When $\text{Na}_2\text{S}_2\text{O}_8$ was the reductant, the average percent reduction was 34.1 with a relative standard deviation of 0.9%.

7. Hydrazine

The most successful reducing agent found for the conversion of As(V) to As(III) was hydrazine sulfate. Reports of the application of hydrazine sulfate as the reducing agent appear in the literature (151, 154, 199-201). This reducing agent is particularly attractive because the

products are N_2 and As(III). The production of N_2 helps drive the reaction to completion because of the volatility of N_2 . The E° value for the $N_2H_5^+ - N_2$ couple is -0.48 V vs. SCE. Any excess $N_2H_5^+$ can be retained on a strong-acid, cation-exchange resin in the eluent stream. A 2.00 ml aliquot of 3.67×10^{-3} M As_2O_5 , 0.2 g $N_2H_2 \cdot H_2SO_4$ and 5 ml concentrated H_2SO_4 were heated in a 30 ml Kjeldahl flask until fumes of sulfuric acid evolved. The solution was then quantitatively transferred to a 100 ml volumetric flask. The sample plus the As(III) standards were injected into a stream of 0.1 M $HClO_4$. According to the calibration curve, the average percent reduction was 95.9 with a relative standard deviation of 0.9%. At least a dozen injections of the sample containing the reduced arsenic and hydrazine sulfate could be made before the hydrazine began to bleed off the strong-acid, cation-exchange resin. At this point, the eluent was switched to 4 M $HClO_4$ so that the elution of the hydrazine from the resin could be accomplished rapidly. After the hydrazine had been flushed from the resin, the eluent was switched back to 0.1 M $HClO_4$. The entire cycle for removing the hydrazine from the resin took approximately 15 minutes.

D. Conclusions

Various reducing agents were investigated for As(V). Hydrazine sulfate was the most successfully applied. The

excess hydrazine can be separated from the As(III) on a strong-acid, cation-exchange resin in 0.1 M HClO₄.

VI. INTERFERENCES

A. Introduction

A wide range of species was investigated to determine which would interfere during the anodic amperometric determination of As(III) in a Pt wire detector. Any species that will pass through the strong-acid, cation-exchange resin unretained and is electroactive at 1.0 V vs. SCE on a Pt surface will interfere. Anions, cations and neutral species were investigated. The only interferences discovered were from Br^- , I^- , NO_2^- and Sb(III).

B. Experimental

1. Reagents

All reagents used were of analytical reagent grade. The water was triply distilled. When anions were being investigated as interferences, the sodium salt was used. When metal cations were being investigated, the nitrate or sulfate salts were used. To study the effect of Se(IV), Se metal was dissolved in hot HNO_3 . Tellurium(IV) was obtained by dissolving Te metal in H_2SO_4 . Germanium(IV) was prepared by the dissolution of GeO_2 in 2 M NaOH. Antimony(III) was prepared by dissolving Sb_2O_3 in H_2SO_4 .

2. Procedure

For the species investigated that were in the form of a salt, 0.10 g was weighed out and placed in a 100 ml volumetric flask. All the solutions containing the species under study were 3.59×10^{-4} M As_2O_3 and 0.1 M HClO_4 as well. The solutions were injected into a flowing stream of 0.1 M HClO_4 which passed through the Pt wire detector potentiostated at 1.0 V vs. SCE. The area of the chromatographic peak was recorded and compared to the area of the peak obtained when simply 3.59×10^{-4} M As_2O_3 in 0.1 M HClO_4 was injected.

For Te(IV), Ge(IV), Se(IV) and Sb(III), the solutions compared to determine the percent current change contained the same type and amount of acid. The concentration of As_2O_3 in all the samples was 3.59×10^{-4} M.

C. Results and Discussion

The results of the interference study are shown in Table VI-1. The relative change in electrode response, as percent, was calculated from the difference in the peak area produced by a solution containing the species under study and arsenic and the peak area produced by a solution containing only arsenic.

The only serious interferences discovered were from I^- , Br^- , NO_2^- and Sb(III). As pointed out in Chapter V, however,

Table VI-1. Interference study

| Species | [Species]/[As(III)] | % Current change |
|------------------------------|---------------------|------------------|
| Cl ⁻ | 23.8 | 1.8 |
| Br ⁻ | 13.5 | >100 |
| I ⁻ | 9.3 | >100 |
| SO ₄ ⁼ | 8.3 | 1.6 |
| PO ₄ ⁻ | 9.1 | 3.4 |
| NO ₃ ⁻ | 8.7 | 1.4 |
| NO ₂ ⁻ | 9.5 | >100 |
| Sr(II) | 4.6 | 2.9 |
| Bi(III) | 4.2 | 0.9 |
| Cd(II) | 6.7 | 2.9 |
| Ti(III) | 9.6 | 1.8 |
| VO(II) | 8.6 | 0.9 |
| Cr(III) | 7.1 | 3.7 |
| Cu(II) | 7.4 | 1.2 |
| Zn(II) | 8.6 | 0.9 |
| Co(II) | 7.6 | 1.5 |
| Ba(II) | 5.3 | 0.3 |
| Mn(II) | 7.6 | 0.9 |
| Ni(II) | 7.6 | 0.9 |
| Fe(III) | 7.0 | 2.5 |
| Pb(II) | 4.2 | 2.0 |
| Fe(II) | 9.2 | 1.0 |

Table VI-1. continued

| Species | [Species]/[As(III)] | % Current change |
|----------------------|---------------------|------------------|
| Ag(I) | 8.2 | 1.9 |
| Tl(I) | 5.2 | 1.3 |
| Al(III) | 4.4 | 0.3 |
| Hg ₂ (II) | 5.3 | 1.3 |
| Hg(II) | 4.3 | 1.9 |
| Se(IV) | 161.8 | 4.9 |
| Te(IV) | 41.7 | 3.5 |
| Ge(IV) | 171.0 | 4.4 |
| Sb(III) | 43.9 | 84.9 |
| Sn(II) | 9.8 | 1.5 |
| Sn(IV) | 8.7 | 2.1 |

if large quantities of Sn(IV) accumulate on the cation-exchange resin, the As(III) is strongly retained by the resin. Consequently, Sn(IV) should also be considered an interference.

The halides, Br^- and I^- , interfere in two ways. First of all, their presence causes the oxidation of As(III) to proceed more irreversibly. Secondly, the halides are electroactive at 1.0 V vs. SCE. Nitrite undergoes oxidation to NO_3^- at the detection potential for arsenic and so it also interferes with the determination. Antimony(III) appears to adsorb on the surface of the Pt electrode and inhibit the oxidation of As(III).

D. Conclusion

The determination of As(III) in a perchloric acid eluent at 1.0 V vs. SCE at a Pt flow-through detector has few interferences. Most of the species commonly found with arsenic do not interfere. The only serious interferences discovered were from Sb(III), NO_2^- , Br^- and I^- .

VII. DETERMINATION OF ARSENIC IN ORCHARD LEAVES

A. Introduction

To verify that the anodic amperometric method for the determination of arsenic in a Pt flow-through detector could be used on real samples, orchard leaves obtained from the National Bureau of Standards were analyzed. This chapter describes the dissolution, reduction and analysis of the NBS orchard leaves.

B. Experimental

The flow-through system and the Pt wire flow-through detector used for the determination of arsenic in the orchard leaves are described in Chapter IV.

C. Results and Discussion

1. Choice of eluent

The eluent used in Chapter IV was 0.1 M HClO₄. The use of 0.1 M HClO₄ as an eluent allowed at least a dozen sample injections to be made before the hydrazine began to bleed off the strong-acid, cation-exchange resin. However, when real samples are being analyzed, a large amount of acid is often necessary to accomplish dissolution. The acid concentration in the sample may be ten times as large as the acid concentration of the eluent. The large acid

concentration in the sample causes the displacement of some of the hydrazine present on the column. Therefore, repetitive injections of a sample containing the reduced arsenic and the excess hydrazine results in peaks which get progressively larger. This is shown in Figure VII-1. The sample volume was 0.226 ml. The flow rate was 1.5 ml min⁻¹. The sample was 1.93×10^{-6} M As(III) and 0.03 g ml⁻¹ hydrazine sulfate in 1.2 M HClO₄ and 1.8 M H₂SO₄. The eluent was 0.1 M HClO₄. To more closely match the concentration of acid in the sample, an eluent stream of 1.0 M HClO₄ was used. The use of a more concentrated eluent would have resulted in very poor separation of the As(III) from the hydrazine. Unfortunately, only one sample could be injected before the hydrazine began to come off the column.

2. Dissolution of orchard leaves and reduction of As(V)

The reduction procedure described in Chapter V using hydrazine was carried out in sulfuric acid. Most samples, however, can not be dissolved simply in sulfuric acid. The dissolution of the orchard leaves, for example, was completed only in the presence of nitric, sulfuric and perchloric acids.

Initially, an aliquot of a standard solution of As(III) was heated in 15 ml HNO₃, 15 ml H₂SO₄ and 15 ml HClO₄ in a 250 ml erlenmeyer flask. A reflux condenser was placed above

Figure VII-1. Effect of hydrazine sulfate on signal peaks for As(III) in samples with high acid concentrations

Pt wire flow-through detector

1.0 V vs. SCE

flow rate = 1.5 ml min⁻¹

0.1 M HClO₄ eluent

0.226 ml sample

1.93 x 10⁻⁶ M As(III)

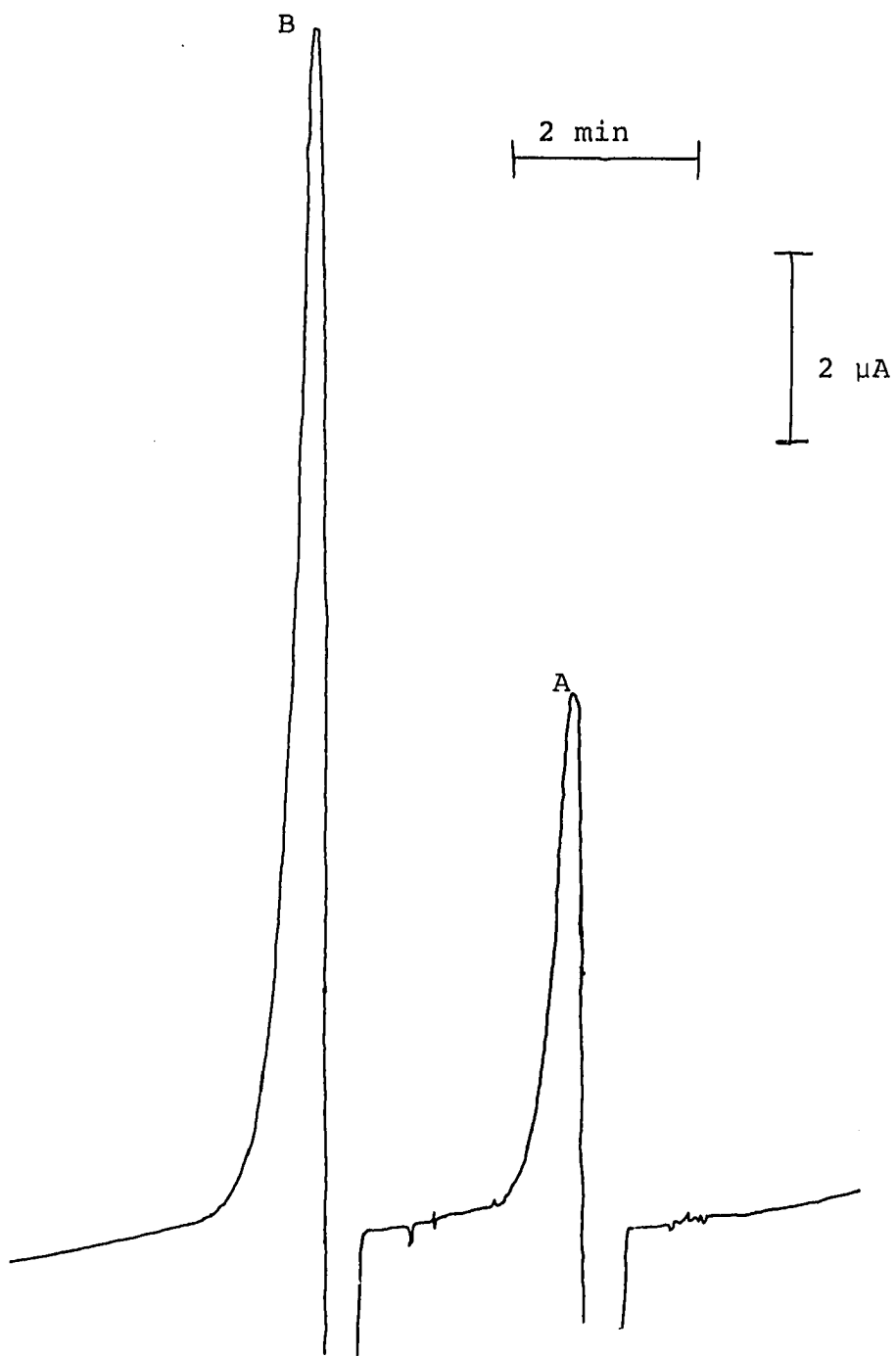
1.8 M H₂SO₄

1.2 M HClO₄

5 x 10⁻² g ml⁻¹ N₂H₄·H₂SO₄

A. First injection

B. Second injection



the flask. Copious fumes of nitrous oxide appeared above the liquid phase during the early stages of dissolution. Eventually the redish brown fumes disappeared and were replaced by white fumes. At this point the dissolution process was discontinued. One hundred ml water and 0.3 g hydrazine sulfate were added next. The solution was boiled down to 50 ml. Upon cooling, the sample was transferred to a 100 ml volumetric flask. Triply distilled water was the diluent. The solution was expected to contain only As(III) and excess hydrazine. However, a second peak appeared between the arsenic and hydrazine peaks as shown in Figure VII-2. According to retention time data, the second peak was tentatively identified as hydroxylamine. Thermodynamically, however, hydroxylamine should not form. When As(V) reacts with hydrazine, the hydrazine should be oxidized all the way to nitrogen gas. When the orchard leaves were subjected to this dissolution and reduction procedure, high results were always obtained.

Because the reduction procedure had worked so beautifully in Chapter V when only sulfuric acid was present, the perchloric acid was removed by distillation prior to the addition of the reducing agent. Again, the sample was dissolved in 15 ml HNO_3 , 15 ml H_2SO_4 and 15 ml HClO_4 . The sample was heated until white fumes of sulfuric acid evolved. This was verified by placing a thermometer in the flask.

Figure VII-2. Reduction of As(III) with $\text{N}_2\text{H}_4 \cdot \text{H}_2\text{SO}_4$ in presence of HClO_4 and H_2SO_4

Pt wire flow-through detector

1.0 V vs. SCE

flow rate = 1.15 ml min^{-1}

1 M HClO_4 eluent

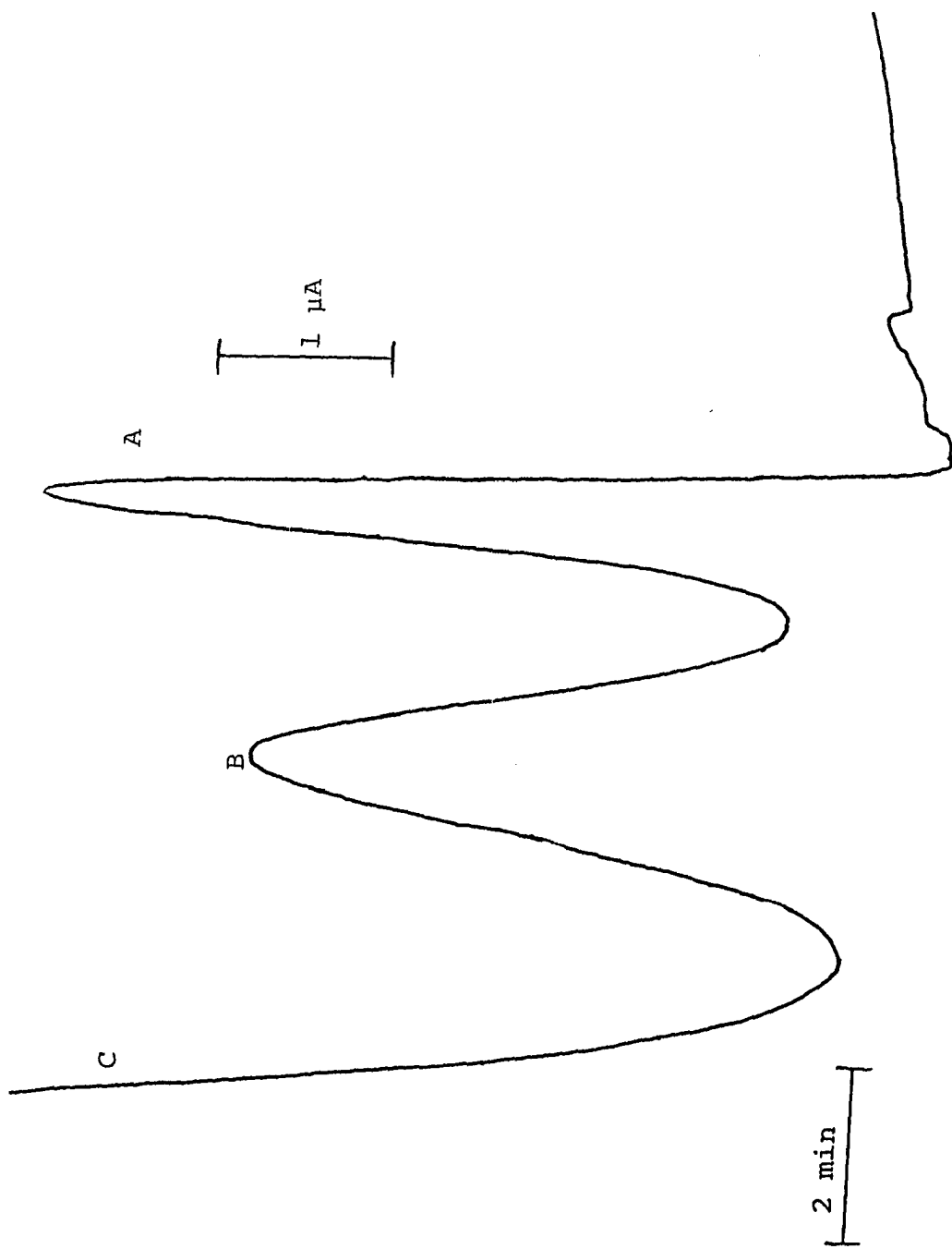
0.226 ml

1.93×10^{-6} M As(III), 1.8 M H_2SO_4 ,

1.2 M HClO_4 , $5 \times 10^{-2} \text{ g ml}^{-1}$

hydrazine sulfate

- A. As(III)
- B. hydroxylamine
- C. hydrazine sulfate



The temperature must be above 204°C, the boiling point of HClO_4 . Upon cooling, 50 ml water and 0.3 g hydrazine sulfate were added. The solution was reheated until fumes of sulfuric acid evolved. The contents of the flask were cooled to room temperature and transferred to a 100 ml volumetric flask. Triply distilled water was the diluent. A 5.00 ml aliquot of the sample was diluted to 10.00 ml. Figure VII-3 contains the data for 3 injections into the flow stream. The first and second peaks correspond to the injection of a sample containing 6.44×10^{-4} M As(III) and 1.35 M H_2SO_4 . The third injection was made from a solution containing the same concentration of As(III) but which was subjected to the dissolution and reduction process. The only acid left in this sample should be H_2SO_4 and the concentration of the H_2SO_4 should be 1.35 M. No extraneous peaks resulted when this dissolution and reduction procedure was used. The size of the peak corresponding to the oxidation of As(III) was the same for both the sample subjected to the dissolution and reduction process and for the sample not subjected to the process. The reduction, therefore, was quantitative and resulted in no loss of As(III).

NBS Standard Reference Material 1571 (orchard leaves) was analyzed. Table VII-1 lists the constituents present in the orchard leaves and their concentration. Standards were prepared from As_2O_3 in H_2SO_4 . The standards contained

Figure VII-3. Reduction of As(III) with $\text{N}_2\text{H}_4 \cdot \text{H}_2\text{SO}_4$ in presence of H_2SO_4

Pt wire flow-through detector

1.0 V vs. SCE

flow rate = 1.15 ml min⁻¹

1.0 M HClO₄ eluent

0.226 ml

A. Injection of 3.22×10^{-4} M As(III) in 1.35 M H₂SO₄

B. Injection of 3.22×10^{-4} M As(III) in 1.35 M H₂SO₄

C. Injection of 3.22×10^{-4} M As(III) and 3×10^{-2} g ml⁻¹
N₂H₄ · H₂SO₄ in 1.35 M H₂SO₄ (subjected to dissolution
and reduction procedure)

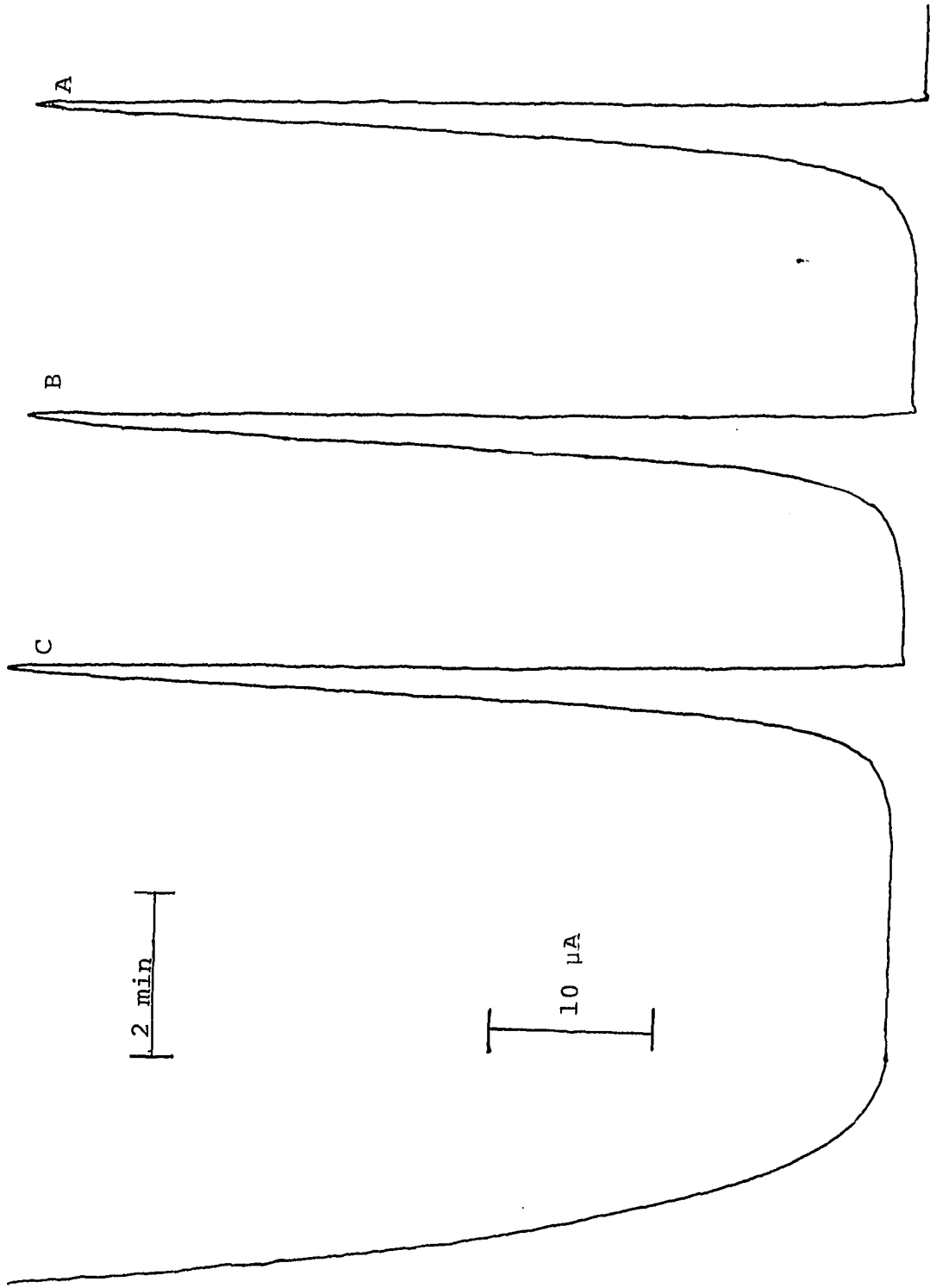


Table VII-1. Constituents present in NBS SRM 1571 (orchard leaves)

| Constituent | Concentration |
|-------------|---------------|
| Nitrogen | 2.76 ± 0.05% |
| Calcium | 2.09 ± 0.03% |
| Potassium | 1.47 ± 0.03% |
| Magnesium | 0.62 ± 0.02% |
| Phosphorus | 0.21 ± 0.01% |
| Iron | 300 ± 20 ppm |
| Manganese | 91 ± 4 |
| Sodium | 82 ± 6 |
| Lead | 45 ± 3 |
| Boron | 33 ± 3 |
| Zinc | 25 ± 3 |
| Arsenic | 14 ± 2 |
| Copper | 12 ± 1 |
| Rubidium | 12 ± 1 |
| Nickel | 1.3 ± 0.2 |
| Mercury | 0.155 ± 0.015 |
| Cadmium | 0.11 ± 0.02 |
| Selenium | 0.08 ± 0.01 |
| Uranium | 0.029 ± 0.005 |

the same concentration of sulfuric acid as was present in the sample. The signal peaks used to construct the calibration curve and the signal peak resulting from the arsenic present in the orchard leaves in one of the samples is shown in Figure VII-4. The calibration curve based on the measurement of peak heights is shown in Figure VII-5 for the same sample. The amount of arsenic in the sample, as reported by the NBS using neutron activation analysis, is 14 ± 2 ppm. The average amount of arsenic in the sample, as determined by the method described in this thesis, is 13.7 ± 1.4 ppm.

Great care must be taken to ensure that the flask containing the sample is heated sufficiently to evolve H_2SO_4 before the reducing agent is added. This will guarantee that the chlorine, a decomposition product of $HClO_4$, has been completely removed. If the reducing agent is added before the chlorine has been removed, $AsCl_3$ can form. $AsCl_3$ can boil off at $130^\circ C$ and cause low results.

D. Conclusion

A sample of NBS Standard Reference Material 1571 (orchard leaves) was analyzed for arsenic. The sample was dissolved in HNO_3 , H_2SO_4 and $HClO_4$. The solution was heated until fumes of sulfuric acid evolved from the flask. Hydrazine sulfate was used as the reducing agent. A calibration curve was prepared.

Figure VII-4. Signal peaks used to construct calibration curve and signal peak due to As(III) in NBS orchard leaves

Pt wire flow-through detector

1.0 V vs. SCE

flow rate = 1.15 ml min⁻¹

1.0 M HClO₄ eluent

0.226 ml

- A. Injection of 1.92×10^{-6} M As(III) in 1.35 M H₂SO₄
- B. Injection of 1.59×10^{-6} M As(III) in 1.35 M H₂SO₄
- C. Injection of 1.27×10^{-6} M As(III) in 1.35 M H₂SO₄
- D. Injection of 9.54×10^{-7} M As(III) in 1.35 M H₂SO₄
- E. Injection of orchard leaves (1.2778 g in 200 ml)

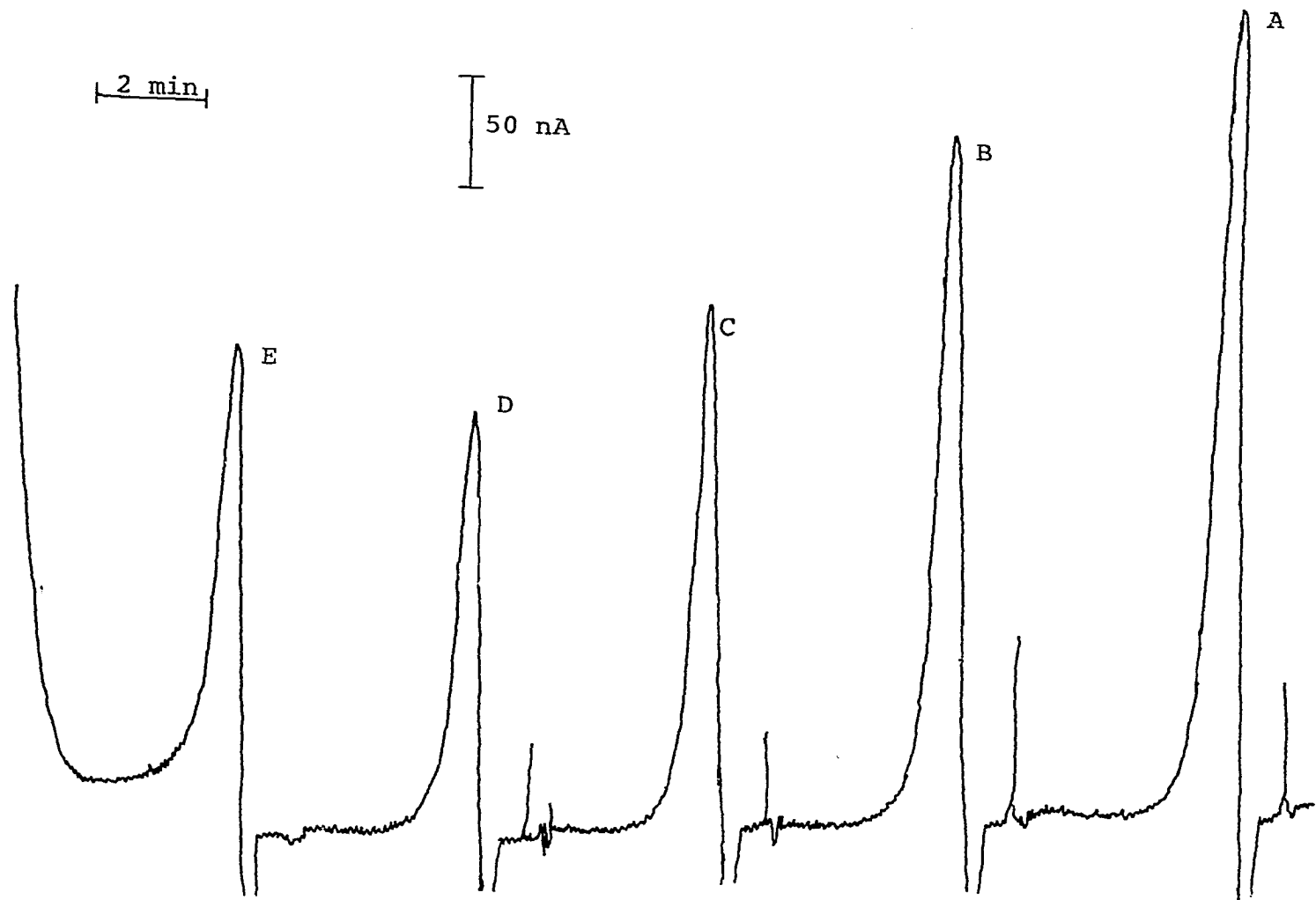


Figure VII-5. Calibration curve for NBS orchard leaves
sample

Pt wire detector

1.0 V vs. SCE

flow rate = 1.15 ml min⁻¹

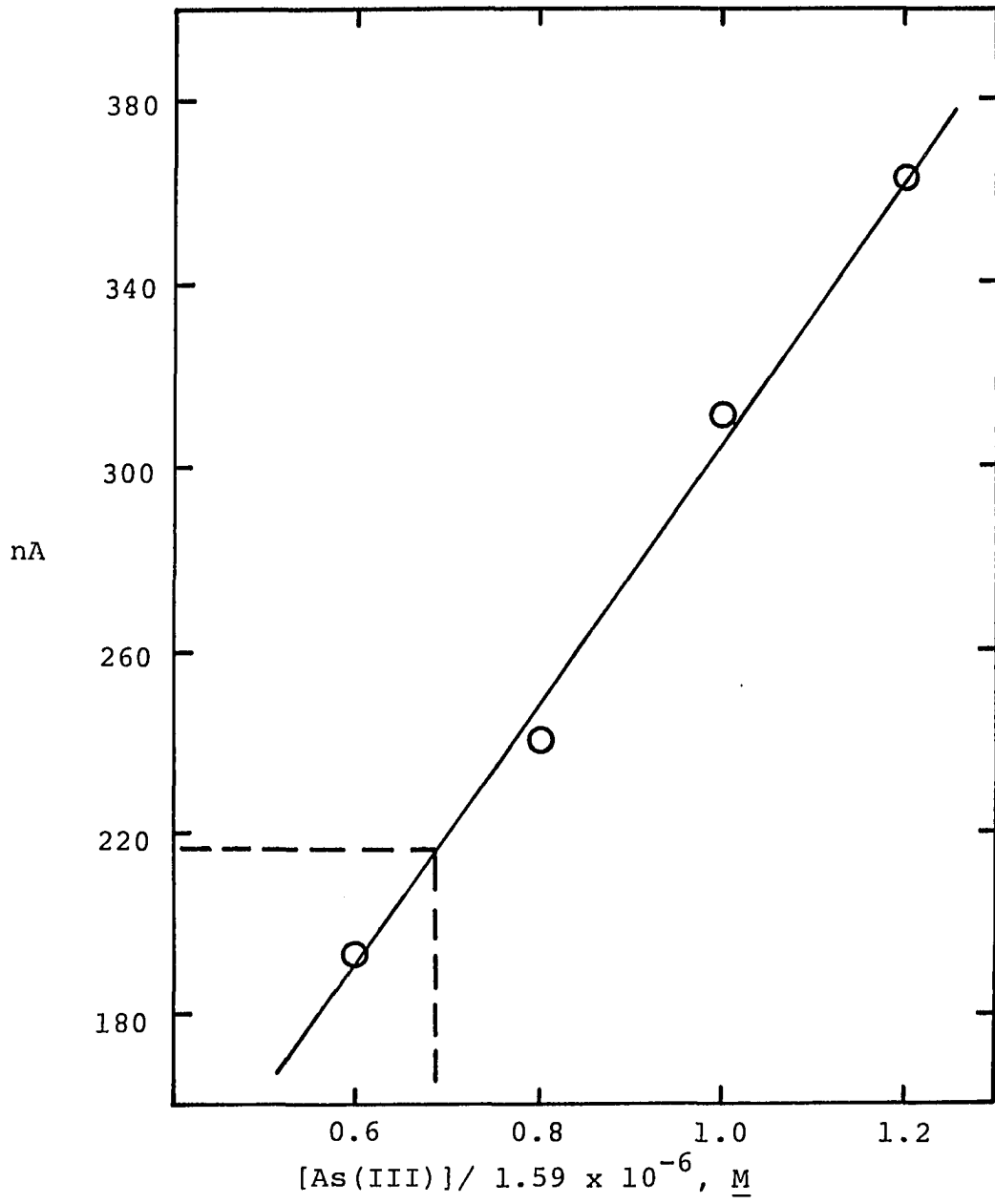
1.0 M HClO₄

0.226 ml

Concentration of As(III):

$$\frac{0.69 (1.59 \times 10^{-6} \text{ moles/l}) (0.2 \text{ l}) (74.9 \text{ g/l mole})}{1.2778 \text{ g}}$$

= 12.9 ppm



VIII. SUGGESTIONS FOR FUTURE RESEARCH

The reduction of As(V) with hydrazine in the presence of perchloric acid needs further investigation. The formation of hydroxylamine, an apparent by-product of the reaction, should not be stable thermodynamically.

The use of redox resins as the reducing agent for As(V) offers exciting possibilities. Oxygen must be removed from the flow-through system. Constructing a flow-through system out of metal lined with plastic, such as that used to make cans for Coca-Cola, would be one approach to the problem. With a column of redox resin placed directly in the eluent stream, the amount of sample pretreatment needed would be greatly reduced.

IX. BIBLIOGRAPHY

1. J. F. Ferguson and J. Gavis, *Water Research*, 6, 1259 (1972).
2. A. L. Reeves, in Health Effects of Occupational Lead and Arsenic Exposure: A Symposium, edited by B. W. Carnow (U.S. GPO, Washington, D.C., 1976), p. 237.
3. B. Fowler, in Health Effects of Occupational Lead and Arsenic Exposure: A Symposium, edited by B. W. Carnow (U.S. GPO, Washington, D.C., 1976), p. 248.
4. H. G. Offner and E. F. Witucki, *J. Amer. Water Works Assoc.*, 60, 947 (1968).
5. J. Savory and F. A. Sedor, in Clinical Chemistry and Chemical Toxicity of Metals, edited by S. S. Brown (Elsevier/North-Holland Biomedical Press, New York, 1977), p. 271.
6. S. A. Peoples, in Arsenical Pesticides, edited by E. A. Woolson (American Chemical Society, Washington, D.C., 1975), p. 1.
7. B. L. Vallee, D. D. Ulmer and W. E. C. Wacker, *Arch. Ind. Health*, 21, 132 (1960).
8. J. J. Dulka and T. H. Risby, *Anal. Chem.*, 48, 640A (1976).
9. A. L. Reeves, in Health Effects of Occupational Lead and Arsenic Exposure: A Symposium, edited by B. W. Carnow (U.S. GPO, Washington, D.C., 1976), p. 265.
10. A. M. Lee and J. F. Fraumeni, Jr., *J. Nat. Cancer Inst.*, 42, 1045 (1969).
11. C. Baroni, G. J. van Esch and U. Saffioti, *Arch. Environ. Health*, 7, 668 (1963).
12. J. E. Milner, *Arch. Environ. Health*, 18, 7 (1969).
13. D. V. Frost, *Fed. Proc.*, 26, 194 (1967).
14. D. V. Frost, *World Rev. Pest Control*, 9, 6 (1970).
15. D. V. Frost, L. R. Overby and H. C. Spruth, *J. Agric. Food Chem.*, 3, 235 (1955).

16. D. V. Frost, *Poultry Sci.*, 32, 217 (1953).
17. W. R. Penrose, *CRC Critical Reviews in Environ. Control*, 4, 465 (1974).
18. K. Nelson, in Health Effects of Occupational Lead and Arsenic Exposure: A Symposium, edited by B. W. Carnow (U.S. GPO, Washington, D.C., 1976), p. 220.
19. H. A. Schroeder and J. B. Balassa, *J. Chronic Diseases*, 19, 85 (1966).
20. E. J. Underwood, in Toxicants Occurring Naturally in Foods, edited by Committee on Food Protection, National Research Council (National Academy of Sciences, Washington, D.C., 1966), p. 43.
21. J. R. Goldsmith, M. Deane, J. Thom and G. Gentry, *Water Research*, 6, 1133 (1972).
22. Y. Talmi and C. Feldman, in Arsenical Pesticides, edited by E. A. Woolson (American Chemical Society, Washington, D.C., 1975), p. 13.
23. Y. Talmi and D. T. Bostick, *J. Chromatogr. Sci.*, 13, 231 (1975).
24. J. E. Portman and J. P. Riley, *Anal. Chim. Acta*, 31, 509 (1964).
25. R. F. Milton and W. A. Walters, Methods of Quantitative Micro-analysis (Edward Arnold, Ltd., London, 1955). Second edition.
26. R. M. Sachs, J. L. Michael, F. B. Anastasia and W. A. Wells, *Weed Sci.*, 19, 412 (1971).
27. W. O. Robinson, H. C. Dudley, K. T. Williams and H. G. Byers, *Ind. Eng. Chem., Anal. Ed.*, 6, 274 (1934).
28. R. C. Chu, G. P. Barron and P. A. Q. Baumgarner, *Anal. Chem.*, 44, 1476 (1972).
29. A. L. Chaney and H. J. Magnuson, *Ind. and Eng. Chem., Anal. Ed.*, 12, 691 (1940).
30. P. H. Davis, G. R. Dulude, R. M. Griffin, W. R. Matson and E. W. Zink, *Anal. Chem.*, 50, 137 (1978).

31. M. V. Susic and M. G. Pjescic, *Analyst*, 91, 258 (1966).
32. E. Sudo and H. Okocki, *Japan Analyst*, 18, 507 (1969).
33. N. G. Elenkova, R. A. Tsoneva and T. K. Nedeltcheva, *Talanta*, 23, 726 (1976).
34. W. R. Nall, *Analyst*, 96, 398 (1971).
35. N. G. Elenkova and R. A. Tsoneva, *Talanta*, 22, 480 (1975).
36. G. M. George, L. J. Frahm and J. P. McDonnell, *J. Assoc. Off. Anal. Chem.*, 56, 793 (1973).
37. W. Holak, *J. Assoc. Off. Anal. Chem.*, 59, 650 (1976).
38. J. L. Morrison and G. M. George, *J. Assoc. Off. Anal. Chem.*, 52, 930 (1969).
39. H. K. Hundley and J. C. Underwood, *J. Assoc. Off. Anal. Chem.*, 53, 1176 (1970).
40. W. Schoniger, *Mikrochim. Acta*, 869 (1956).
41. W. Schoniger, *Mikrochim. Acta*, 123 (1955).
42. M. R. Masson, *Mikrochim. Acta*, 399 (1976).
43. G. Schwedt and H. A. Russel, *Chromatographia*, 5, 242 (1972).
44. J. A. James and D. H. Richards, *Nature*, 175, 769 (1955).
45. H. Onishi and E. B. Sandell, *Mikrochim. Acta*, 34 (1953).
46. G. R. Kingsley and R. R. Schaffert, *Anal. Chem.*, 23, 914 (1951).
47. N. G. Elenkova and R. A. Tsoneva, *Zh. Anal. Khim.*, 29, 289 (1974).
48. V. I. Plotnikov and L. P. Usatova, *Zh. Anal. Khim.*, 19, 1183 (1964).
49. W. Reichel and B. G. Bleakley, *Anal. Chem.*, 46, 59 (1974).
50. J. I. Hoffman and G. C. Lundell, *J. Res. Nat. Bur. Std.*, 22, 465 (1936).

51. V. V. Sergeeva, J. J. Levin, L. I. Tishchenko and V. Dankova, *Zh. Anal. Khim.*, 27, 2188 (1973).
52. H. Asaoka, *Bunseki Kagaku*, 23, 1049 (1974).
53. L. Rozanski, *Chem. Anal.*, 17, 55 (1972).
54. P. F. Wyatt, *Analyst*, 80, 368 (1955).
55. H. Malissa and E. Schoffman, *Mikrochim. Acta*, 187 (1955).
56. Y. V. Morachevskii and A. I. Kalinin, *Zav. Lab.*, 27, 272 (1961).
57. A. I. Kalinin, *Zh. Anal. Khim.*, 17, 390 (1962).
58. H. J. Morris and H. O. Calvery, *Ind. Eng. Chem., Anal. Ed.*, 9, 447 (1937).
59. F. J. Fernandez and D. C. Manning, *Atom. Abs. Newslett.*, 10, 86 (1971).
60. E. N. Pollock and S. J. West, *Atom. Abs. Newslett.*, 12, 6 (1973).
61. F. E. Lichte and R. K. Skogerboe, *Anal. Chem.*, 44, 1480 (1972).
62. G. C. Whitnack and R. C. Brophy, *Anal. Chim. Acta*, 48, 123 (1969).
63. R. Frache and A. Dadone, *Chromatographia*, 6, 475 (1973).
64. F. W. E. Strelow, R. Rethemeyer and C. J. C. Bothma, *Anal. Chem.*, 37, 106 (1965).
65. Y. Yoshimo, *Bull. Chem. Soc. Japan*, 24, 39 (1951).
66. J. T. Odenchantz and Wm. Rieman, *Anal. Chem.*, 22, 1066 (1950).
67. Z. I. Otmakhova, O. V. Chashchina and N. I. Slezko, *Zav. Lab.*, 35, 685 (1969).
68. F. Nelson, T. Murase and K. Kraus, *J. Chromatogr.*, 13, 503 (1964).
69. A. K. De and T. Chakrabarty, *Ind. J. Chem.*, 7, 180 (1969).

70. M. D. Seymour and J. S. Fritz, *Anal. Chem.*, 45, 1394 (1973).
71. P. van den Winkel, F. De Corte, A. Speecke and J. Hoste, *Anal. Chim. Acta*, 42, 340 (1968).
72. P. van den Winkel, F. de Corte and J. Hoste, *Anal. Chim. Acta*, 56, 241 (1971).
73. Wm. F. Carey, *J. Assoc. Off. Anal. Chem.*, 51, 1300 (1968).
74. H. N. Das-Gupta, *J. Ind. Chem. Soc.*, 9, 95 (1932).
75. G. Newberry, *J. Chem. Soc.*, 127, 1751 (1925).
76. M. M. Tuckerman, J. H. Hodecker, B. C. Southworth and K. D. Fleischer, *Anal. Chim. Acta*, 21, 463 (1959).
77. I. M. Kolthoff and E. Amdur, *Ind. Engr. Chem., Anal. Ed.*, 12, 177 (1940).
78. D. E. Ryan and G. D. Lutwick, *Can. J. Chem.*, 31, 9 (1953).
79. E. Gastinger, *Mikrochim. Acta*, 4, 526 (1972).
80. E. Troug and A. H. Meyer, *Ind. Eng. Chem., Anal. Ed.*, 1, 136 (1929).
81. A. E. Heron and D. Rogers, *Analyst*, 71, 414 (1946).
82. H. J. Morris and H. O. Calvery, *Ind. Eng. Chem., Anal. Ed.*, 13, 760 (1941).
83. H. J. Rodden, *J. Res. Nat. Bur. Std.*, 24, 7 (1940).
84. A. J. Williams, *Analyst*, 93, 611 (1968).
85. P. Pakalns, *Anal. Chim. Acta*, 47, 225 (1969).
86. D. F. Bolz, *CRC Critical Reviews Anal. Chem.*, 3, 147 (1973).
87. G. F. Kirkbright, M. Sargent and T. S. West, *Atom. Abs. Newslett.*, 7, 5 (1968).
88. G. F. Kirkbright and L. Ranson, *Anal. Chem.*, 43, 1238 (1971).

89. J. E. Allen, *Spectrochim. Acta*, 18, 259 (1962).
90. R. M. Dagnall, K. C. Thompson and T. S. West, *Atom. Abs. Newslett.*, 6, 117 (1967).
91. A. U. Shaikh and D. E. Tallnan, *Anal. Chem.*, 49, 1093 (1977).
92. G. W. Dickinson and V. A. Fassel, *Anal. Chem.*, 41, 1021 (1969).
93. G. F. Kirkbright, A. F. Ward and T. S. West, *Anal. Chim. Acta*, 64, 353 (1973).
94. K. Heydron and E. Damsgaard, *Talanta*, 20, 1 (1973).
95. Y. Maruyama and K. Komiya, *Radioisotope*, 5, 279 (1973).
96. B. J. Ray and D. L. Johnson, *Anal. Chim. Acta*, 62, 196 (1972).
97. E. Steinnes, *Analyst*, 97, 241 (1972).
98. R. C. Leake and D. Peachey, *Inst. Mining Met. Trans.*, Sect. B, 82, 25 (1973).
99. H. Tanaka, Y. Moriguchi, T. Yamamoto and G. Hashizume, *Bunseki Kagaku*, 21, 1456 (1972).
100. F. J. Marcie, *Environ. Sci. Tech.*, 1, 164 (1967).
101. J. Tadmor, *J. Gas Chromatogr.*, 2, 385 (1964).
102. D. Vranti-Piscoue, J. Kontoyannokos and G. Parissakas, *J. Chromatogr. Sci.*, 9, 499 (1971).
103. R. S. Jewet, Jr. and R. L. Fisher, *Anal. Chem.*, 37, 1752 (1965).
104. W. C. Butts and W. T. Rainey, Jr., *Anal. Chem.*, 43, 1538 (1971).
105. G. Schwedt and H. A. Russel, *Chromatographia*, 5, 242 (1972).
106. G. Schwedt and H. A. Russel, *Z. Anal. Chem.*, 264, 301 (1973).
107. R. S. Braman and C. C. Foreback, *Science*, 182, 1247 (1973).

108. D. P. Cox and M. Alexander, *Bull. Environ. Contam. Toxicol.*, 9, 84 (1973).
109. Y. Talmi and V. E. Norvell, *Anal. Chem.*, 47, 1510 (1975).
110. W. Reichel and B. G. Bleakley, *Anal. Chem.*, 46, 59 (1974).
111. G. G. Rao, M. Gandikota and S. G. Viswanath, *Anal. Chim. Acta*, 87, 511 (1976).
112. T. Tanaka, K. Hiroy and A. Kawahara, *Z. Anal. Chem.*, 272, 44 (1974).
113. W. Selig, *Mikrochimica Acta*, 349 (1973).
114. R. Shaw, B. Riedel and W. Harris, *Can. Pharm. J.*, 90, 303 (1957).
115. Y. Bradshaw, *Analyst*, 88, 559 (1963).
116. M. Kobrova, *Chem. Listy*, 67, 762 (1973).
117. S. Yang, C. C. Tien and H. H. Kao, *Chem. Abst.*, 54, 626 (1945).
118. J. M. Issa, M. A. Ghanddour and A. M. Hammam, *J. Ind. Chem. Soc.*, 51, 872 (1974).
119. R. J. Myers and E. H. Swift, *J. Am. Chem. Soc.*, 70, 1047 (1948).
120. I. M. Kolthoff, *Zav. Lab.*, 11, 626 (1945).
121. S. Bruckenstein and D. C. Johnson, *Anal. Chem.*, 36, 2187 (1964).
122. N. Y. Chokina, O. A. Songina and V. A. Zakharov, *Zh. Anal. Khim.*, 31, 720 (1976).
123. A. A. Ramadan, P. K. Agasyan and S. I. Petrov, *Zh. Anal. Khim.*, 30, 89 (1975).
124. B. B. Prasad and G. D. Khandelwal, *Israel J. Chem.*, 9, 281 (1971).
125. R. K. Simon, G. D. Christian and Wm. C. Purdy, *Am. J. Clin. Path.*, 49, 207 (1968).

126. W. M. Wise and J. P. Williams, *Anal. Chem.*, 36, 19 (1964).
127. A. A. Ramadan, P. K. Agasyan and S. I. Petrov, *Zh. Anal. Khim.*, 31, 322 (1976).
128. A. A. Ramadan, P. K. Agasyan and S. I. Petrov, *Zav. Lab.*, 41, 641 (1975).
129. V. J. Jennings, A. Dodson and A. M. Atkinson, *Analyst*, 97, 923 (1972).
130. A. P. Tomilov and N. E. Chomutov, in Encyclopedia of Electrochemistry of the Elements, edited by A. J. Bard (Marcel Dekker, Inc., New York, 1974), p. 21.
131. J. P. Arnold and R. M. Johnson, *Talanta*, 16, 1191 (1969).
132. L. Meites, *J. Am. Chem. Soc.*, 76, 5927 (1954).
133. S. M. White and A. J. Bard, *Anal. Chem.*, 38, 61 (1966).
134. M. V. Susic and M. G. Pjescic, *J. Electroanal. Chem. Interfac. Electrochem.*, 34, 535 (1972).
135. W. B. Swann, J. F. Hazel and W. M. McNabb, *Anal. Chem.*, 32, 1064 (1960).
136. E. G. Vasilyeva, S. I. Zhdanov and T. A. Krjukova, *Elektrokhimiya*, 4, 25 (1968).
137. N. J. Holpin, N. A. Rafalovich and G. P. Aksenova, *Zh. Anal. Khim.*, 3, 16 (1948).
138. D. Everest and G. Finch, *J. Chem. Soc.*, 704 (1955).
139. J. Suzuki, *Japan Analyst*, 15, 548 (1966).
140. N. G. Elenkova and R. A. Tsoneva, *Anal. Chim. Acta*, 62, 435 (1972).
141. H. S. Mahanti, *Z. Anal. Chem.*, 274, 303 (1975).
142. N. G. Elenkova and R. A. Tsoneva, *Zh. Anal. Khim.*, 29, 1344 (1974).
143. N. G. Elenkova and R. A. Tsoneva, *Zh. Anal. Khim.*, 29, 244 (1974).

144. N. G. Elenkova and R. A. Tsoneva, Zh. Anal. Khim., 28, 501 (1973).
145. N. G. Elenkova and R. A. Tsoneva, Russ. J. Inorg. Chem., 17, 356 (1972).
146. R. Geyer and M. Geissler, Z. Anal. Chem., 201, 16 (1964).
147. P. Beran, J. Cihalik, J. Dolezal, V. Simon and J. Zyka, Chem. Listy, 47, 1315 (1953).
148. D. Cozzi and S. Vivarelli, Anal. Chim. Acta, 5, 215 (1951).
149. G. Haigh, J. Am. Chem. Soc., 75, 3848 (1953).
150. D. J. Myers, M. E. Heinbrook, J. Osteryoung and S. M. Morrison, Environ. Lett., 5, 53 (1973).
151. K. Hagiwara and I. Murase, Japan Analyst, 13, 788 (1964).
152. D. J. Myers and J. Osteryoung, Anal. Chem., 45, 267 (1973).
153. W. Holak, J. Assoc. Off. Anal. Chem., 60, 1015 (1977).
154. E. Temmerman and F. Verbeek, Anal. Chim. Acta, 43, 263 (1968).
155. A. A. Kaplin, N. A. Veits and A. G. Stromberg, Zh. Anal. Khim., 28, 2192 (1973).
156. G. Forsberg, J. W. O'Laughlin and R. G. Megargle, Anal. Chem. 47, 1586 (1975).
157. L. F. Trushina and A. A. Kaplin, Zh. Anal. Khim., 25, 1616 (1970).
158. T. Kuwabara, S. Suzuki and S. Araki, Bull. Chem. Soc. Jap., 46, 1690 (1973).
159. E. S. Pilkington and C. Weeks, Anal. Chem., 48, 1665 (1976).
160. V. F. Toropova, Y. N. Polyakov and L. N. Soboleva, Zh. Anal. Khim., 32, 985 (1977).

161. T. Y. Belova, I. B. Berengard and B. Y. Kaplan, *Zav. Lab.*, 41, 1314 (1975).
162. T. A. Krapivkina, E. M. Roizenblat, V. V. Nosacheva, L. S. Zaretskii and V. S. Utenko, *Zh. Anal. Khim.*, 29, 1818 (1974).
163. A. A. Kaplin, N. A. Veits, N. M. Mordvinova and G. G. Glukhov, *Zh. Anal. Khim.*, 32, 687 (1977).
164. D. T. Napp, D. C. Johnson and S. Bruckenstein, *Anal. Chem.*, 39, 481 (1967).
165. P. Delahay, Double Layer and Electrode Kinetics (Interscience Publishers, New York, 1977).
166. R. N. Adams, Electrochemistry at Solid Electrodes (Marcel Dekker, Inc., New York, 1969).
167. Z. Galus, Fundamentals of Electrochemical Analysis (John Wiley and Sons, Inc., New York, 1976).
168. D. C. Johnson and E. W. Resnick, *Anal. Chem.*, 49, 1918 (1977).
169. R. J. Davenport and D. C. Johnson, *Anal. Chem.*, 45, 1755 (1973).
170. F. Anson, *J. Electrochem. Soc.*, 110, 436 (1963).
171. R. Parsons, *J. Electroanal. Chem.*, 21, 35 (1969).
172. R. De Levie, *J. Electrochem. Soc.*, 118, 185C (1971).
173. Y. Takato and G. Muto, *Bunseki Kagaku*, 14, 543 (1965).
174. Y. Takato, T. Kuwabara and G. Muto, *Bunseki Kagaku*, 17, 1491 (1968).
175. Y. Takato and G. Muto, *Bunseki Kagaku*, 15, 269 (1966).
176. D. C. Johnson and J. H. Larochele, *Talanta*, 20, 959 (1973).
177. L. R. Taylor and D. C. Johnson, *Anal. Chem.*, 46, 262 (1974).
178. R. W. Andrews and D. C. Johnson, *Anal. Chem.*, 48, 1056 (1976).

179. Y. Takato and G. Muto, *Anal. Chem.*, 45, 1864 (1973).
180. P. L. Joynes and R. J. Maggs, *J. Chromatogr. Sci.*, 8, 427 (1970).
181. M. D. Seymour, J. P. Sickafoose and J. S. Fritz, *Anal. Chem.*, 43, 1734 (1971).
182. J. H. Larochelle, Ph.D. Thesis, Iowa State University, Ames, Iowa, 1977.
183. H. Diehl, Quantitative Analysis (Oakland Street Science Press, Ames, Iowa, 1974).
184. D. C. Johnson and S. Bruckenstein, *J. Electrochem. Soc.*, 117, 460 (1970).
185. P. L. Meschi, private communication, I.S.U. Chemistry Department, 1978.
186. V. G. Levich, Physiochemical Hydrodynamics (Prentice-Hall, Englewood Cliffs, New Jersey, 1962).
187. T. K. Ross and A. A. Wragg, *Electrochim. Acta*, 10, 1093 (1965).
188. D. C. Johnson and S. Bruckenstein, *J. Am. Chem. Soc.*, 90, 6592 (1968).
189. W. J. Blaedel, C. L. Olson and L. R. Sharma, *Anal. Chem.*, 35, 2100 (1963).
190. H. G. Cassidy, *J. Am. Chem. Soc.*, 71, 402 (1949).
191. I. H. Updegraff and H. G. Cassidy, *J. Am. Chem. Soc.*, 71, 407 (1949).
192. M. Ezrin, I. H. Updegraff and H. G. Cassidy, *J. Am. Chem. Soc.*, 75, 1610 (1953).
193. H. G. Cassidy, M. Ezrin and I. H. Updegraff, *J. Am. Chem. Soc.*, 75, 1615 (1953).
194. L. Erdey, J. Inczidy and I. Markovits, *Talanta*, 4, 25 (1960).
195. G. E. Janauer, G. O. Ramseyer and J. W. Lin, *Anal. Chim. Acta*, 73, 311 (1974).
196. W. E. Bernier and G. E. Janauer, *Trace Substances in Environ. Health*, 10, 323 (1976).

196. W. E. Bernier and G. E. Janauer, Trace Substances in Environ. Health, 10, 323 (1976).
197. R. G. Pats, S. I. Zhdanov, T. V. Semochkina, E. D. Shuvalova and S. V. Rudakova, Zav. Lab., 38, 1053 (1971).
198. K. A. Kraus and F. Nelson, Proc. of First U.N. International Conf. on Peaceful Uses of At. Energy, 7, 113 (1956).
199. K. Hagiwara, Japan Analyst, 19, 563 (1970).
200. H. N. Heckner, Z. Analyt. Chem., 261, 29 (1972).
201. W. Holak, J. Assoc. Off. Anal. Chem., 60, 478 (1977).

X. ACKNOWLEDGEMENTS

I would like to thank Dr. Dennis C. Johnson and the members of his research group for their contribution to my graduate education.

The financial support from the National Science Foundation through grant GP-40646X and from the Pine Instrument Co. is gratefully acknowledged.

The various forms of support extended to me by my family are deeply appreciated.

A special thanks is offered to St. Jude, the patron saint of hopeless causes.